Title
Variation in forest richness, density, and size is explained by environmental gradients from the plot to landscape scale

Author
Fricker, Geoffrey Andrew

Publication Date
2015

Peer reviewed|Thesis/dissertation

UNIVERSITY OF CALIFORNIA

Los Angeles

Variation in forest richness, density, and size is explained by environmental gradients from the plot to landscape scale

A dissertation submitted in partial satisfaction of the requirements

for the degree Doctor of Philosophy in Geography

by

Geoffrey Andrew Fricker

2015

ABSTRACT OF THE DISSERTATION

Variation in forest richness, density and size is explained by environmental gradients from the plot to landscape scale

by

Geoffrey Andrew Fricker

Doctor of Philosophy in Geography

University of California, Los Angeles, 2015

Professor Thomas Welch Gillespie, Chair

A spatial gap exists between fine scale forest census plot dynamics and coarse scale landscape processes. Patterns observed at the plot scale do not necessarily continue outside plot boundaries and how such patterns scale across the landscape remains poorly understood. The sparse geographic extent of census plot data and the prohibitive cost of high resolution remote sensing remain the largest obstacles to extending the study of plot scale dynamics across the landscape, however this situation is changing rapidly and methods must be developed to integrate new data and close this spatial gap. The research presented in this dissertation utilizes

plot level census data to study how plant richness, density and size vary across environmental gradients and presents a methodological framework for 1) predicting species richness where no plot data currently exists, 2) investigating guild level differences between plant growth forms in relation to resource gradients and 3) studying how forests vary across environmental gradients at the continental scale. The methodology utilizes spatial and non-spatial modeling to identify associations between plant richness, density and size at the plot scale. These associations are used to predict forest dynamics at the landscape scale and study forest structure at the continental scale.

First, the findings provide evidence that increased tree species richness is associated with environmental heterogeneity in both the canopy and hydrologic environment. These associations explain nearly half of the variation in tree species richness and are used to make hectare scale predictions of tree species richness on Barro Colorado Island, Panama. Secondly, there is strong evidence of habitat filtering along resource gradients of light and water caused by guild level differences between plants. In particular, free-standing plant guilds are non-randomly arranged along the hydrologic gradient with short understory trees and shrubs clustered in wetter environments and midstory and canopy level trees clustered in drier environments. Finally, when compared to climatic predictors, topography and terrain slope in particular appear to be exerting strong controls on forest structure across Mesoamerica. Taller forests occur on steep slopes, high elevation, on well drained soils and these effects are insensitive to land cover, biome and spatial scale.

The dissertation of Geoffrey Andrew Fricker is approved.

Yongwei Sheng

Stephen Hubbell

Thomas Welch Gillespie, Committee Chair

University of California, Los Angeles

2015

DEDICATION

I would like to dedicate this work to my parents and my wife. Geoffrey Fricker Sr. and Sandra Machida raised me with a wonder for science, the natural world and taking pictures. I credit them with my passion for science, remote sensing and sense of stewardship for the environment. I would also like to dedicate this work to my loving wife Haylea Drysdale, who has provided unconditional support, patience and has kept me grounded throughout the dissertation process.

TABLE OF CONTENTS

ACKNOWLEDGMENTS

Chapter 1:

Chapter 1 is in press for the journal *Ecological Applications*. Special thanks for Chapter 1 is owed to Thomas Gillespie, Jeffrey Wolf, and Sassan Saatchi for helping provide feedback throughout the writing process as co-authors. Airborne LiDAR data was provided by Sassan Saatchi and Jim Dalling. Fernando Espirito-Santo provided valuable input on the analysis and methods. The LiDAR data collection was made possible with financial support from the Smithsonian Tropical Research Institute and National Science Foundation (DEB-0939907) to Jim Dalling. Geoffrey A. Fricker was financially supported by the NSF Dissertation Improvement Grant (Award No: BCS-1333701). Technical GIS programming assistance was provided by Evan Lyons and Jida Wang. This research was also supported by the Dimensions of Biodiversity Distributed Graduate Seminar Series made possible by a National Science Foundation Dimensions of Biodiversity grant (1050680) to Sandy Andelman and Julia Parish.

Chapter 2:

Acknowledgments for Chapter 1 also are owed for Chapter 2. Chapter two uses nearly identical information and is currently in preparation. Special thanks is owed to Jeffrey Wolf who facilitated the collaboration between Liza Comita and Stephan Schnitzer which made this chapter possible in addition to helping organize and process the guild level plot data. Liza Comita and Stephan Schnitzer deserve special thanks for contributing their additional plant census data from BCI The LiDAR data collection was made possible with financial support from Smithsonian Tropical Research Institute and National Science Foundation (DEB-0939907) to Jim Dalling. Geoffrey Fricker was financially supported by the NSF Dissertation Improvement Grant (Award

No: BCS-1333701). This research was also supported by the Dimensions of Biodiversity Distributed Graduate Seminar Series made possible by a National Science Foundation Dimensions of Biodiversity grant (1050680) to Sandy Andelman and Julia Parish. Special thanks are owed to thank Claudio Monteza and Amaranto Cabezon for their help in the field on BCI and to Sean Bowers of Geodigital International Corporation for assisting in Differential GPS post-processing of plot corner coordinates. Research on the BCI 50-ha FDP has been made possible by US National Science Foundation grants to S.P. Hubbell: DEB-0640386, DEB-0425651, DEB-0346488, DEB-0129874, DEB-00753102, DEB-9909347, DEB-9615226, DEB-9615226, DEB-9405933, DEB-9221033, DEB-9100058, DEB-8906869, DEB-8605042, DEB-8206992, DEB-7922197, support from the Center for Tropical Forest Science, the Smithsonian Tropical Research Institute, the John D. and Catherine T. MacArthur Foundation, the Mellon Foundation, the Small World Institute Fund, and numerous private individuals, and through the hard work of over 100 people from 10 countries over the past two decades. The plot project is part of the Center for Tropical Forest Science, a global network of large-scale demographic tree plots.

Chapter 3:

Thomas Gillespie, Stephen Hubbell, Gregory Okin, Yongwei Sheng, and Sassan Saatchi all contributed valuable feedback which will be incorporated into this Chapter before it is submitted for publication in a peer-viewed journal. Thanks to Michael Lefsky for processing the GLAS laser profiles and performing the slope correction and to Yifan Yu who provided GLAS structural metrics across Mesoamerica. Special thanks to Jeffrey Wolf who performed an independent test of the Random Forest Regression modelling to verify the results for this

chapter. Geoffrey Andrew Fricker was financially supported through the UCLA Graduate Division Dissertation Year Fellowship for the academic year of 2014/2015.

BIOGRAPHICAL SKETCH

Geoffrey Andrew Fricker

EDUCATION:

Ph.D. Candidate	Geography, University of California, Los Angeles (graduation June 2015)
M.A.	Geography, University of California, Los Angeles, 2009
B.S.	Physical Geography, University of California, Santa Barbara, 2005

AWARDS

Dissertation Year Fellowship, 2014/2015. Graduate Division, UCLA. Award date 2014, Award amount $35,208.38.

National Science Foundation, Social Behavioral and Economic Sciences (SBE) Doctoral Dissertation Research Improvement Grant in Geography and Spatial Sciences. Award date 2013, Award amount $8,820.

REFEREED PUBLICATIONS (Accepted)

Wolf, J.A., Hubbell, S.P., Fricker, G.A., Turner, B.L., Geospatial observations on tropical forest subsurface soil chemistry (Data Paper). Ecology. Accepted 5/19/2015.

Fricker, G.A., Wolf, J.A., Saatchi, S.S., Gillespie, T.G., Predicting spatial variations of tree species richness in tropical forests from high spatial resolution remote sensing. *Ecological Applications*. In Press, preprint available at: http://www.esajournals.org/toc/ecap/0/0.

Fricker, G.A.; Saatchi, S.S.; Meyer, V.; Gillespie, T.W.; Sheng, Y. Application of Semi-Automated Filter to Improve Waveform Lidar Sub-Canopy Elevation Model. *Remote Sens.* 2012, *4*, 1494-1518.

Wolf, J.A.; Fricker, G.A.; Meyer, V.; Hubbell, S.P.; Gillespie, T.W.; Saatchi, S.S. Plant Species Richness is Associated with Canopy Height and Topography in a Neotropical Forest. *Remote Sens.* 2012, *4*(12), 4010-4021.

Meyer, V., Saatchi, S.S., Chave, J, Dalling, J., Bohlman, S., Fricker, G.A., Robinson, C.M., Neumann, M. Detecting tropical forest biomass dynamics from repeated airborne Lidar measurements. *Biogeosciences*. 2013, 10(2)1957-1992.

CONFERENCE PAPERS AND RESEARCH PUBLICATIONS

Gillespie, T.W., Fricker, G.A., Robinson, C.M. "Biodiversity of the world: A study from space". *Remote Sensing Handbook*. Oxford, UK: Taylor and Francis (in preparation).

Fricker, G.A.; Saatchi, S.S.; Meyer, V.; Gillespie, T.W.; Sheng, Y. "Correction of Waveform Lidar Sub-canopy Elevation Model Using a Semi-automated Filter". *ForestSAT 2012 Oregon State University, Corvallis, Oregon.* September 2012 (invited presentation).

Meyer, V.; Saatchi, S.S.; Fricker, G.A.; Chave, J.; Neumann, M.; Bohman, S.; Dalling, J. "Detecting Tropical Forest Biomass Dynamics from Lidar Measurements". *ForestSAT 2012 Oregon State University, Corvallis, Oregon.* September 2012 (poster).

Fricker, G.A.; Wolf, J.; Saatchi, S.S.; Hubbell, S.P.; Gillespie, T.W.; Meyer, V.; Robinson, C.; Rovzar, C. Sheng, Y. "Coupling forest structure and sub-canopy topography to Alpha diversity across spatial scales in the 50 ha plot Barro Colorado Island, Panama". Ecological Society of America, Portland, Oregon. August 2012 (poster).

Robinson, C.; Saatchi, S.S.; Clark, D.; Gillespie, T.; Fricker, G.A.; Andelman, S.; Wolf, J.; Rovzar, C. Assessment of Variations in Taxonomic Diversity and Forest Structure Along an Altitudinal Gradient in Tropical Montane Forest of Costa Rica". Ecological Society of America, Portland, Oregon. August 2012 (poster).

Fricker, G.A.; Saatchi, S.S.; Meyer, V.; Gillespie, T.W.; Sheng, Y. "Using a semi-automated filtering process to improve waveform lidar sub-canopy elevation models and forest structure metrics" American Geophysical Union, San Francisco, CA. 2011 (poster).

Fricker, G.A.; Gillespie, T.G.; Sheng, Y. "Deriving tropical forest stand characteristics from large footprint waveform lidar". *Association of America Geographers*, Las Vegas, NV. 2009.

PROFESSIONAL SERVICE

Referee for journals (number of manuscripts reviewed)

International Journal of Remote Sensing (5)

IEEE Transactions on Geoscience and Remote Sensing (1)

CHAPTER 1

[Chapter 1 is formatted as a paper in Ecological Applications]

[A preprint of Chapter 1 is available at: http://www.esajournals.org/doi/abs/10.1890/14-1593.1]

Section 1.1: Predicting spatial variations of tree species richness in tropical forests from high resolution remote sensing

ABSTRACT

There is an increasing interest in identifying theories, empirical datasets, and remote sensing metrics that can quantify tropical forest alpha diversity at a landscape scale. Quantifying patterns of tree species richness in the field is time consuming, especially in regions with over 100 tree species per ha. This study examines species richness in a 50 ha forest dynamics plot (FDP) on Barro Colorado Island (BCI), Panama and tests if biophysical measurements of canopy reflectance from high resolution satellite imagery combined with detailed vertical forest structure and topography from light detection and ranging (LiDAR) are associated with species richness across four tree size classes (> 1, 1-10, > 10, > 20 cm dbh) and three spatial scales (1, 0.25, 0.04 ha). This study uses the 2010 tree inventory, including 204,757 individuals belonging to 301 species of freestanding woody plants or 166 ± 1.5 species per ha (mean ± SE), to compare with remote sensing data. All remote sensing metrics become less correlated with species richness as spatial resolution decreased from 1.0 ha to 0.04 ha and tree size increased from 1 cm to 20 cm dbh. When all stems > 1 cm in 1 ha plots were compared to remote sensing metrics, standard deviation in canopy reflectance can explain 13% of the variance in species richness. The

standard deviations of canopy height and the topographic wetness index (TWI) derived from LiDAR were the best metrics to explain the spatial variance in species richness (15% and 24% respectively). Using multiple regression models, this study makes predictions of species richness across Barro Colorado Island (BCI) at the 1-ha spatial scale for different tree size classes. Models can predict variation in tree species richness amongst all plants (adjusted $r^2 = 0.35$) and trees > 10 cm dbh (adjusted $r^2 = 0.25$). However, the best model results were for understory trees and shrubs (1-10 cm dbh) (adjusted $r^2 = 0.52$), that comprise the majority of species richness in tropical forests. The results indicate that high resolution remote sensing can predict a large proportion of variance in species richness and potentially provide a framework to map and predict alpha diversity amongst trees in diverse tropical forests.

Key words: Barro Colorado Island, high-resolution satellite imagery, LiDAR, remote sensing, spatial scale, tree species richness

INTRODUCTION

Tropical forests are experiencing high rates of deforestation and degradation causing a significant contribution to increasing atmospheric CO_2 and a large adverse impact on biodiversity and other ecosystem services (Clark et al. 2011, Bellard et al. 2012, Harris et al. 2012, Hansen et al. 2013). Yet there is a lack of spatial information on the distribution of biodiversity at the landscape to regional scales that can be used for achieving specific Aichi Biodiversity Targets by 2020, outlined in the Global Biodiversity Outlook from the Intergovernmental Science-Policy Platform on Biodiversity and Ecosystem Services (IPBES). In particular, a recent mid-term analysis of progress toward international biodiversity targets found that a global analysis will not reflect finer scale spatial variation at local to regional scales and that taxonomic coverage is a key limiting factor. The analysis could not locate any indicators meeting the criteria to measure progress toward measuring ecosystem resilience and contribution of biodiversity to carbon stocks (Aichi Target 15) (Tittensor et al. 2014). It is therefore a pressing issue to develop baseline targets against which to assess future progress and test assessments with additional taxonomic and landscape scale assessments of alpha diversity. With accelerated declines in tropical forests across the world, there is an urgent need to identify patterns and processes associated with the distribution and maintenance of species richness (alpha diversity), turn over (beta diversity), and traits (functional diversity). An analysis of 100 time series from biomes across the planet did not find a systematic loss of alpha diversity, however community composition changed systematically through time (Dornelas et al. 2014). The results suggested that the extent to which biodiversity change in local assemblages contributes to global

biodiversity loss is poorly understood. Furthermore, the authors emphasized that monitoring and understanding change in species composition should be a conservation priority.

Most remote sensing studies of tree species richness in the tropics use 1 ha plots and examine tree species >10 cm in diameter at breast height (dbh), but there has been an increase in the number of large plots (i.e. 50 ha) that quantify species richness of stem >1 cm dbh (Condit et al. 1996, Saatchi et al. 2008, Keith et al. 2009). However, quantifying patterns of species richness in regions with over 100 tree species per ha is expensive, time consuming, requires skilled individuals to identify trees to species, and currently field plots cover a small geographic extent of the tropical landscape. Thus there is an increasing need to develop methods for mapping predictions of alpha diversity across tropical forest landscapes at a high spatial resolution (Nagendra and Rocchini 2008).

There are a number of physical and environmental conditions that have been hypothesized to be associated with tree species richness in tropical forest landscapes. Primary productivity has been hypothesized to be associated with alpha diversity based on the species-energy or diversity-productivity theory (Lo Seen Chong et al. 1993, Evans et al. 2005). There have been an increasing number of studies that have found significant associations between spectral indices of productivity and diversity (Nagendra 2001, Kerr and Ostrovsky 2003, Chambers et al. 2007, Leyequien et al. 2007, Saatchi et al. 2008), and many studies have reported significant positive correlations between plant species richness and diversity from plot data and productivity indices in tropical ecosystems (Bawa et al. 2002, Feeley et al. 2005, Gillespie 2005, Cayuela et al. 2006).The most commonly used and most intensively studied vegetation index is the normalized difference vegetation index (NDVI), capturing the greenness or chlorophyll content of vegetation and photosynthesis processes relating to productivity.

However a host of other vegetation indices are also available. Some may be better adapted for tree diversity applications such as the simple ratio vegetation index (RVI) which more directly measures leaf area index (LAI) (Chen et al. 2002) or the enhanced vegetation index (EVI) which can resolve differences in LAI without being impacted by background soil reflectance (Rocha and Shaver 2009).

Amongst canopy trees, there is often high interspecific variation in the chemical and physical properties that influence light absorption and reflectance. New airborne imaging technologies such as the Carnegie Airborne Observatory (CAO) offer higher spectral resolution and analytical methods which provide a way to detect and map canopy species richness based on biochemical variation across landscapes (Asner et al. 2007). A range of airborne and space-based remote sensing technologies hold real promise for overcoming the challenges posed by the biogeochemical complexity of the tropical biome (Townsend et al. 2008, Schimel et al. 2014). Spectral heterogeneity may be positively associated with species richness due to chemical and structural variability. Measurements of spectral heterogeneity derived from satellite imagery have been proven to be correlated with species richness in temperate environments (Gould 2000, Rocchini et al. 2004a) as well as from airborne remote sensing platforms in the tropics (Asner and Martin 2008a, Asner et al. 2011). This relationship with species richness is based on the hypothesis that heterogeneity in spectral indices or spectral variability within a landscape is an indicator of either habitat heterogeneity, or in the case of canopy trees a diversity of foliar chemistry (Palmer et al. 2002, Carlson et al. 2007, Rocchini et al. 2007). Variation in spectral indices has been shown to be positively associated with species richness and diversity for a number of taxa in different regions, but there are few studies in tropical forest landscapes (Gould 2000, Fairbanks and McGwire 2004, Levin et al. 2007). Since differences in vertical canopy

structure create a heterogeneous light environment with shadows, gaps and volumetric scattering in tree canopies, there is a powerful signal from canopy structure in remote sensing measurements of spectral heterogeneity. Canopy texture measurements from digital aerial photographs showed highly significant correlations with tree density ($r^2 = 0.80$), mean basal area ($r^2 = -0.71$), distribution of dbh size classes ($r^2 = 0.64$) and mean canopy height ($r^2 = 0.57$) in 12 1-ha control plots in a tropical rainforest in French Guiana for trees greater than 10 cm dbh (Couteron et al. 2005). High-resolution Quickbird satellite imagery (200 km^2) has also been employed to demonstrate the feasibility of large scale assessment of rain forest canopy structure across the Amazon (Barbier et al. 2010).

The complexity of tropical forest structure has long been identified as associated with high diversity in tropical forests (MacArthur and MacArthur 1961). Studies in temperate forests have shown that the development of structurally complex canopies comprising various tree species enhances stand productivity by promoting complementary resource utilization among species through spatial, physiological, and temporal differentiation (Ishii et al. 2004). Recent studies have shown that upper canopy variability is correlated with increased species richness among trees (>1 cm dbh) possibly due to partitioning of light resources (Wolf et al. 2012). Highly complex vertical canopy structure also enhances biodiversity of canopy-dwelling organisms by creating a resource-rich habitat (Terborgh 1985, Ishii et al. 2004).

It has been hypothesized that topography has a large influence on the distribution of both alpha diversity and community composition in tropical forests (Denslow 1995, Baldeck et al. 2013b). Slope has been found to be positively correlated with species richness of seedlings (1.0-3.9 cm dbh) (Hubbell et al. 1999) and this may also be the case for larger stems. It has been shown that slope specialists have significantly higher survival rate on the slope vs. plateau

habitat during the dry season, but plateau specialists show no difference in performance between habitats. This suggest that associations with plateau habitats result from a numerical advantage of drought-tolerant species in dry habitats where drought-sensitive species are unable to persist (Comita and Engelbrecht 2009). It is believed that topographic variation will create more physical space and different hydrologic conditions for species to co-exist. For instance, of the 171 commonly occurring species in the forest plots in Panama, 64% were associated with at least one topographically defined habitat (Harms et al. 2001). This suggests that niche differentiation with respect to micro-topography and soil water availability is a direct determinant of both local and regional scale distributions of tropical trees (Engelbrecht et al. 2007). Simple measurements of the heterogeneity of growth limiting factors in the light and hydrologic environments are expected to be associated with increased tree richness due to resource partitioning.

Advances in spaceborne and airborne sensors may allow for quantifying metrics of productivity, forest structure, and topography associated with alpha diversity in tropical forest landscapes. Spaceborne sensors such as Landsat, SPOT, and MODIS, with pixels sizes of 20 m to 250 m have been useful for quantifying species richness in tropical forest regions using spectral metrics (i.e. NDVI, EVI) associated with photosynthetic activity and primary productivity (Gillespie 2005). More recently airborne and spaceborne LiDAR and radar remote sensing systems have been used to characterize three-dimensional canopy structure for the purposes of modeling biodiversity (Goetz et al. 2007, Bergen et al. 2009, Gillespie et al. 2009, Müller and Brandl 2009, Goetz et al. 2010). Spatially explicit, high-precision LiDAR measurements of forest structure from airborne platforms allow for a more detailed characterization of the forest canopy across larger areas than previously possible using field based methods.

This research is focused on examining the relationship between tree species richness and canopy light reflectance, vertical forest structure, and surface topographical variations derived from fine scale (<1-m) remote sensing. This study is based on more than 200,000 tree inventory data on a single 50-ha plot at Barro Colorado Island (BCI) CTFS plot, but extends to cover the entire island (> 1500 ha) with forests along landscape and successional gradients (Condit et al. 1996). First, we examine relationships between species richness and remote sensing data across different tree size classes and spatial scales. In particular the analysis seeks to identify which environmental conditions have the strongest associations with tree richness and aim to test the hypotheses that tree species richness will be insensitive to different tree size classes and spatial scales. Second, the results identify which combinations of remote sensing derived metrics can explain the largest proportions of variance in tree species richness across a tropical forest landscape. Finally, the statistical relationships between multiple remote sensing metrics are used to predict tree species richness across Barro Colorado Island outside the boundaries of the 50 ha plot.

MATERIALS AND METHODS

Site area

The study was conducted on the 15.6 km^2 Barro Colorado Island (BCI) centered in Barro Colorado Nature Monument in the Republic of Panama (9°10'N, 79°51'W). The climate of BCI is seasonal, with an average four-month dry season from late December through late April (Engelbrecht et al. 2007). The vegetation is mainly tropical evergreen and semi-deciduous forest with high diversity (Croat 1978). The flora and vegetation of BCI have been investigated within the Forest Dynamics Plot (FDP) on the central plateau of BCI (Hubbell and Foster 1983). The

FDP was established in 1982, and all free standing trees > 1 cm dbh have been mapped and measured every 5 years since 1985. The study is focused on the 50 ha FDP on the central plateau, however maps of predicted species are projected across BCI (Figure 1.1)

Forest census plot data

Data on tree species richness across four different tree size classes and three spatial scales was analyzed. First, all freestanding woody plants (lianas and herbaceous plants excluded) in the 50 ha BCI FDP were categorized from the 2010 census for all tree size classes (Condit 1998, Hubbell et al. 1999). To study the effects of tree size, the plant stem data is sorted into four categories based on dbh size thresholds commonly used in the literature: 1) all stems (>1 cm dbh), 2) small trees and shrubs (<10 cm dbh), 3) medium and large trees (>10 cm dbh) and 4) large trees (>20 cm dbh). To calculate species richness across difference spatial scales, three different grid systems (0.04 ha, 0.25 ha or 1.0 ha) were defined across the 50 ha FDP. Iteratively, all individuals in the census are recorded as belonging to their respective subplot cell. Then the number of unique species per cell, the stem density, and the cumulative basal area of each subplot is counted or summed in the case of basal area. Basal area was calculated based on the largest stem for multi-stemmed plants.

Remote sensing

Airborne LiDAR and high spatial resolution Quickbird satellite imagery were used to quantify canopy reflectance, canopy structure, and sub-canopy micro-topography across each vegetation subplot (Figure. 1.2). The average and the standard deviation of each variable were computed across the subplot area, at each spatial scale for each remote sensing derived predictor

variable. A full description of remote sensing pre-processing is available in Appendix 1.1 and all remote sensing data can be downloaded at: http://www.esajournals.org/doi/abs/10.1890/14-1593.1.

Canopy reflectance

Multispectral Quickbird satellite imagery (2.4 m spatial resolution) was utilized to quantify the reflectance of the forest canopy. The image was collected on March 4th 2004 and available through the Smithsonian Tropical Research Institute GIS web portal. The Quickbird imagery contains four bands, blue (450 - 520 nm), green (530 - 600 nm), red (630 - 690 nm) and near-infrared (760 - 900 nm). Reflectance was corrected using the Fast-Line-of-sight Atmospheric correction tool (FLAASH) in ENVI 5.0 (Exelis Visual Information Solutions, Inc., Boulder, CO, USA). Three common vegetation indices were used, including the Ratio Vegetation Index (RVI), the Normalized Difference Vegetation Index (NDVI) and the Enhanced Vegetation Index (EVI). The variance in panchromatic image texture was also calculated as a predictor variable due to its sensitivity to vertical structure, shadows and light gaps. Image texture is categorized as a structural variable in the results, despite being derived from satellite imagery. Finally, spectral heterogeneity is quantified by performing a principle components analysis (PCA) and using the standard deviation in the first principle component band for each vegetation subplot. Most of the variance in the Quickbird image is in the infrared band and the majority of total variance captured by the PCA was in the first axis (>96%) (Appendix 1.1). We also calculated spectral distance between the 1st, 2nd and 3rd PC bands; however the results were not qualitatively different and were excluded from the reported results. This intermediate result indicates that a large proportion of the spectral variability in the satellite imagery derived

variables is due to forest stand structure and volumetric light scattering in the canopy (Couteron et al. 2005, Barbier et al. 2010). Therefore when interpreting the results variability in satellite derived metrics should be considered as being more indicative of complex canopy structure and not necessarily differences in canopy chemistry. There is a temporal gap between satellite imagery collection (2004), LiDAR collection (2009) and plot census (2010) wherein changes in forest composition have occurred, particularly in the understory. Since the Quickbird imagery primarily measures upper canopy reflectance I am making the assumption it will be less sensitive to understory demographic changes. The majority (89%) of large/emergent canopy trees in the 2005 census (>20 cm dbh) survived the 5+ years from photo acquisition to 2010 plot census and it is acknowledged some upper canopy changes may be present due to temporal misalignment.

Canopy structure

Airborne LiDAR was used to measure the vertical canopy structure and sub-canopy micro-topography (Figure 1.3). The airborne LiDAR data were acquired with an Optech ALTM Gemini system by BLOM Sistemas Geoespaciales in 2009 (Meyer et al. 2013). The number of returns ranged between 4 and 27 points per m^2 and field measured vertical errors were an average in height of -0.069 m, an RMS value of 0.076 m and standard deviation of 0.032 m from 36 control points in open un-vegetated areas (BLOM 2009, unpublished quality-assurance report). The geo-positioning of the 50 ha plot was based on the known location of coordinates of the corners published on the STRI GIS portal. The plot location was projected in the Universal Transverse Mercator (UTM) projection 17N, (meters) to match the native projection and units of the LiDAR. Classified LiDAR point cloud data was manually edited in LP360 (QCoherent) in ArcGIS 10.2 (ESRI, Redlands, CA, USA) to remove canopy towers or other high points from the

canopy point class. To measure vertical canopy structure the canopy surface model was rasterized at 1 m using first-return points defined by the highest LiDAR return (ground or canopy class) within each 1 m pixel. By subtracting the 1 m digital surface model (DSM) from the canopy surface model (CSM), a 1 m canopy height model (CHM) with terrain removed is generated. The CHM is how canopy structure is defined within each subplot, by computing both the mean and standard deviation of the CHM at each spatial scale.

Topography

The sub-canopy micro-topography variables were calculated from an unsmoothed 1 m LiDAR derived topographic DSM. The topography model was created by triangulating last-return LiDAR points to form a continuous surface from which all micro-topography variables were derived. Sub-canopy micro-topography is defined as topographic variables which are derived from the 1 m last-return LiDAR DSM and which vary at or below the smallest spatial scale (0.04 ha). I calculated terrain aspect, curvature, slope, and the TWI. To convert aspect measurements (0-360 degrees) into meaningful values, the cosine of aspect is calculated to transform it to a measure of 'northness'. Terrain slope is the first derivative of elevation and is calculated in degrees, and curvature is the unitless second derivative of elevation which describes whether the ground is upwardly concave or convex (positive curvature indicates upward convexity). The TWI includes terrain slope (in radians) and upslope contributing area to calculate a weighted estimation of water availability (Sørensen 2006, Sørensen and Seibert 2007). The TWI is modified by adding a small constant (C = 0.01) to the denominator to ensure no data voids in the TWI, when the slope is zero (Figure 1.4). For the final analysis, a fine scale (1 m) unsmoothed DSM was tested to provide the highest level of detail in the underlying

topography, however it is likely that there is some topographic 'noise' introduced by the fine scale and lack of smoothing. By testing DSMs with varying spatial resolutions the results indicate that while qualitatively similar, the finer DSM produced higher correlation coefficients between species richness and all micro-topography variables and was therefore of greater utility for the purposes of prediction. All remote sensing variables were calculated in ENVI 5.0 and ArcGIS 10.2 and extracted for each vegetation subplot using arcpython scripts in ArcGIS. The revised TWI arcpython script is available online: (https://github.com/africker/Topographic-Wetness-Index).

Statistical analysis

Species richness data is summarized for three tree sizes classes and three spatial scales and compared results to stem density and basal area from the 50 ha plot. The analysis is primarily focused on tree species richness amongst all stems (> 1 cm dbh), however discrete size classes were created by sub-setting the tree census data based on dbh size thresholds. The primary motivation for setting these discrete size thresholds was to analyze how different sized stems respond to the environmental variables, in particular the understory vegetation and the largest canopy trees. To study pairwise associations, Pearson correlation coefficients (r) and simple linear regression models were used to quantify the relationships between observed species richness and each remote sensing derived variable using ordinary least-squares (OLS) and Generalized Least Squares (GLS) regression in the R programming language (Team 2013).

Ordinary Least Squares and Generalized Least Squares

Relative to the island as a whole, the large cluster of samples in the 50 ha plot requires that spatial modeling be considered. OLS regression assumes independence of individual

observations (i.e. a non-spatial model). GLS regression on the other hand provides an opportunity to measure spatial autocorrelation by fitting a variogram to model results. Since the purpose of the predictive models is to use general associations trained in the 50 ha plot and expand them across the landscape and in different forest plots we opt to use non-spatial models (OLS) using variables informed by spatial models (GLS). Therefore testing a simple linear relationship in other locations is highly repeatable, easy to interpret and does not require the optimization of a spatial GLS model. OLS regression is the starting framework which can be expanded to include spatial effects as well modeling non-linear processes in future studies. The method to select remote sensing variables for the prediction models requires three separate steps. First, the pairwise OLS regression must account for a minimum 10% (r^2>0.10) of observed species richness to capture only the strongest associations amongst all remote sensing predictor variables. Second, the AIC score for three variograms (Exponential, Spherical, and Gaussian) is computed for each variable using GLS regression using the 'Linear and Nonlinear Mixed Effects Models' package (nlme). The model with the lowest AIC score is considered to be the 'optimal' GLS model. Lastly, the correlation coefficients for OLS and optimal GLS models for each predictor variable are compared. If the correlation coefficient changes sign, I consider that the variable has considerable differences between OLS and optimal GLS model outputs. This indicates that the residuals are highly spatially auto-correlated and therefore unfit for a non-spatial OLS prediction. In this way, models account for spatial autocorrelation in the non-spatial regression and increase repeatability of the methods.

Prediction Models of Species Richness

Based on the results of the OLS regression and optimized GLS regression models, variables are selected for the predictive models which characterized environmental heterogeneity in the imagery reflectance, the LiDAR derived canopy CHM and sub-canopy topography DSM. The variables selected were chosen because they characterized the hydrologic, topographic and light environments and could explain a minimum portion of the variance in tree richness in the FDP ($r^2 > 0.10$). At least one variable from the canopy reflectance, structure and topography variables were included in each predictive model. The threshold of $r^2 > 0.10$ was chosen to include only the strongest associations amongst all available variables. Multiple regression models with a maximum of four predictor variables were used to predict patterns of species richness across BCI. Depending on tree size class, different predictor variables were used for each model depending on model fit (Appendix 1.2). Terrain curvature was included in the predictive model due to known associations with the hydrologic network, forest structure and previously published correlations with species richness on BCI (Wolf et al. 2012, Detto et al. 2013). Using the 'predict' function in R, remote sensing variables are used to make predictive maps across the landscape at 1 ha spatial scale for each tree size class. The specific variables used for each tree size prediction change depending on their relative importance in each tree size class. Predictions for BCI were made across the island by creating a grid of 1 ha cells that align with the 50 ha plot but extend to the margins of the island. Cells which cross the margin of the island boundary are excluded so that only 1 ha cells which fall completely inside the island boundary are included in predictions. Both Quickbird and LiDAR derived variables were extracted to the common 1 ha grid where no ground census data were available. Using the remote sensing predictor values the multivariate OLS regression equations were applied to estimate how many tree species were present in each 1 ha cell across BCI. There is a small gap

(15 ha) in coverage where a cloud and shadow are present in the satellite image on the western edge of BCI, which is subsequently omitted from the predictive maps. Each environmental variable is computed for each hectare of forest on BCI using ArcGIS 10.2 and the OLS models are applied in R to predict the number of tree species in each hectare. Model predictions from OLS and GLS model predictions are generally very similar and the difference between spatial and non-spatial model predictions never exceed 2 species/ha. The results of the models are a 1 ha scale prediction of tree species richness for the whole island at every tree size class.

RESULTS

The 2010 census included 204,757 individuals in the 50 ha plot (4,095 ± 46 individuals per ha, mean ± S.E.) belonging to 301 species (166 ± 1.5 species per ha, mean ± SE) of freestanding woody plants. Species richness varied based on tree size in the 50 ha plot (Table 1.1). Small stems < 10 cm dbh composed the largest proportion of variation in tree species richness. In the largest subplot size (1 ha), stem density (stems/ha) alone can explain minimal variation in species richness per subplot ($r^2 = 0.08$, $P < 0.042$) (Table 1.2), but as plot size decreases stem density can explain increasingly more variance in tree richness (0.25 ha $r^2 = 0.21$, $P < 0.001$, 0.04 ha $r^2 = 0.34$, $P < 0.001$). Basal area was inversely correlated with species richness amongst all stems at 1 ha in the 50 ha plot ($r^2 = 0.25$, $P < 0.001$).

Species richness and remote sensing metrics

Remote sensing measurements of variability in canopy reflectance, forest structure, and micro-topography were positively associated with species richness but the relationships were highly scale dependent (Table 1.2). OLS regression correlation coefficients for remote sensing predictor variables were the highest at the 1 ha spatial scale and decreased as subplot size

decreased in nearly all cases. In relation to all stem sizes, the correlation coefficients between species richness and remote sensing predictor variables were higher for stems <10 cm dbh and lower for stems >10 and >20 cm (Table 1.2 and Appendix 1.3). The strongest associations of the remote sensing predictor variables were the standard deviation of variables such as EVI, TWI, mean canopy height and terrain concavity. Generally, the mean values of the same metrics were less correlated with tree species richness across spatial scales (Table 1.2, Appendix 1.3).

Predictive models of tree species richness

The strongest statistical associations were used for the predictive models at the 1 ha spatial scale (Figure 1.5). Although the study included three spatial scales in the analysis to test the effects of subplot size, model fits were lower ($r^2 < 0.13$, $P < 0.001$) at the 0.25 ha scale and nearly uncorrelated at the 0.04 ha scale ($r^2 < 0.04$, $P < 0.001$). The variables used to model species richness amongst all tree size classes were the standard deviation of mean canopy height, standard deviation of EVI, standard deviation of TWI, and mean terrain curvature (Appendix 1.4). The different characterizations of environmental heterogeneity and terrain curvature were used to make three OLS prediction models of species richness across BCI for three tree size classes based on the 50 ha plot (Figure 1.6). The models could predict variation in tree species richness amongst all stems (adjusted $r^2 = 0.35$) and trees >10 cm dbh (adjusted $r^2 = 0.25$). However, the best model results were for understory trees and shrubs (1 to 10 cm dbh) (adjusted $r^2 = 0.52$). The results of the predictive models indicate that high spatial resolution remote sensing can explain the up to half of variation in tree species richness amongst smaller and medium tree sizes classes across a tropical landscape.

DISCUSSION

Tree size and spatial scale

The results indicate that tree size and spatial scale of analysis provides significantly different results that should be considered when mapping species richness across tropical forest landscapes. Explanations of variation in species richness were much lower amongst large canopy trees and at fine spatial scales, meaning similar predictions should not be made for large trees (>20 cm dbh) or at subplot sizes smaller than 1 ha. The analysis highlights two important findings and two limitations regarding tree size and spatial scale. The first finding is that such models are not reliable or informative at the finest spatial scale (0.04 ha) due to small stem counts per plot, the models are possibly informative at the mid-scale (0.25 ha), and potentially useful at the coarsest spatial scale (1.0 ha). The second finding is that including all tree size classes (>1 cm dbh) at the coarsest spatial scale is optimal for prediction and models are not informative for only larger tree size classes (>10-20+ cm dbh). The first limitation is that Quickbird imagery cannot resolve differences in spectral/structural characteristics and that airborne LiDAR may be more appropriate for such predictive modeling. Higher spectral and spatial resolution imagery may be necessary to characterize large tree canopy chemistry, because the canopy structural signal using this sensor is strong. The second limitation is that the 1 ha spatial scale may be useful when all stems are analyzed, however to expand the study to analyze only the largest canopy trees (>10 cm dbh), a larger geographic area and a coarser plot scale is necessary (Appendix 1.3).

Species richness and canopy reflectance

It was expected that Quickbird derived spectral variables associated with mean productivity would be correlated with tree species richness, however the standard deviations had stronger statistical associations than mean values at the 1 ha spatial scale. Currently, individual crown level analysis is difficult for all but the largest trees (> 1 m dbh) from spaceborne platforms (Clark et al. 2004). The strength of simple vegetation indices to predict species richness from high spatial resolution (2.4 m) satellite imagery as compared to high spectral resolution has interesting implications for modeling biodiversity across remote landscapes in the tropics. Simple indices derived from high-resolution satellite imagery may provide some utility for making predictions of species richness at coarse spatial scales across the landscape. In 4-band imagery, differences in canopy reflectance and upper canopy structure are virtually indistinguishable and the spectral resolution of this sensor is too coarse to decouple the structural signal (i.e. gaps and shadows) from variation in spectral signal. Quickbird is therefore is not appropriate for analyzing variance in canopy chemistry. Higher spatial and spectral resolution sensors such as the Carnegie Airborne Observatory (Asner et al. 2007) are necessary for such chemical characterizations at the tree or subplot scale. However, in the absence of airborne LiDAR/imagery, satellite imagery may help characterize the structural heterogeneity and gap fraction across landscape scales. Although simple Quickbird derived vegetation indices (EVI/NDVI/RVI) may provide some utility to predict species richness, the standard deviation in these indices or the image texture was more strongly associated with increased tree richness. This result confirms that the structural signal cannot be de-coupled from the spectral signal at this resolution (spatial and spectral).

Currently, high spatial resolution LiDAR measurements of forest structure do not exist across the pan-tropics, therefore readily available high-spatial resolution imagery must be used to

help set baseline assessments of alpha diversity to achieve international Aichi biodiversity targets. As new spaceborne LiDAR sensors become operational and airborne LiDAR coverage in tropical forest expands in the next decade, widespread prediction of alpha diversity leveraging structural information from LiDAR will become a reality. Such predictions which can explain 50% in the variance in forest richness may be valuable to conservation planners looking to maximize biodiversity value per unit area and may offer useful predictions of alpha diversity trained using forest census plot data. Models utilizing only canopy reflectance from satellite imagery rarely explain over 20% of the variance in species richness, highlighting the need for additional three-dimensional LiDAR measurements. These results do confirm suggestions that spectral indices will improve estimates of species richness as the spatial scale of the study increases from a 1 ha plot to 50 ha plot and across the landscape (Bawa et al. 2002, Feeley et al. 2005, Gillespie 2005, Cayuela et al. 2006).

Species richness and canopy structure

Airborne LiDAR was an effective tool for measuring the characteristics of forest structure and biophysical properties of tropical forest environments at high spatial resolutions (Lefsky et al. 2002, Tang et al. 2012). Environmental heterogeneity in the canopy was positively correlated with species richness amongst the small and medium size trees but becomes de-correlated with progressively larger tree size classes. Species richness was generally highest in open canopy and medium stature forest where trees can exist in higher densities. Large trees (> 20 cm dbh) appear to reduce diversity under their large canopies and trunks. However, variability in the height of the upper canopy had the strongest correlation with species richness. Increased variability in upper canopy height was associated with increased species richness across spatial

scales and was the strongest predictive canopy structure variable (r^2=0.15, P = 0.0048), suggesting that a heterogeneous light environment (greater light availability in the understory) is capable of supporting a greater variety of tree species. These metrics can easily be calculated and applied to LiDAR datasets for tropical forest landscape to estimate species richness for different tree size classes. Careful consideration should be given to LiDAR point density as measurements of gap fraction and understory vegetation is highly dependent on average LiDAR point density and sufficient penetration through the canopy profile. Generally, higher average point densities will yield a more complete characterization of the mid/understory layers of vegetation as well as a more accurate sub-canopy DSM.

Species richness and micro-topography

The variability in the TWI had the highest correlation with increased species richness amongst all stems in the 50 ha FDP (1 ha scale). This result suggests that sub-plots including heterogeneous hydrologic environment can support a higher variety of tree species due to partitioning of water resources. Concave up curvature (i.e. valleys), average slope, and variability in slope were all positively correlated with species richness across spatial scales. These results confirm previous research which report slope and curvature both have statistical associations to species richness amongst all stems at the 1 ha scale. (Wolf et al. 2012) found these micro-topography effects on species richness to be highly dependent on spatial scale and this study shows that topography may be more important for the small tree sizes as the statistical associations weaken or disappear when considering only medium and large (>10 cm dbh) canopy trees. A potential explanation for increase seedling diversity on sloped terrain is that steep slopes may be too unstable for large trees which would mean those areas are subject to a more rapidly

cycling disturbance regime and a higher proportion of tree fall gaps (Lobo and Dalling 2013). Upward concave terrain curvature is positively correlated to species richness indicating the hydrologic controls may be important to structuring the forest environment. (Detto et al. 2013) found that mean canopy height was correlated with terrain curvature and Laplacian convexity, pointing to topographic and hydrologic controls over forest structure. Habitat suitability models using LiDAR derived DSM in Hawaii found that topographic depressions protected species from prevailing winds and improve the survival of planted individuals. Plant height and nutrient content were greater in high suitability areas indicating topographic control over plant physiology (Questad et al. 2014).

It should be noted that these effects of micro-topography may be influenced by forest age more than some underlying topographic control. The landscape across BCI is more topographically variable compared to the 50 ha plot which is located on a plateau composed primarily of old growth forest. These results should be tested over across BCI (i.e. in younger and more topographically variable locations) and other 50 ha plots to test whether the associations found in this study hold across the landscape and in different forest types. Also, since the TWI takes the contributing upslope area into consideration it may be a better estimate of water availability compared to lower order elevation derivatives like slope and curvature. Further exploration into the relationship between the hydrologic network and species richness and forest structure is necessary as many of the wetness indices are highly influenced by the algorithms used to derive overland flow accumulation (Sørensen 2006).

Ecological applications and limitations

Combining spectral and LiDAR remote sensing metrics can predict between 25% and 50% of the total variance in tree species richness across a Panamanian tropical moist forest landscape. In particular, spectral and LiDAR remote sensing identifies species diversity of shrubs and small trees in the understory and the next generation of canopy trees that make up a majority of tree diversity on Barro Colorado Island (Croat 1978). Chance, land use history, disturbance, soil nutrient properties, and micro-fungal communities may explain the remaining proportions of the variance in tree species richness for all stems and different tree size classes (Hubbell et al. 1999, Keith et al. 2009). However, these variables are difficult to quantity with space and airborne remote sensors. This study focused on a relatively undisturbed and well-protected tropical forest with high diversity and low variation in species richness. We would expect spectral and LiDAR metrics to explain higher proportions of variation in tree species richness across gradients of anthropogenic disturbance, such as logging, fire, grazing, which can be common in tropical forests and generally results in reduced stem diversity in the understory.

These results should be interpreted with cautious optimism. This study has shown that using airborne LiDAR and satellite imagery, approximately 50% of tree alpha diversity can be mapped across the landscape. Using associations observed in forest plots, remote sensing is used to extend predictions over the local landscape to predict local patterns of alpha diversity. In order to achieve international goals of conserving and studying biodiversity, baseline estimates need to be set for tropical forest diversity from the plot to the landscape scale. Large forest census plots are the logical points to start for such modeling and the associations found in the 50 ha plot on BCI should be tested at other large plots across forest types (Condit et al. 1996). These results suggest that while airborne LiDAR remote sensing may be more effective when studying the plot

scale (< 50 ha), satellite imagery still may provide some utility in mapping tree alpha diversity and should be explored in future studies.

The importance of large trees is well known in biomass studies (Keith et al. 2009), but associations between remote sensing variables and tree species richness in stems larger than 20 cm dbh were unclear. The main reason associations remain unidentified at the largest tree sizes (>20 cm) is because of the low stems numbers at the scale being analyzed (1.0 ha). This is a numerical and scale dependent limitation of the tree plot data, not necessarily the scale of the remote sensing data being used. To repeat the methods and model species richness amongst only the largest canopy trees, a larger geographic would need to be censused in the field with the same taxonomic accuracy as the 50 ha plot. In order of importance, the most challenging issues with the spatial extrapolation of such a framework to be the lack of precise taxonomic plot data, lack of high-resolution LiDAR to measure canopy structure and topography at fine scales and difficulties in mosaicking high-resolution satellite imagery in the moist tropics. If such methods were scaled up to include large mosaics of satellite images, substantial satellite geometry reflectance corrections would be necessary when interpreting the canopy conditions from space (Morton et al. 2014).

Future research

The results of the study lead to recommendations for future work analyzing tree species richness using high resolution remote sensing. Using airborne hyperspectral remote sensing, individual large canopy trees can be characterized in terms of their species-specific foliar chemistry at spectral and spatial resolutions that are currently unattainable from space (Asner and Martin 2008b, Asner et al. 2011). The four-band Quickbird imagery provides a coarse

spectral resolution characterization of the forest, however this framework could be applied using higher spatial/spectral remote sensing and improve the predictions for large canopy trees through a more comprehensive view of canopy chemistry and structure. More sophisticated methods to quantify the fluvial environment should be tested to explore whether patterns of species richness are spatially structured around the hydrologic network. The tropical rainforest exists under a dynamic hydrologic regime and field tests of wetness indices like the TWI should be implemented in dynamic studies of both the wet and dry seasons to examine the validity of such derived indices. Soil water availability will vary throughout the year in forests with a distinct dry season and models should be developed which help capture this variance. Exploring the details of the micro-topography variables such as directional curvature (parallel and perpendicular to slope) may be an interesting direction for future research as well as investigating the topographic depressions which may provide high suitability for a greater range of tree species.

Plants richness should also be analyzed by guild (growth form) to determine whether smaller understory shrubs, trees and lianas partition resources (light, water) differently than mid-story or upper canopy trees. Finally, LiDAR and imagery over plot data is needed to study alpha diversity in different common anthropogenic disturbance regimes. Such an analysis would require the methods be extended to dynamic data sets to monitor change over time to model niche, dispersal and disturbance through space and time. Implementing a verified stakeholder requirement to test predictions is the first step in creating a monitoring and verification system comprising a baseline estimate of alpha diversity at high spatial resolution. A spatially explicit map of alpha tree diversity in the tropics is critical to understanding how species shift their ranges spatially and temporally (beta diversity). Achieving international biodiversity targets by 2020 is predicated upon having reliable baseline estimates of forest diversity across the forest

landscape. Such a baseline will not be possible unless there is a collective implementation of ground based landscape scale stem mapping which should be collected in concert with high resolution remote sensing. Using future plot data and high-resolution remote sensing, similar methods could be used to study regional patterns of beta diversity, particularly in a changing climate.

CONCLUSION

This study has shown that high resolution satellite imagery and airborne LiDAR data can explain nearly half of the variation in tree species richness at 1 ha spatial scales in the moist forests of central Panama. Associations between tree species richness and remotely sensed characterizations of environmental heterogeneity, three-dimensional vertical forest structure and topography can be used to predict species richness across the landscape. High resolution remote sensing can explain variance in tree richness at the census plot spatial scale, particularly amongst shrubs, small and medium sized trees, however the results were in conclusive for the largest canopy trees. This study presents a multi-scale framework that can be applied to existing and new forest vegetation plots. This framework utilizing census plot data, high resolution satellite imagery and airborne LiDAR data can explain about half of the variation in tree species richness at 1 ha spatial scales in the moist forests of central Panama, however little is known about how these predictions might perform outside the island, the isthmus or across the region. For such predictions of tree species richness to be useful, extensive field plots must be added to cross-validate and improve current estimates. This study has shown high resolution remote sensing can be used to make predictions at the landscape scale and may provide a methodological framework for studying tropical tree ecology beyond existing forest plot boundaries.

Section 1.2: FIGURES

FIGURE LEGENDS

Figure 1.1. The 50-hectare forest dynamics plot over the LiDAR derived 1 m canopy height image (a), Barro Colorado Island including forest plot data over the LiDAR derived digital elevation hillshade model (b), the study area in the Panama Canal Zone over a 90 m digital elevation hillshade model (c).

Figure 1.2. Quickbird true color high spatial resolution satellite image for two different spatial scales: full plot (top) and the south-eastern section zoomed in on 1 ha plots (outlined in yellow) boundaries (bottom).

Figure 1.3. Four vertical cross sections (10 m depth) of the forest inside the 50 ha plot showing Coefficient of Variation (CV) in forest structure. The CV is the ratio of the standard deviation over the mean and defined as $CV = (\sigma/\mu)$. Low CV scores indicate a low variation in upper canopy height and a high average canopy height (upper-left, -2 sigma) while a high CV score indicate a higher variation in upper canopy height and low average canopy height (lower-right, +2 sigma).

Figure 1.4. Topographic Wetness Index at two spatial scales, full plot (left) and zoomed view of the swamp area (right). Darker shades of blue indicate higher wetness index values.

Figure 1.5. Pairwise ordinary least squares (grey line) and generalized least squares (black line) regression results for important spectral and LiDAR metrics. R-squared and P-values are the results of the ordinary least squares regression. Plots are colored by forest age: darker green = older forest, light green = old forest and secondary, yellow green = secondary).

Figure 1.6. OLS linear model predictions of tree diversity across BCI for different tree size classes. Plots are colored in 5 equal intervals varying based on tree size class:

Figure 1.1.

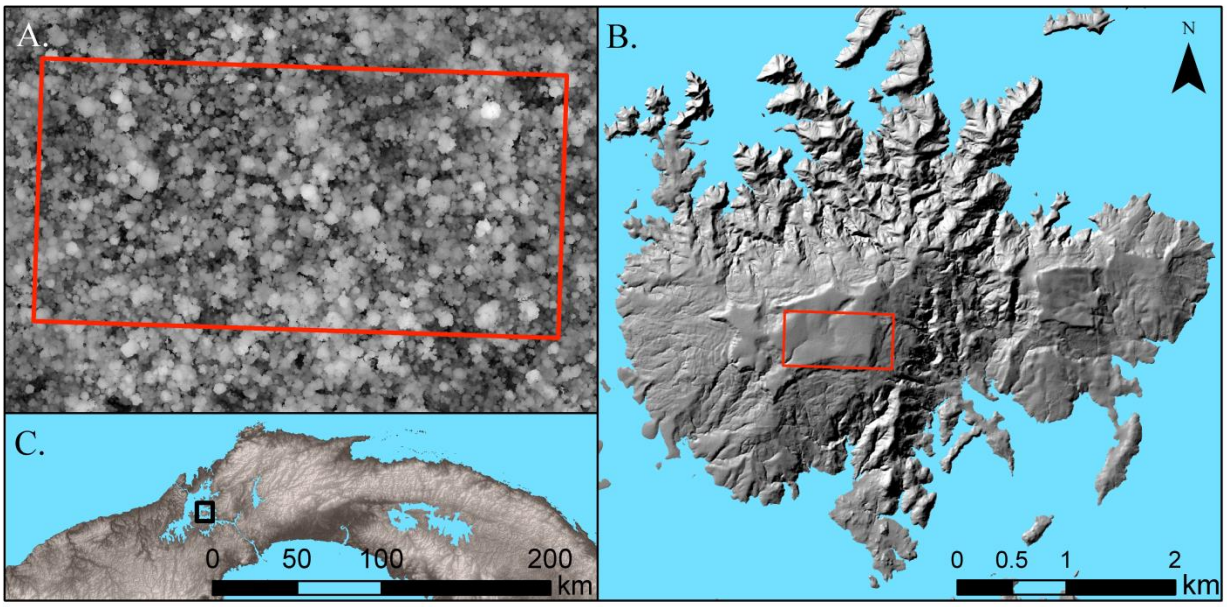

Figure 1.2.

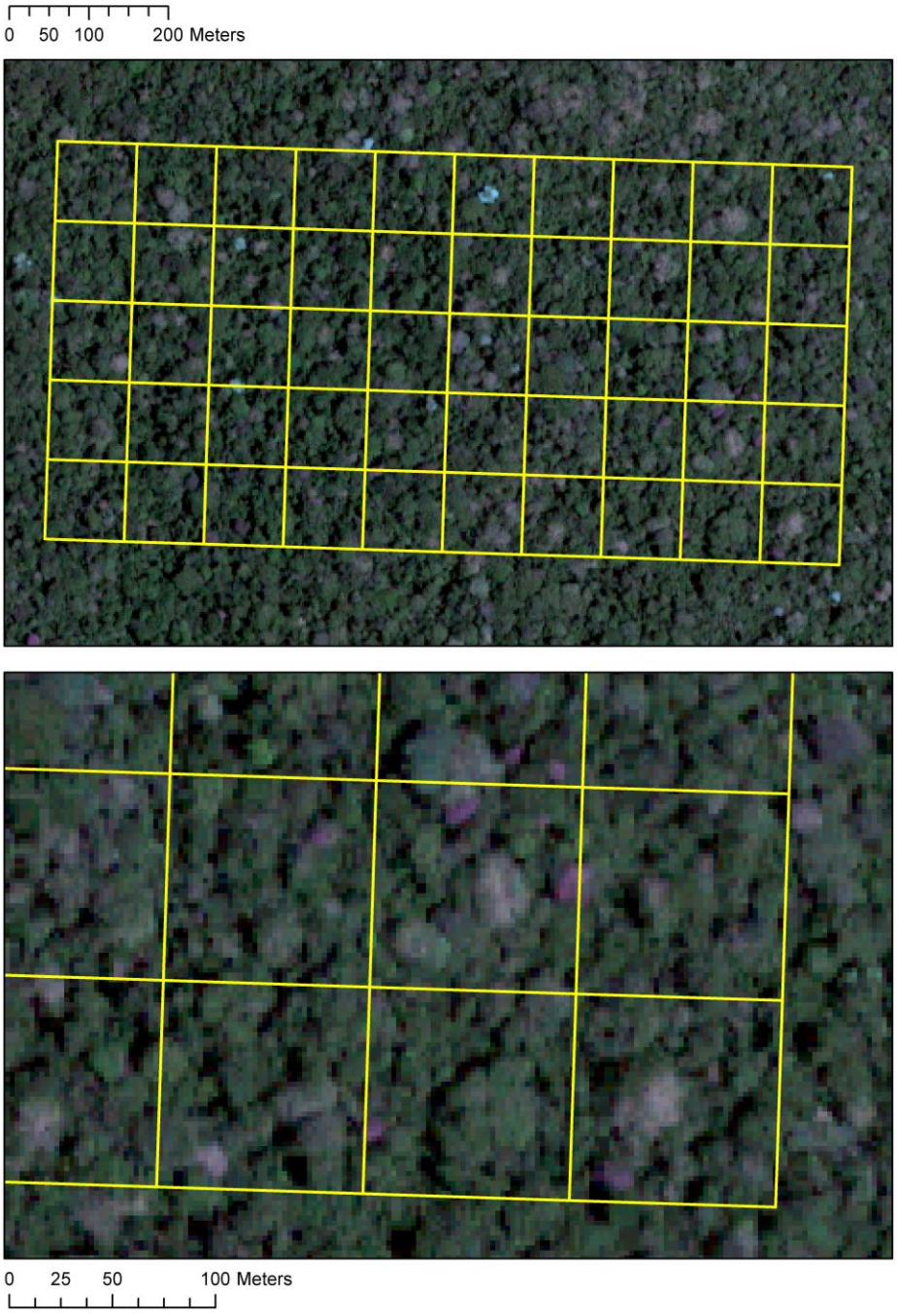

Figure 1.3.

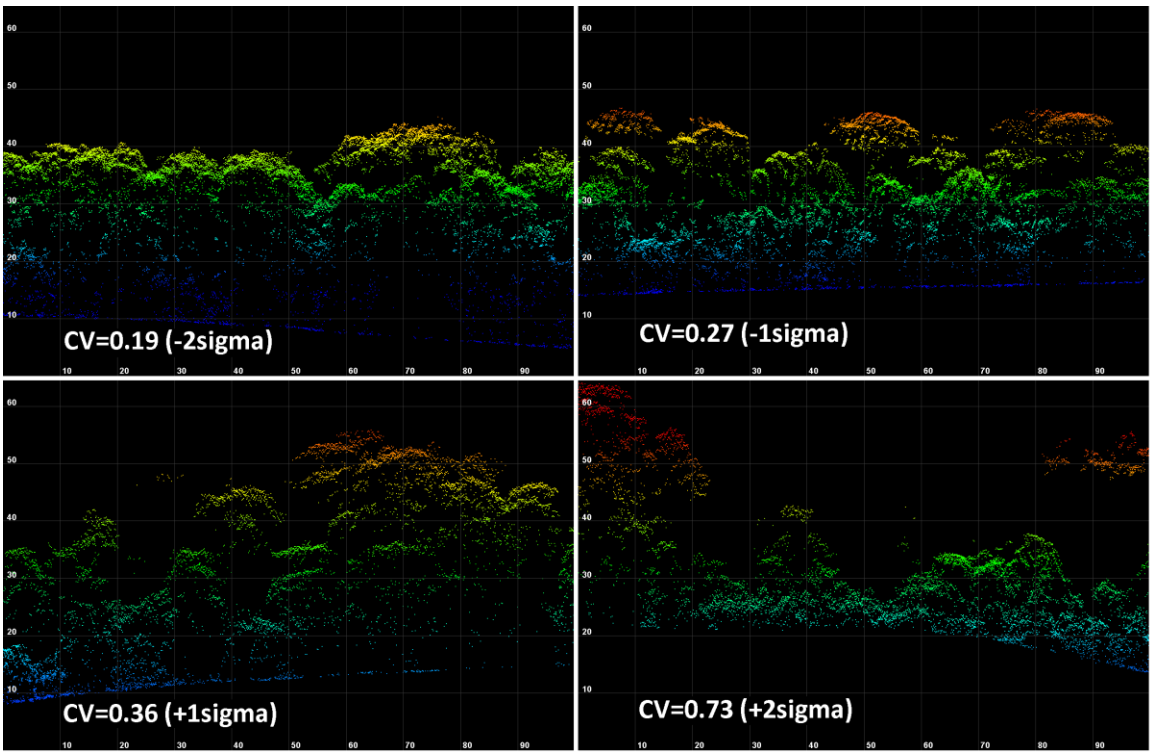

Figure 1.4.

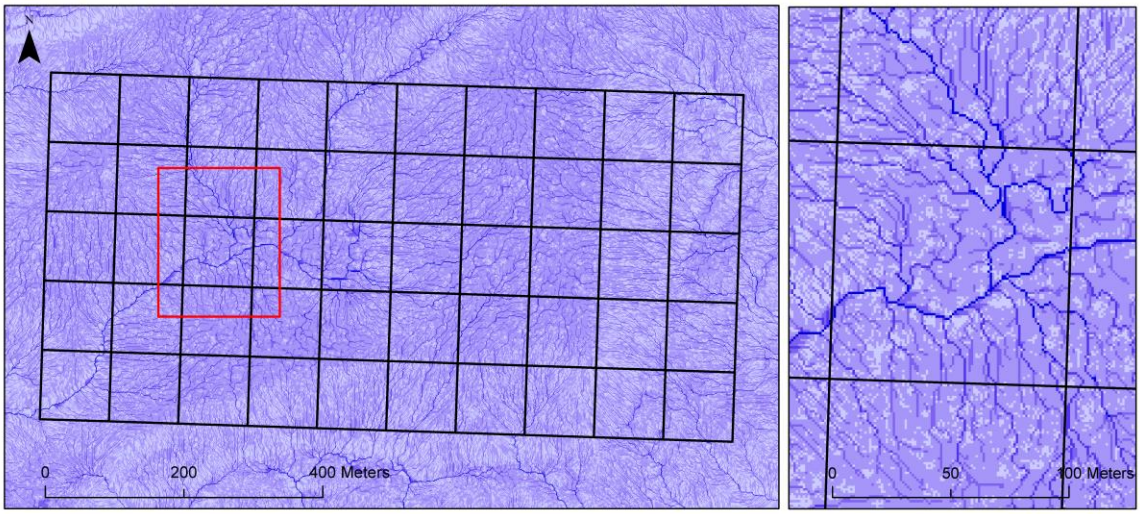

Figure 1.5.

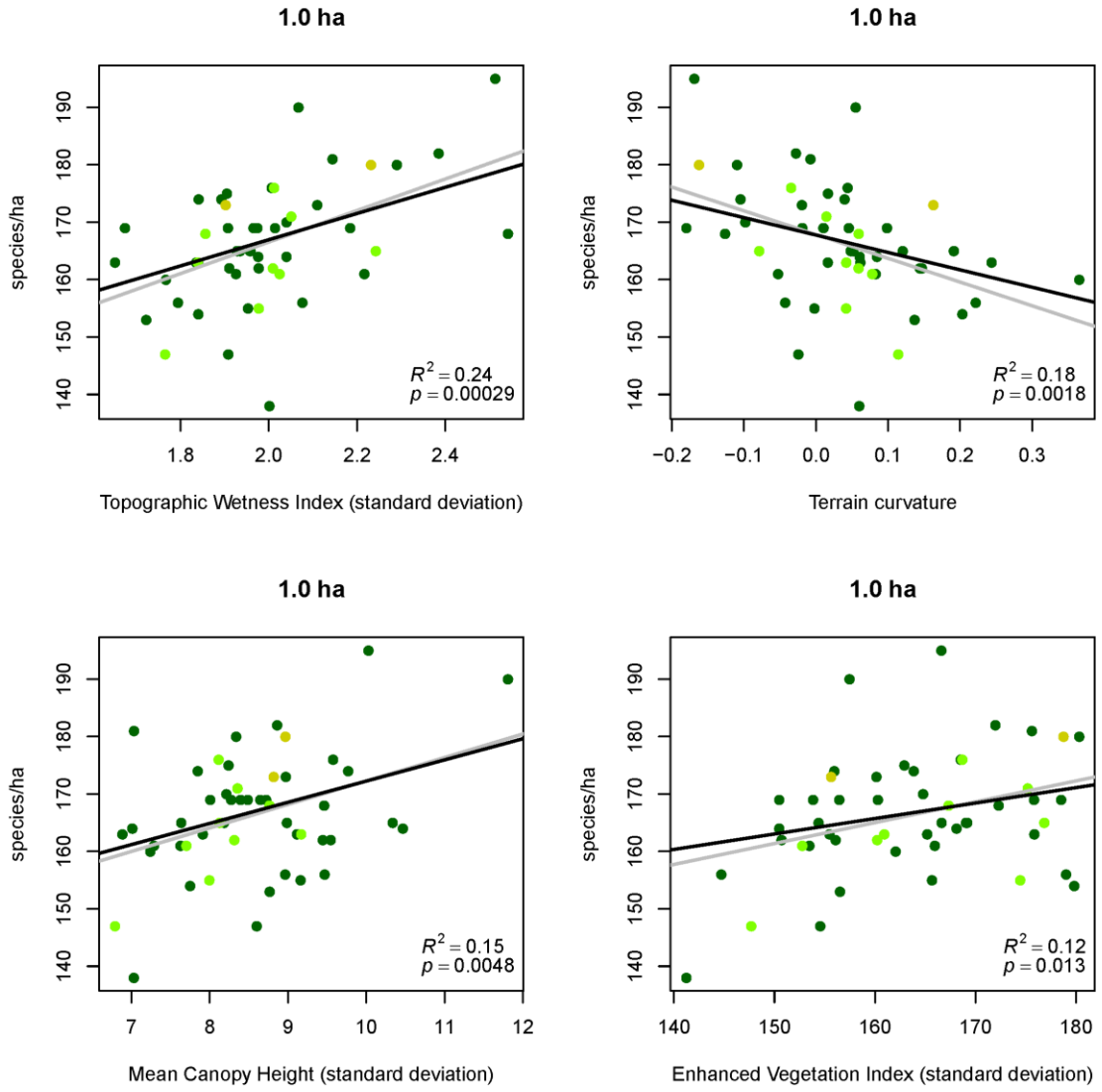
1.0 ha
species/ha
140
150
160
170
180
190
1.8
2.0
2.2
2.4
Topographic Wetness Index (standard deviation)
$R^2 = 0.24$
$p = 0.00029$
1.0 ha
species/ha
−0.2
−0.1
0.0
0.1
0.2
0.3
Terrain curvature
$R^2 = 0.18$
$p = 0.0018$
1.0 ha
species/ha
7
8
9
10
11
12
Mean Canopy Height (standard deviation)
$R^2 = 0.15$
$p = 0.0048$
1.0 ha
species/ha
140
150
160
170
180
Enhanced Vegetation Index (standard deviation)
$R^2 = 0.12$
$p = 0.013$

Figure 1.6.

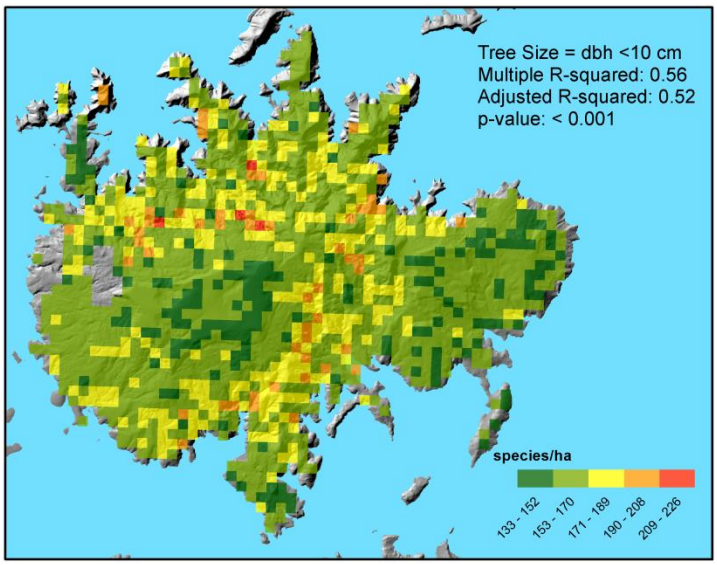
Tree Size = dbh <10 cm
Multiple R-squared: 0.56
Adjusted R-squared: 0.52
p-value: < 0.001
species/ha
133 - 152
153 - 170
171 - 189
190 - 208
209 - 226

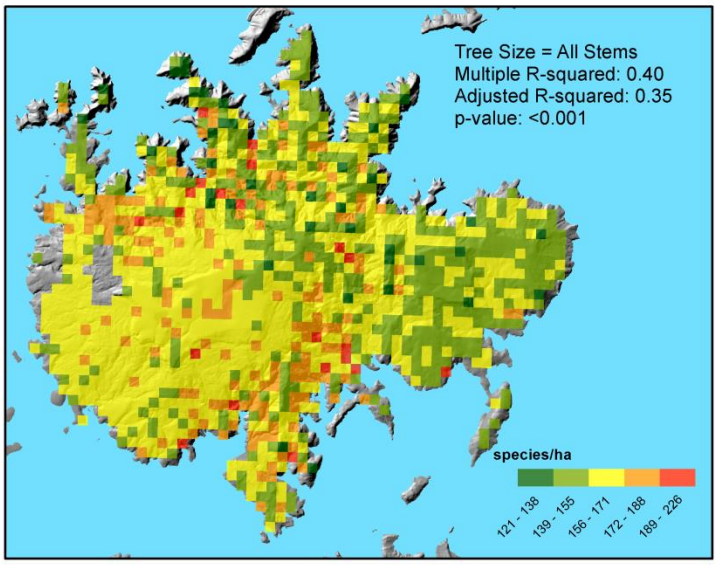
Tree Size = All Stems
Multiple R-squared: 0.40
Adjusted R-squared: 0.35
p-value: <0.001
species/ha
121 - 138
139 - 155
156 - 171
172 - 188
189 - 226

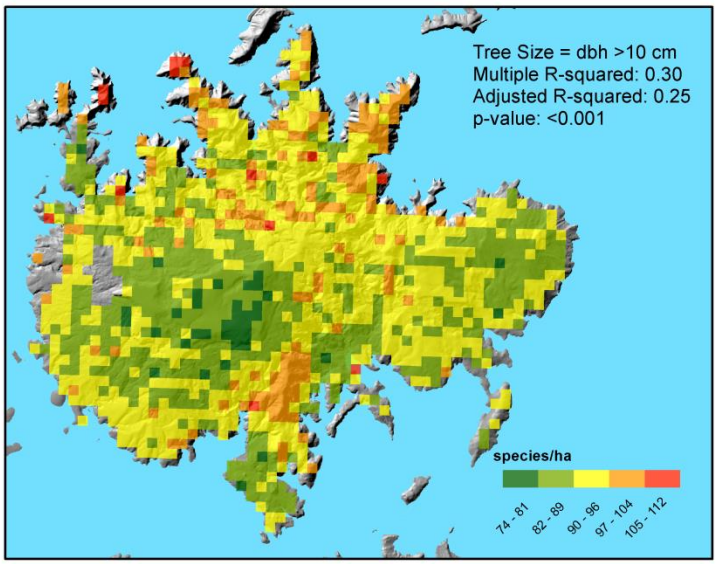
Tree Size = dbh >10 cm
Multiple R-squared: 0.30
Adjusted R-squared: 0.25
p-value: <0.001
species/ha
74 - 81
82 - 89
90 - 96
97 - 104
105 - 112

Section 1.3: TABLES

Table 1.1. The number of species, stems, stem density and average dbh in each tree size class. Table includes pre-processing results of stems and species present as well as average size in diameter in each class.

Description	Size min (cm)	Size max (cm)	Tree species	Stems	Stems/ha	Mean dbh (cm)
All stems	1	+	301	204,759	4,095	4.7
Understory trees and shrubs	1	10	290	186,202	3,724	2.8
Medium to large canopy trees	10	+	217	18,914	378	22.8
Large canopy trees	20	+	174	7,216	144	37.9

Table 1.2. Ordinary least squares Pearson's product moment correlation coefficient (r) and corresponding r^2 value between species richness (all stems) per subplot and the remote sensing predictor variables at each spatial scale.

	Pearson's r			r^2		
	1-ha	0.25 ha	0.04 ha	1 ha	0.25 ha	0.04 ha
			Plot variables			
Stems	**0.29**	**0.46**	**0.59**	**0.08**	**0.21**	**0.34**
Basal area	**-0.50**	**-0.29**	**-0.07**	**0.25**	**0.08**	**0.01**
			Remote sensing variables			
			Canopy Structure			
Canopy height	**-0.30**	**-0.30**	**-0.19**	**0.09**	**0.09**	**0.04**
Canopy height sd*	**0.39**	**0.28**	**0.19**	**0.15**	**0.08**	**0.04**
Image texture	0.08	**0.16**	**0.09**	0.01	**0.02**	**0.01**
			Canopy Reflectance			
EVI	0.03	0.01	**-0.06**	0.00	0.00	**0.00**
EVI sd*	**0.35**	**0.23**	**0.08**	**0.12**	**0.05**	**0.01**
NDVI	0.11	0.03	-0.04	0.01	0.00	0.00
NDVI sd	-0.11	-0.03	0.04	0.01	0.00	0.00
RVI	**0.30**	**0.16**	0.01	**0.09**	**0.03**	0.00
RVI sd	**0.36**	**0.22**	**0.07**	**0.13**	**0.05**	**0.00**
PC 1 sd	**0.34**	**0.24**	**0.08**	**0.12**	**0.06**	**0.01**
			Micro-Topography			
Aspect	0.23	-0.03	0.03	0.05	0.00	0.00
Aspect sd	0.06	0.03	-0.02	0.00	0.00	0.00
Curvature*	**-0.43**	-0.05	0.05	**0.18**	0.00	0.00
Curvature sd	**0.38**	**0.36**	**0.27**	**0.14**	**0.13**	**0.07**
TWI	-0.10	**-0.26**	**-0.29**	0.01	**0.07**	**0.08**
TWI sd*	**0.49**	0.10	-0.05	**0.24**	0.01	0.00
Slope	0.18	**0.28**	**0.27**	0.03	**0.08**	**0.07**
Slope sd	0.26	**0.25**	**0.25**	0.07	**0.06**	**0.06**

* included in the predictive model (1-ha)

Bold = p-value < 0.05

sd=standard deviation

Section 1.4: APPENDICES

Appendix 1.1. A full description of remote sensing pre-processing

Imagery preprocessing

All imagery pre-processing was performed in ArcGIS 10.2 and ENVI 4.8/5. A single Quickbird (QB) satellite image scene was used to calculate canopy reflectance indices for all vegetation plots on BCI. Atmospheric correction was applied using the FLAASH correction tool in ENVI-5.0. The QB satellite imagery was used to calculate the Ratio Vegetation Index (RVI), the Normalized Difference Vegetation Index (NDVI), and Enhanced Vegetation Index (EVI) in ENVI and spectral heterogeneity was calculated using a principle components analysis in ArcGIS. To calculate spectral heterogeneity we clipped the image to the vegetation plots so no water or clouds were included in the imagery. Using the clipped imagery, we applied a principal components analysis (PCA) to the satellite imagery to compute a 4-band principle component image. We found that >96 % of the spectral variation was composed in the first principle component, and focused the spectral heterogeneity calculation on only that first principle component. We also used 'two-dimensional' spectral variability using the second principal component; however the results were qualitatively similar and were not reported in the final results. The standard deviation of the pixels in the first band of the principle component, compose the spectral heterogeneity for each vegetation sub-plot and were highly correlated to the standard deviation of the EVI (r=0.91). The Quickbird variance in imagery texture was calculated from the panchromatic (0.6 m resolution) using a 3 x 3 window in ENVI. We investigated additional spectral indices which were not included in the final analysis. For

instance we calculated mean values of pairwise Euclidean distance (MED) and distances from the mass centroid (MCD) as indicators of spectral heterogeneity (in two spectral dimensions) (Rocchini et al. 2004b).

LiDAR preprocessing

The remote sensing data with the highest spatial accuracy and precision is the LiDAR data collected by Blom Corporation and Northrup Grumman over BCNM. These data were collected during the wet season between August 15th 2009 and September 10th 2009 during eleven flights by a fixed-wing aircraft equipped with an Optech 3100 (Optech, Vaughan, ON, Canada) system capable of four returns per pulse. The mean flying height was 457.2 m and mean flight speed was 66.9 m/second. The system operated at a scan angle of 17°, using a scanning frequency of 48 Hz and laser frequency of 70 KHz. All flights produced a total of > 233 million laser shots and > 528 million individual data points, resulting in a point density of 5.6 points per square meter (ppm^2) and 8.1 returns per square meter (rpm^2). We used a 1 m digital surface model (DSM) and 1 m digital canopy surface model (DCSM) (Figure 1.1). The DSM and DCSM were created by Blom Corp. who calibrated and filtered unprocessed LiDAR data using Bentley's Microstation (Bently, Exton, PA) and then manually edited the product to make a bare-earth DSM. Blom Corp. verified vertical accuracy of the DSM using 36 Differential GPS survey points in flat open areas around the island. The average error in height between the ground survey points and the DSM was 6.9 cm with RMSE value of 7.6 cm. Blom Corp. produced the DCSM from the point of highest return above each cell on a 1-m grid. We compared the DCSM to ground-based canopy height measurements from 2009 that were collected every 5 m across the entire 50-ha plot (Hubbell et al. 1999), which were in general agreement with the 1 m

DCSM. No additional efforts were made to minimize artifacts where understory vegetation may present commission errors in the ground point classification. In addition to a classified point cloud, the LiDAR data also provides an un-calibrated intensity value as well as the return type. Possible return types include only return, first of many, intermediate of many or last of many returns. The return type and intensity information is used in the calculation of the canopy/gap fraction statistics.

In addition to the mean canopy height and the standard deviation of canopy height we also tried additional methods to quantify vertical forest structure. Relative height metrics (rh25/rh50/rh75) were calculated which measured relative canopy distribution throughout the vertical canopy profile. Additionally, canopy closure/canopy fraction with four different methods were computed approximating light penetration using LiDAR return ratios (first/last/intermediate), LiDAR classification (canopy/ground/all) and LiDAR intensity following a study by (Hopkinson and Chasmer 2009). We found these measurements of forest structure did not yield stronger associations with the response variables and were slightly more difficult to interpret from an ecological point of view. The mean canopy height and standard deviation of canopy height within a singular forest plot are much easier to interpret and likely to be repeated. Three dimensional LiDAR point cloud profiles from four 10 x 100 m horizontal transects to illustrate the coefficient of variation (CV) in the standard deviation of maximum canopy height (main text Figure 1.3). Transects were selected based on the CV for the LiDAR derived maximum canopy height variable. CV = Standard deviation of max canopy height/average canopy height. CV values were selected to represent the statistical distribution of values (1 sigma and 2 sigma+) on both sides of the distribution. Each grid cell represents 10 m of vertical and horizontal change.

Appendix 1.2. Statistical Analysis

Ordinary Least Squares, Generalized Least Squares and cross-validation

Non-spatial Ordinary Least Squares (OLS) regression was used for modelling tree species richness across the landscape, however we also performed Generalized Least Squares (GLS) spatial regression models to account for spatial autocorrelation. Predictive models were calculated in R using both OLS and GLS regression to observe the effects of non-spatial and spatial models. OLS modelled residual errors may be spatially autocorrelated and as such, a spatial (GLS) model is necessary to determine the effect of spatial autocorrelation in the predictions across the landscape. The purpose of the GLS modelling is to test spatial predictions against the OLS non-spatial predictions to determine whether an OLS model is inappropriate (i.e. no change in coefficient sign). If a predictor variable has a significantly different spatial and non-spatial prediction, it is not considered to be a good predictor. For the GLS models, three methods of fitting a parametric correlation function (Gaussian, Spherical, and Exponential) were tested for the residual co-variance matrix. The model with the lowest Akaike information criterion (AIC) score was selected for each remote sensing predictor variable. Variograms for each variable were created and 'Moran's I' was calculated to measure the spatial auto-correlation using an inverse distance weighted residual error matrix. Then multi-modeled inference was used to determine the optimal model using different combinations of the four remote sensing variables. Finally the models were cross-validated using 5-fold cross validation to train and test the data. The 'dredge' function was used in the multi-model inference library to judge the general importance of predictor variables and cross validate the results. The following list contains the statistical

package in R associated with each stage of analysis: GLS (nlme), Variogram (gstat), Moran's I (ape), Multi-model Inference (MuMIn).

Appendix 1.3. Pearsons's r, adjusted r-squared and p-values for the Ordinary Least Squares regression models for tree species richness 1 – 10 cm, ≥ 10 cm, ≥ 20 cm dbh.

	DBH 1-10 cm			DBH >10 cm			DBH > 20 cm		
	R	r-squared	p	r	r-squared	p	r	r-squared	p
Stems	0.423	0.162	**0.0022**	-0.137	-0.002	0.3427	-0.048	-0.018	0.7407
Basal area	0.303	0.073	**0.0322**	-0.566	0.306	**0.0000**	-0.154	0.003	0.2863
Canopy height	-0.367	0.117	**0.0087**	-0.439	0.176	**0.0014**	-0.075	-0.015	0.6058
Canopy height sd*	0.455	0.191	**0.0009**	0.022	-0.020	0.8805	0.168	0.008	0.2436
Image texture	0.165	0.007	0.2516	0.220	0.029	0.1244	0.021	-0.020	0.8828
EVI	0.150	0.002	0.2990	0.094	-0.012	0.5167	0.041	-0.019	0.7749
EVI sd*	0.316	0.081	**0.0254**	0.275	0.056	0.0536	0.160	0.005	0.2683
NDVI	0.159	0.005	0.2699	0.201	0.020	0.1626	0.145	0.001	0.3134
NDVI sd	-0.155	0.004	0.2824	-0.230	0.033	0.1075	-0.160	0.005	0.2676
RVI	0.337	0.095	**0.0167**	0.306	0.075	**0.0305**	0.073	-0.015	0.6126
RVI sd	0.279	0.059	**0.0494**	0.149	0.002	0.3013	0.099	-0.011	0.4937
PC 1 sd	0.371	0.120	**0.0080**	0.325	0.087	**0.0214**	0.161	0.006	0.2648
Aspect	0.140	-0.001	0.3333	0.163	0.006	0.2578	-0.148	0.002	0.3039
Aspect sd	0.107	-0.009	0.4607	-0.023	-0.020	0.8754	-0.077	-0.015	0.5962
Curvature*	-0.325	0.087	**0.0212**	-0.112	-0.008	0.4405	-0.077	-0.015	0.5953
Curvature sd	0.405	0.147	**0.0035**	0.162	0.006	0.2608	0.219	0.028	0.1263
TWI	-0.140	-0.001	0.3322	-0.120	-0.006	0.4080	-0.163	0.006	0.2594
TWI sd*	0.417	0.157	**0.0026**	0.117	-0.007	0.4166	0.120	-0.006	0.4078
Slope	0.192	0.017	0.1822	0.118	-0.007	0.4148	0.157	0.004	0.2777
Slope sd	0.289	0.065	**0.0416**	0.095	-0.012	0.5100	0.196	0.018	0.1735

Bold = p-values less than 0.05

Appendix 1.4. Ordinary Least Squares regression models for tree species richness predictions across BCI. Each OLS model is particular to the prediction map for each tree size class in Figure.1.6.

Small trees and shrubs (<10 cm)

	Estimate	Std. Error	t value	Pr(>|t|)
(Intercept)	109.6460	15.4984	7.0750	7.9e-09 ***
twi sd	17.0827	6.0136	2.8410	0.00674 **
mch sd	3.6476	1.1447	3.1860	0.00262 **
mch	-1.5906	0.3561	-4.4670	5.3e-05 ***
curv sd	1.0862	0.3923	2.7690	0.00814 **

Residual standard error: 7.541 on 45 degrees of freedom
Multiple R-squared: 0.5584
Adjusted R-squared: 0.5191
F-statistic: 14.23 on 4 and 45 DF
p-value: 1.40E-07

All Stems (>1 cm)

	Estimate	Std. Error	t value	Pr(>|t|)
(Intercept)	67.1419	26.5788	2.5260	0.0151 *
twi sd	13.1195	9.5722	1.3710	0.1773
curv	-16.2735	15.9501	-1.0200	0.3130
mch sd	3.1779	1.2378	2.5670	0.0136 *
evi sd	0.2843	0.1232	2.3080	0.0257 *

Residual standard error: 8.433 on 45 degrees of freedom
Multiple R-squared: 0.4034
Adjusted R-squared: 0.3504
F-statistic: 7.606 on 4 and 45 DF
p-value: 9.05E-05
Signif. codes: 0 '***' 0.001 '**' 0.01 '*' 0.05 '.' 0.1 ' ' 1

code	variable
mch	mean canopy height
mch sd	mean canopy height sd
curv	curvature
curv sd	curvature sd
twi sd	Topographic Wetness Index sd
slp	Terrain slope
evi sd	Enhanced Vegetation Index sd

Medium and large trees (>10 cm)

	Estimate	Std. Error	t value	Pr(>|t|)
(Intercept)	94.8818	19.8047	4.7910	1.77e-05 ***
mch	-1.1497	0.3225	-3.5640	0.000863 ***
evi sd	0.0757	0.0922	0.8210	0.4161
slp	0.8585	0.3328	2.5800	0.013143 *

Residual standard error: 5.794 on 46 degrees of freedom
Multiple R-squared: 0.3011
Adjusted R-squared: 0.2555
F-statistic: 6.604 on 3 and 46 DF
p-value: 0.00083

Linear model equations for each tree size

The following regression equations are the basis for the tree species richness prediction maps

Small Trees (1-10 cm dbh)

Species/ha = 17.0827 (twi sd) + 3.6476 (mch sd) + -1.5906 (mch) + 1.0862 (curv sd)

All Stems (> 1 cm dbh)

Species/ha = 13.1195 (twi sd) + 3.1779 (mch sd) + 0.2843 (evi sd) + -16.2735 (curv)

Medium and Large Trees (>10 cm dbh)

Species/ha = -1.14969 (mch) + 0.07570 (evi sd) + 0.85846 (slope)

CHAPTER 2

Section 2.1: Predicting spatial patterns of plant guild richness, density and basal area across gradients of water and light in a tropical forest

ABSTRACT

Local scale habitat heterogeneity in the form of topographic and edaphic variations impacts availability of resources in terms of water, light, and nutrients that shapes tropical tree communities. This study broadens its scope to include additional plant communities in the 50-ha forest dynamics plot on the Barro Colorado Island, Panama to capture the guild level patterns of richness, stem density, and basal area along the local scale gradients of light and moisture derived from airborne LiDAR (Light Detection and Ranging). The analysis first investigates whether variations of forest structure defining the light condition and topography relating to moisture gradients can predict community level diversity, density, and basal area. Then, the analysis investigates whether patterns of diversity, density and size within guilds coincided with community-level patterns or whether strong evidence for alternative responses to resource gradients occurs at the guild level. Lianas and trees > 1 cm in diameter and three-dimensional LiDAR structure at sub meter scales were used to perform the statistical and spatial analysis. Results show there is strong evidence of habitat filtering and that the plant guilds do respond differently to light and water resource gradients. When considering all plant species, richness and stem density were uncorrelated (r = -0.115, r = -0.128) with water availability at the 1.0 ha plot scale. When considering individual plant guilds, the density of shrubs and small understory trees were positively associated (r = 0.258, r = 0.661) with water availability while midstory and tall canopy tree species were negatively associated (r = -0.608, r = -0.622), suggesting a partitioning

of water resources by plant species of different freestanding guilds. For liana species, richness, density and basal area were negatively correlated (r = -0.671, r = -0.686, r = -0.758) with average canopy height, but not strongly associated with topographic metrics. Canopy trees and lianas predominately occur on opposite ends of the canopy height gradient with canopy trees occupying the tallest, densest plots in the forest while lianas have a strong spatial tendency towards large canopy gaps. This research takes a novel approach to analyzing plant species richness and density at the guild level. Observations indicate that plant guilds respond differently to water and light availability and that remote sensing has the ability to detect fine scale environmental gradients which can be used to predict the guild composition of plant communities across the landscape.

Keywords: plant guilds, alpha diversity, Barro Colorado Island, Forest Dynamics Plot, remote sensing, LiDAR

INTRODUCTION

Plants are subject to filtering along resource gradients of light and water in tropical forest environments (Kobe 1999, Kembel and Hubbell 2006). Habitat filtering refers to the non-random germination, establishment and survival of individuals with respect to variation in habitat characteristics (Baldeck et al. 2013a). Numerous studies have supported the importance of habitat filtering via variation in resource availability in tropical forests by documenting non-random patterns in tropical plant distributions and variation in community composition with respect to topographic, edaphic and light variation over local to landscape scales (Clark et al. 1998, Harms et al. 2001, Schnitzer and Bongers 2002, John et al. 2007, Dalling et al. 2012, Baldeck et al. 2013b). Research into the relationships between species richness, stem density, basal area and ecosystem function is motivated by interest in understanding ecological communities as well as a practical interest in managing and conserving ecosystem services (Schwartz et al. 2000, Srivastava and Vellend 2005). Among ecosystem services, carbon storage and biodiversity are particularly important in tropical forests as they contain more than 70% of carbon in global live forests, and over 50% of total terrestrial biodiversity (Wilson 1988, Pan et al. 2011). Carbon dense, species rich tropical forests largely occur in developing countries in tropical regions of Latin America, sub-Saharan Africa and Southeast Asia where ecologists have used remote sensing to produce maps of carbon (Saatchi et al. 2011) and taxonomic diversity (Asner and Martin 2008a). Particularly in the humid tropics, estimates of forest carbon storage at the individual tree or stand scale can vary widely depending on species specific differences in wood density , life-stage and plant type (Chave et al. 2004). Key parameters controlling ecosystem carbon responses, such as plant traits, are also sparsely observed in the tropics, with the most diverse biome on the planet treated as a single type in models (Schimel et al. 2014).

Differences in plant traits, guilds, species allometry and nutrient availability are all difficult to quantify remotely and field plots are necessary to train models. For these reasons, this study focuses on a forest with rich ground observations and remote sensing data to develop new techniques to be used to monitor ecosystem structure, diversity, and function in the future as additional plot data becomes available.

This analysis focuses on gaining a better understanding of how understory and overstory plants compete for light and water, both at the community and guild level. The inclusion of lianas, understory shrubs and seedlings to the tree census, allows the partitioning of the canopy into vertical strata based on species-specific maximum possible height. By combining plant guild classification with high resolution three-dimensional characterizations of the canopy and sub-canopy topography this study investigates how different plant guilds are spatially arranged along resource gradients. Observations from the Barro Colorado Island (BCI) 50 ha FDP report that 63% of liana species were associated with low canopy height (i.e. tree fall gaps) but significantly less strongly associated with soil chemical or topographic habitat variables (Dalling et al. 2012). These findings support the contention that increases in forest disturbance, fragmentation and degradation has driven a global increase in liana/tree competition for light resources and the subsequent increase in liana size, abundance and biomass (Phillips et al. 2002, Schnitzer and Bongers 2011, Dalling et al. 2012, Schnitzer et al. 2012).

A plot scale analysis of an understory ‘species swarm’ (Gentry 1982), the hyperdiverse genus *Psychotria* on BCI, found that the evolutionary conservation of hydraulic traits related to drought tolerance largely explains phylogenetic clustering in the local assembly. It is suggested that close relatives are unlikely to exclude one another from shared habitats because resource availability is determined largely by asymmetric competition with the overstory, rather than

competition with the neighboring understory plants (Sedio et al. 2012). Recent studies have highlighted the importance of seedling abundance and liana community associations in tropical forests (Comita et al. 2007, Dalling et al. 2012). Seedling and tree abundance is higher in canopy gaps, but tree species composition was unpredictable in tree fall gaps, even for pioneer species (Hubbell et al. 1999). Topographic and edaphic habitat heterogeneity were found to have small and inconsistent effects on the structuring of tropical tree community composition among life stages, indicating tropical tree community composition may be established by the time trees are large enough to be included in the forest census (Baldeck et al. 2013a). Seasonal and spatial variation in water availability, particularly in dry years, determine spatial patterns of species-specific seedling growth and mortality, which in turn shape local species distributions (Comita and Engelbrecht 2009). On a macro spatial scale, climate and soil (i.e. dry season intensity and soil phosphorus) were shown to limit tropical tree distributions across Central Panama (Engelbrecht et al. 2007, Condit et al. 2013). Tree species richness, forest biomass and productivity are dominated by sampling effects and niche complementarity at fine spatial scales (0.04 ha), while environmental gradients drive patters at slightly larger scales (0.25-1 ha) (Chisholm et al. 2013).

In this study, three separate plant surveys (trees, seedlings and lianas) are combined to measure plant species richness, density and basal area at the community and guild level in relation to LiDAR derived remote sensing estimates of water and light availability. The research question is, how does species richness, stem density and basal area vary at the community-level compared to the guild-level, and to what extent do plant guilds vary along gradients of water and light? A previous analysis of tree species richness in the 50-ha plot found that tree species richness was positively associated with the variability in water and light availability within the

plot at the community level (Fricker et al. 2015). Therefore, I hypothesized this species richness effect may be caused by differences in habitat filtering among plants at the guild level. To address these questions, statistical models between the LiDAR derived light condition and water index and guild and community level parameters were developed in the 50ha FDP.

MATERIALS AND METHODS

Study Area & Census Data

The 50 ha Forest Dynamics Plot (FDP) on Barro Colorado Island (BCI), Republic of Panama is the study site (Figure 2.1). The forest on BCI is a classified as a seasonal moist forest and receives a mean of 2600 mm of rain per year, most of which falls during the 8 month wet season from May to December (Windsor 1990). Further details about BCI's climate, geology and flora can be found in Croat (1978). The BCI FDP was established in 1980, and all trees and shrubs > 1 cm dbh in the plot were mapped, identified to species and measured between 1982 and 1983, and re-censused at 5-year intervals since 1985 (Hubbell and Foster 1983, Condit 1998). The BCI FDP represents a unique site due to the long research history spanning over three decades and the wealth of biological census data available including liana and seedling censuses (Hubbell and Foster 1983, Comita et al. 2007, Schnitzer et al. 2012). The BCI FDP was the first large forest dynamics plot of its kind and similar 50-ha plots have been censused around the world in different forest types (Condit et al. 1996, Anderson-Teixeira et al. 2015). This research is novel because it is the first to combine a tree, liana and seedling census including all censused plants into an analysis of habitat filtering at the community and individual guild level.

The study includes data on all free-standing plants > 1 cm dbh (Condit 1998, Hubbell et al. 1999), all lianas (Schnitzer and Carson 2001), and seedlings (Comita et al. 2007). Census data

on lianas was collected by identifying, tagging, mapping and measuring all rooted lianas. Liana stem diameter was measured at 1.3 m from the rooting point and each liana was mapped in relation of the existing 20,000 5x5 m grid markers to aid in mapping the precise location of each stem (within 0.5 m) (Schnitzer et al. 2012). Seedling data were collected for all woody seedlings $\geq$ 20 cm tall and < 1 cm BDH in 20,000 1 m^2 quadrats within the BCI FDP (Comita et al. 2007). The census which was as close to the remote sensing data acquisition were preferred, so the 2010 main census data was used, both the 2009-2011 seedling censuses and the liana census from 2007. All census data available for the BCI 50 ha FDP were compiled into a single PostGIS spatial database. For the main census, individual plants were included which were alive during the 2010 census and with available dbh information. For the liana census, all rooted stems were included. For the seedling census, plants not recorded in either the main or liana censuses were included.

LiDAR Data

To estimate gradients of light and water, airborne LiDAR was used to measure the vertical canopy profile and sub-canopy topography within the 50-ha FDP on BCI. High resolution airborne LiDAR was collected in August 2009 using an Optech ALTM Gemini LiDAR instrument (Optech, Vaughan, ON, Canada) with a first return density of 6.5 per m^2 (BLOM Sistemas Geospaciales SLU) (Lobo and Dalling 2013). In the field, plot locations were surveyed by taking differential GPS coordinates for the plot corners in April 2014. An 'affine' spatial transformation was parameterized with differential GPS coordinates for plot corners to georeference all stems from the censuses. Multiple static GPS measurements were recorded at each plot corner (minimum 15 minute observation) and post-processed using nearby

Continuously Operating Reference Stations (CORS) to obtain a differential solution. The post-processed solution for each point with the lowest residual error was used as the final position and it should be noted that the positions used are different than used in Chapter 1 (published by SRTI). A full description and list of positions is available in Appendix 2.3. To study the patterns of the guild diversity and structure, we considered three spatial scales by dividing the LiDAR and census data into subplots of 20 x 20 m (0.04 ha), 50 x 50 m (0.25 ha) and 100 x 100 m (1.0 ha). The LiDAR data at these three scales to were used to derive water and light availability indices.

Water Index

The Topographic Wetness Index (TWI) was developed to provide a physically based, variable contributing area model of basin hydrology (Beven and Kirkby 1979). The TWI is commonly used to quantify topographic control on hydrological processes and has been used in previous studies to assess ground water contamination risk in China at large spatial scales (Rodríguez-Lado et al. 2013) and in a boreal forest in Sweden, the TWI was used to explain 30% of the variation in vascular plant number and correlated quite well ($r^2 = 0.50$) with groundwater level (Zinko et al. 2005). A study of topographic position on BCI concluded that large variation in water regime over small spatial scales may play a role in maintaining high species richness through providing opportunities for niche specialization (Daws et al. 2002). Topographically defined environments such as the average elevation, terrain slope, curvature or water flow accumulation can approximate hydrologic conditions at the plot to landscape scale (1- 50+ ha) (Moore et al. 1991, Detto et al. 2013). Upward concave terrain (i.e. valleys) was found to be associated with increased species richness across spatial scales in the BCI FDP (Wolf et al. 2012)

and with higher mean canopy height at the landscape scale (Detto et al. 2013). To approximate the availability of water in the BCI FDP, the derived TWI metric was computed from the topographic DSM. The TWI is defined as ln(α/tanβ) where α is the local upslope area draining through a certain point per unit contour length and tanβ is the local slope measured in radians (Sørensen 2006).

$$TWI = \frac{\alpha}{tangent\ (\beta)}$$

The revised TWI arcpython script used in this study is available online (https://github.com/africker/Topographic-Wetness-Index). The mean and standard deviation of TWI were computed for each sub-plot at each spatial scale. These metrics are referred to as the TWI and TWI_{sd}. Visualizations of the TWI are provided in Figure 2.1 A, B, C and Appendix 2.1.

Light Index

Tropical forests are highly light-limited first by extensive cloud cover in the wet season, but also by large upper canopy trees which extinguish photosynthetic flux densities exponentially with distance beneath forest canopies (Wright and Schaik 1994). Light availability in the lower canopy is particularly important for shrubs, treelets, and understory trees and is the primary driver of regenerative competition in tree-fall gaps (Wright et al. 2004). Similarly, physiological and life-history trade off in pioneers versus shade-tolerant mature forest trees vary in their degree of dependence on light and light gaps for germination, growth and survival (Hubbell et al. 1999). Airborne LiDAR has proven effective in detecting fine scale changes in vertical forest structure as non-native trees displace the native forests in Hawaii at the tree and stand scale (Asner et al. 2008). The three-dimensional nature of LiDAR data allows a spatially-explicit characterization of the vertical light environment as well as the sub-canopy vegetation structure. Combining

spectral and LiDAR sensors can quantify a number of biophysical characteristics associated with forests in different stages of succession that may be used to predict the distribution of species richness (Gillespie et al. 2004) and baseline estimates of species richness have been made using LiDAR and high resolution spaceborne optical imagery on BCI (Fricker et al. 2015).

To measure light availability from three-dimensional vertical forest structure data across the BCI FDP, the first-return LiDAR canopy surface model (CSM) is generated by computing the highest recorded LiDAR return within each 1 x 1 m pixel. The digital surface model (DSM) is subtracted from the CSM to compute a canopy height model (CHM). The two canopy structure variables include the mean of the maximum canopy height (MCH) and the standard deviation of the maximum canopy height (MCH_{sd}) in each census subplot. Both MCH and MCH_{sd} are the light indices used and visualizations of the MCH are provided in Figure 2.1 D, E, F and Appendix 2.1.

Guilds

Available information on plant growth form (Schnitzer and Carson 2001, Comita et al. 2007) was used for species-level classification of plants into growth form 'guilds' (Croat 1978, Putz 1984, Hubbell and Foster 1986, Comita et al. 2007). Plant guilds are defined by each species maximum adult stature for freestanding stems or as lianas (climbing woody vines) which use freestanding stems as structural support and therefore are categorized into their own guild. The five plant guilds include: lianas, shrubs (0-4 m), understory trees (4-10 m), midstory trees (10-20 m) and canopy level trees (20 m+). Nineteen individuals were excluded from four tree species in the genus Ficus (Moraceae) that first establish as hemi-epiphytes as well as all stems which were only identified to family or genus level (i.e. species is not known, 975 plants total,

<0.01% of total plants). For the spatial analysis, the 50 ha FDP ground census data was divided into subplots of 20 x 20 m (0.04 ha), 50 x 50 m (0.25 ha) and 100 x 100 m (1.0 ha). For each spatial scale, the number of species, stems, and total basal area is computed within each subplot for all plant species. This process was repeated for each plant guild yielding the total number of species, stems per subplot and total basal area at the individual plant guild level. Based on adult architecture and maximum plant height, species are assigned one of five guilds shown in Table 2.1 and diversity, density and total basal area is reported in Table 2.2 for each guild and the whole community.

Statistical Approach

To address the questions of the study, a statistical approach was developed to analyze the data at two levels. First, the diversity, density and the basal area is analyzed in relation to both water and light availability at the community and secondly examined at the guild level. The statistical approach is based on the spatial and non-spatial regression models to identify statistical associations between plant and guild level diversity, density and size. Pearson's 'r' correlation coefficient is computed for plant richness, density and basal area per subplot in relation to the mean and standard deviations for both TWI and MCH. Remote sensing predictor variables were analyzed using pairwise linear regression models to the response variables: species richness, stem density and basal area. All statistics were calculated in R software (Team 2013).

To determine the effects of spatial autocorrelation amongst variables, both non-spatial ordinary least squares (OLS) regression and spatial generalized least squares (GLS) regression models were tested. Generalized least squares regression is applied when the variances of the

observations are unequal or when there is spatial autocorrelation between observations. To account for spatial autocorrelation in model residuals, the 'gls' function in R was used to fit a model where residual errors are allowed to be correlated and/or have unequal variances. Three variograms are fit to the OLS models (Exponential, Spherical, Gaussian) and the GLS model is optimized by choosing the model with the lowest Akaike information criterion (AIC) score. The OLS and optimized GLS models are compared to determine whether model fits remain similar after accounting for spatial autocorrelation. If the sign of the OLS and GLS models are not the same (generally seen in weak statistical correlations), I consider spatial autocorrelation to be a strong factor and the OLS model assumptions may not be valid. Since GLS models do not have an R-squared statistic, only R-squared and p-value statistics are reported for OLS regression models. Identical modelling methods are used in Chapter 1 (see Appendix 1.4).

Species richness, stem density and basal area calculated from all three plant surveys (tree, seedling and liana) are reported both at the community and the guild level in Table 2.2. For the basal area analysis, seedling diameters were not recorded and were not included in the calculations of basal area. The diversity, density and basal area are summarized in Table 2.2. Lianas are the most species rich and numerous guild followed by canopy trees and midstory trees. Shrub and understory guilds have the lowest number of species with 67 each, but both have more individuals than the midstory guild. All plants are classified within guilds based on species maximum possible height, regardless of actual size in the field (Table 2.1). Pearson product-moment correlation coefficients (r) for all OLS regressions between species richness, stem density and basal area with each of the 4 remote sensing predictor variables in Table 2.3. All results are reported for the 1-ha spatial scale (n = 50).

RESULTS

Effects of subplot size

Since stem density has a measurable effect on species richness, this effect was tested based on the spatial scale (size) of the subplots. Stem density explains varying proportions of the species richness for each subplot and predictably this effect increases with decreasing subplot sizes. At the 1.0 ha subplot size, stem density can explain approximately 18% of the variation in species richness (r = 0.420), 26 % at the 0.25 ha (r = 0.509), and 38% at the 0.04 ha (r = 0.614) subplot scale. This indicates that at the coarsest subplot size (1.0 ha) over 80% of the total variance in species richness cannot be explained by the density of plants alone and may be explained by other environmental factors, chance or history. All subsequent results are reported at the 1.0 ha spatial scale.

Community Level

Species Richness

At the community level (considering all plant guilds), heterogeneity in both the hydrologic and light environments (TWI_{sd} and MCH_{sd}) are positively associated with species richness (r^2 = 0.197 and r^2 = 0.168 respectively (Figure 2.2, Table 2.3). Mean canopy height was negatively associated with species richness (r^2 = 0.206) presumably due to higher plant abundance in tree fall gaps. TWI was weakly negatively associated with species richness (r^2 = 0.013).

Stem Density

Heterogeneity in the light environment (MCH_{sd}) and low MCH were positively associated with community stem density (r^2 = 0.103 and r^2 = 0.093) respectively. There were only weak associations between the stem density of all plants and the TWI or TWI_{sd} (r^2 = 0.013 and r^2 = 0.012) which indicates that if plant stems are non-randomly arranged along the water gradient, these differences must occur at the guild level.

Basal Area

Average basal area is tightly correlated with MCH amongst all plants (r^2 = 0.671), it should be considered that majority (72.6%) of total basal area within the plot is comprised of canopy tree species, with midstory (14.1%), understory (8.4%), lianas (3.1%) and shrub (1.8%) guilds all contributing decreasing relative percentages to total basal area. Mean canopy height and the total canopy tree guild basal area was the strongest statistical relationship found in the analysis (r^2 = 0.774) which confirms that the largest plot measured trees are in the same subplots as the highest measured MCH.

Guild Level

Species Richness

Liana species richness is positively associated (r^2 = 0.450) with low MCH, but not strongly associated with any other predictors. Canopy tree species richness is slightly positively associated (r^2 = 0.101) with the MCH_{sd}, but was more strongly associated (r^2 = 0.217) with TWI_{sd}. Midstory tree species richness was not strongly associated with TWI, TWI_{sd} or MCH, but

there is a positive association (r^2 = 0.262) with MCH_{sd}. While there were no strong associations between the species richness of all plants and the TWI, understory tree species richness is positively association with TWI_{sd} (r^2 = 0.375), but shows no strong association with the other three predictor metrics. Shrub and treelet species richness is positively associated with both TWI_{sd} (r^2 = 0.295) and MCH_{sd} (r^2 = 0.144) predictors, but not strongly associated with the mean values of either. Complete species richness results are reported for all plants and for each guild in Appendix 2.1.1.

Stem Density

At the guild level differences in resource acquisition become apparent. At the individual guild level, liana density is strongly associated with low MCH (r^2 = 0.471), but generally uncorrelated with MCH_{sd} or any topographic variable. When only considering tree guilds (shrubs, understory, midstory or canopy), the strongest association is the midstory species have a higher density in plots with a higher MCH_{sd} (r^2 = 0.120), otherwise stem density among tree guilds does not show strong associations with canopy height metrics. The results of stem density between tree guilds in relation to the TWI reveal a stark trends indicating habitat filtering between guilds. Canopy (r^2 = 0.387) and midstory (r^2 = 0.370) tree density is negatively associated with high water availability (i.e. high TWI). Conversely, understory tree density (r^2 = 0.437) and to a lesser degree shrub and treelet density (r^2 = 0.066) are positively associated with high TWI plots (Figure 2.3, Table 2.3). Generally, plants which reach a taller maximum height occur at higher densities in drier subplots while shorter understory plants occur in higher densities in wetter subplots. Complete stem density results are reported for all plants and for each guild in Appendix 2.1.2.

Basal Area

Liana basal area, while only around 3% of total plot basal area is inversely correlated with MCH (r^2= 0.575) showing that canopy trees and lianas occupy different ends of the light availability gradient (Figure 2.4). With regard to water availability, filtering patterns are similar (but of lesser statistical significance) to those of stem density. Lianas and shrubs show weak statistical associations with TWI ($r < 0.05$). However, amongst trees, canopy (r^2= 0.098) and midstory tree (r^2 = 0.167) basal area are negatively associated with high TWI, while understory trees show a strong filtering effect (r^2 = 0.564) being positively associated with wetter subplots. Complete basal area results are reported for all plants and for each guild in Appendix 2.1.3.

DISCUSSION

The results reveal patterns of spatial partitioning of water and light resource gradients, particularly between different plant guilds. Patterns of plant diversity, density and size are non-randomly spatially structured across water and light availability gradients in the 50-ha plot. At the community level, heterogeneity in both the water and light environments are associated with increased species richness. I assert that these patterns are due to the specific ways in which different plant guilds preferentially occupy gradients of water and light. Environmental filtering of lianas and canopy trees along the light resource gradient have confirmed previous observations (Dalling et al. 2012), however the apparent habitat filtering of freestanding plant species along the water resource gradient is a novel finding.

Water

There appears to be a distinct break in how freestanding plants are spatially arranged in relation to the water gradient at the guild level. Mean water availability is weakly positively associated with diversity and density in small shrubs, and more strongly positively associated with understory trees, while water availability is negatively associated with midstory and canopy tree guilds. Previous research found hydrologic heterogeneity is associated with increased tree species richness on BCI (Wolf et al. 2012) and these results provide evidence to indicate this may be due to differences in resource acquisition traits between plant guilds. When considering all plant guilds, species richness is positively associated with hydrologic heterogeneity (Figure 2.2). However when the contribution of each guild to overall richness is analyzed, there are striking contrasts which highlight the importance of considering plant growth form when analyzing alpha diversity (Figures 2.3, Table 2.3). Shallow root depth serves as the most plausible explanation for an increase in smaller tree species density in wetter areas whereas larger trees likely possess deeper and more horizontally expansive root networks which can survive in drier soil conditions. This explanation is contrary to observational data on BCI which suggests that smaller trees appear to preferentially tap deeper sources of soil water than larger trees, however this study analyzed tree size and did not subset the community into individual plant guilds (Meinzer et al. 1999). Meinzer et al. (1999) suggested that the extensive horizontal area explored by root systems of large trees may partially compensate for the reduced water content in the upper portion of the soil profile and also that large tree stem water storage capacity increases exponentially with tree size. This would explain why shrub and understory plants are clustered in wet areas due to smaller root networks which need direct access to surface water, compounded by the fact that understory guilds have reduced stem water storage capacity compared with their overstory counterparts. This apparent contradiction in results can reasonably

be explained by the fact that smaller diameter trees must tap deeper sources of water to survive long and intense dry seasons, however relative to plant size, larger canopy trees will still have sufficiently deep roots to tap deep soil water, as well as horizontally extensive root systems which untether those individuals from local, topographically induced water stress. While there was a clear signal of hydrologic partitioning amongst tree species richness, density and size, lianas had weak associations with topographically derived predictors (Appendix 2.2.1-Appendix 2.2.3). Since the life history of a liana is much shorter and characterized by rapid growth it stands to reason that lianas are more sensitive to gradients of light rather than water.

Light

The results indicate there is a clear partitioning of light resources amongst different plant guilds, particularly amongst lianas and canopy level trees which confirm previous observations by Dalling et al (2012) (Figure 2.4). Lianas display a strong spatial clustering pattern in subplots with low mean canopy height (i.e. higher proportion of gaps) and can explain 45%, 47% and 57% of the total variance in liana species richness, density and basal area respectively. It has been well documented that lianas are associated with suppressed gap regeneration, and lateral movement into canopy gaps (Schnitzer and Bongers 2002). The results confirm previous findings of a strong guild-level association between lianas and low canopy height (i.e. gaps), and the lack of partitioning of any hydrologically defined habitat is a new finding. Liana species richness, stem density and basal area were weakly correlated with both topographic variables ($r <$ 0.26).

Considering all plant species richness and species richness at the guild level, the standard deviation of canopy height was positively associated with species richness, but differences between guilds becomes evident (Appendix 2.2.1 and Appendix 2.2.2). Less than 10% of the total variation in species richness among canopy trees, understory trees and lianas could be explained by variability in upper canopy height (MCH_{sd}). The same variable could explain 14% and 26% of shrubs and midstory tree species richness respectively. Although the diversity for all plants is associated with low canopy subplots, these increases in diversity can be attributed to increases in liana diversity and increased stem density. Although lianas represent a relatively small fraction of total plot basal area (3.1%), this guild represents a substantially larger proportion (36%) of the total species richness and has a very different life cycle than freestanding plants. Lianas represent a forest carbon pool which is highly light sensitive, uses more energy in the production of photosynthetically active biomass and less energy on the generation of woody biomass for structural support (Schnitzer and Bongers 2002). Therefore, in a spatially heterogeneous manner, lianas cycle carbon at a much faster rate than their freestanding woody counterparts. Since liana censuses have not yet achieved widespread adoption in traditional forest demographics plots, there is a missing component of species richness and biomass estimates using only tree census data. In areas which normally might have a low estimation of biomass (i.e. large canopy gaps), there is a rapidly cycling carbon pool with high species richness which is currently ignored and should be considered in future estimates. As forest fragmentation, disturbance and degradation increase, this 'missing' carbon pool will become increasingly important to global terrestrial biomass budgets and must be analyzed further.

CONCLUSION

This study is the first of its kind to analyze plant richness, density and basal area at the guild level in relation to resource gradients and provide explanations for the spatial partitioning of plant species at this scale. By separating plant species richness, stem density and basal area by individual plant guilds, this study addresses ways in which a plant's growth form and life history influences how it partitions light and water resources in space. The study of plant guild dynamics using airborne LiDAR across the FDP on BCI proves to be a novel way to explain variation in how plants partition light and water resources. Simple metrics which can approximate light and water availability in an existing 50 ha forest census plot demonstrate that plant species have non-random affinities for particular spatially variable environments. Light conditions in the canopy are strongly associated with tree species richness and liana richness in particular. Low average canopy height can explain nearly half of the total variation in liana diversity, however lianas were weakly or not associated with topographic predictors. When considering water availability, there appears to be a pronounced difference between smaller understory and larger over-story tree species guilds and how they are spatially arranged along the hydrologic gradient. Tree species within mid or upper canopy level tree species guilds (>10 m max. height) can be found in higher densities in drier subplots, whereas the smaller (< 10 m max. height) treelets, shrubs and understory guild species are found at higher densities in wetter subplots regardless of growth stage. This study provides some of the first observational evidence of habitat filtering along the water resource gradient between plant guilds with different resource acquisition strategies.

Section 2.2: FIGURES

FIGURE LEGENDS

Figure 2.1. Study Site: The 50 ha Forest Dynamics Plot on Barro Colorado Island, Republic of Panama (bottom). Resource gradients of water and light are measured using the Topographic Wetness Index (A-C) and Mean Canopy Height (D-F). A. Topographic Wetness Index draped over a DEM hillshade model, blue to white is wet to dry. B. Three-dimensional view of the plot (exaggerated 2.5x) viewed from the South-West corner (A, red arrow) superimposed over hillshade model. C. One-hectare scale view of the subplot with the highest standard deviation in wetness index (A, yellow box). D. Canopy surface model, green to white is high to low maximum canopy height. E. Vertical cross section (200 m long x 20 m wide) of hectares with the highest average canopy height (red lines) and the lowest average canopy height (blue lines). F. One-hectare scale view of the subplot with the highest standard deviation in canopy height (D, yellow box).

Figure 2.2. Scatterplots of species richness of the whole plot community (all plant guilds) in relation to both the mean and standard deviation of the Topographic Wetness Index and Mean Canopy Height.

Figure 2.3. Scatterplots of stem density in relation to the Topographic Wetness Index by tree guild (shrubs, understory, midstory and canopy species).

Figure 2.4. Scatterplots of basal area in relation to the Topographic Wetness Index (top-left) and Mean Canopy Height (top-right). The inverse relationship between liana (bottom left) and canopy (bottom-right) tree guilds are plotted against Mean Canopy Height.

Figure 2.5. Maps of species richness, stem density and basal area for all plants and for each individual guild.

Figure. 2.1.

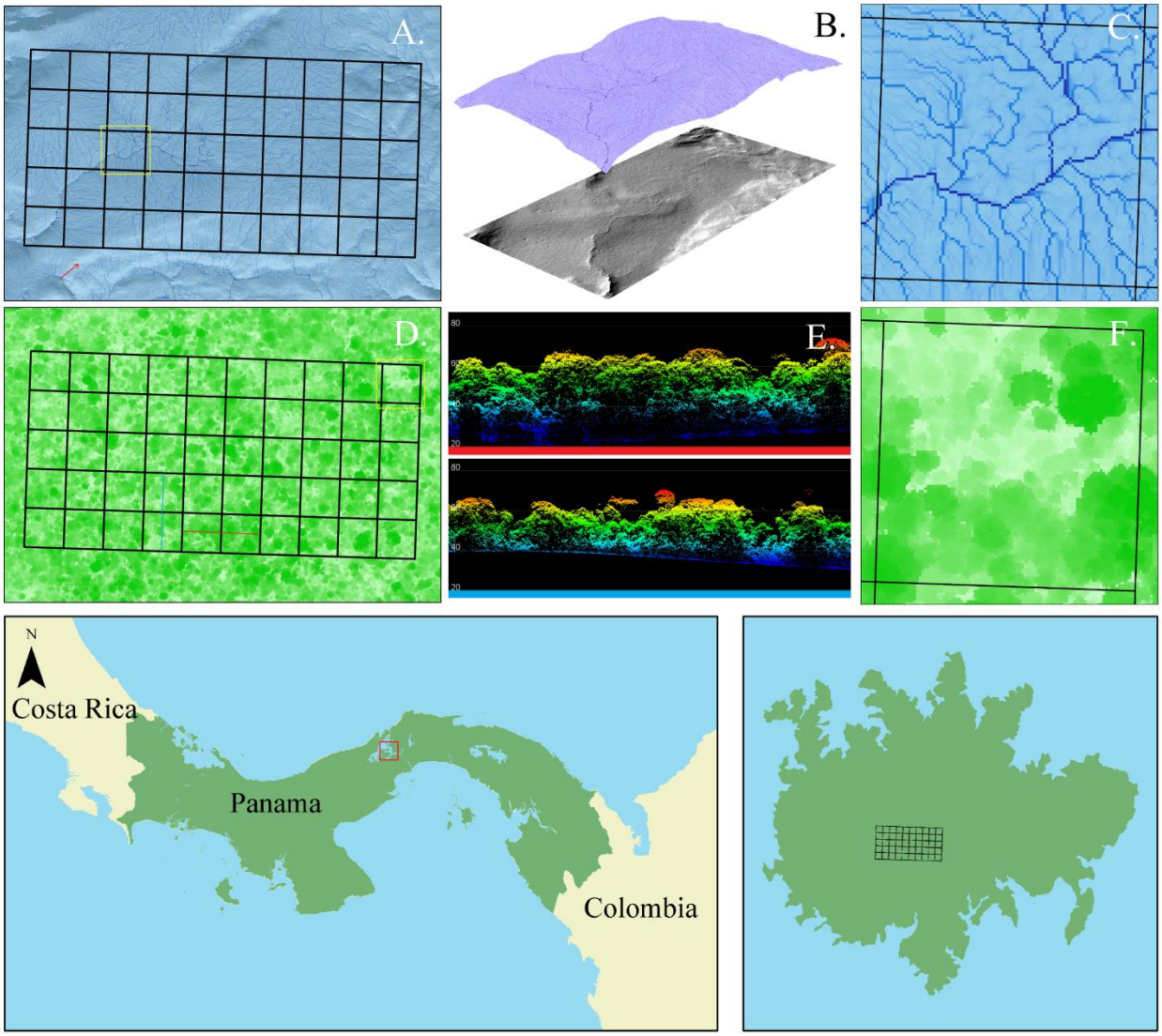

Figure 2.2.

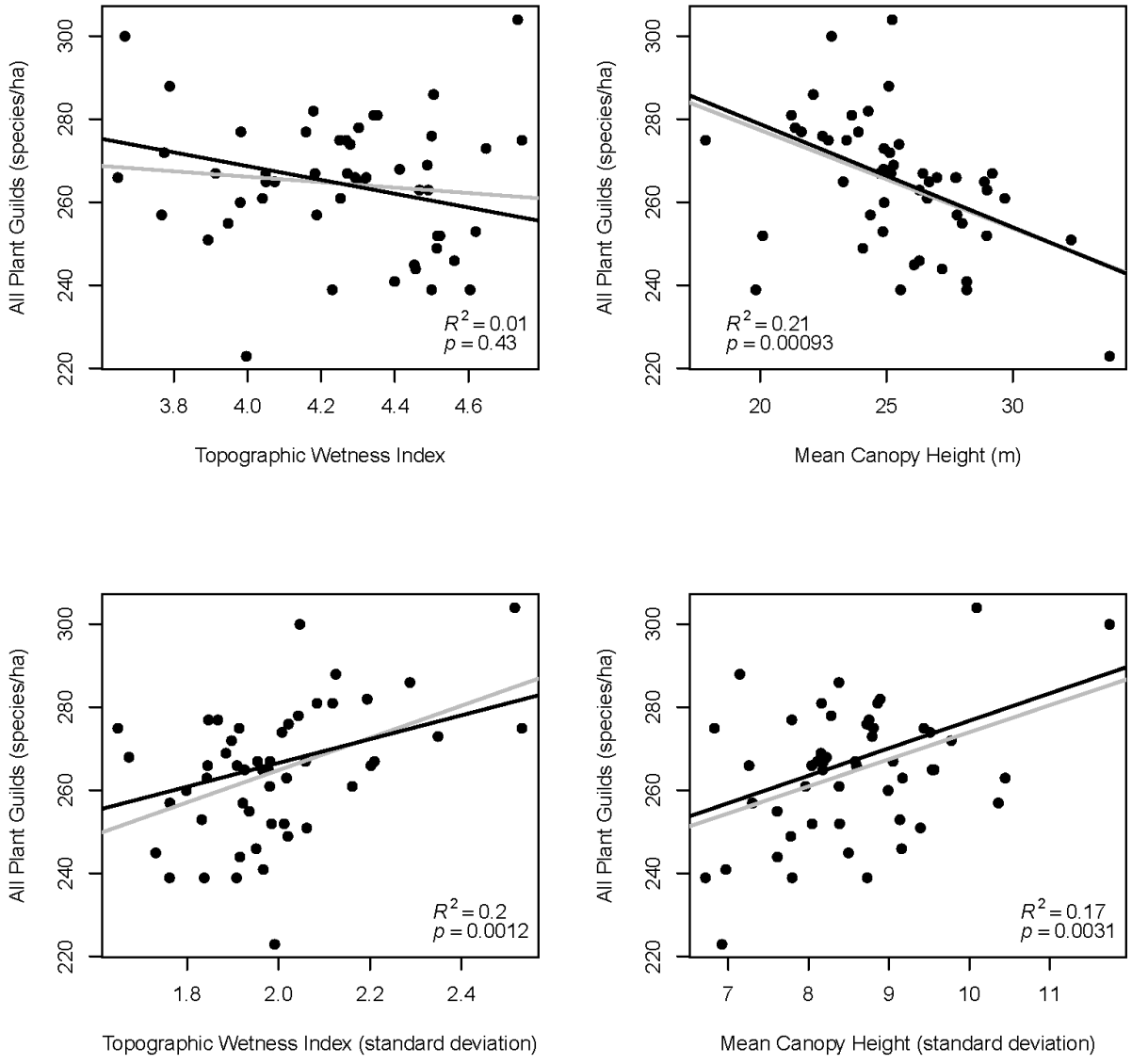
All Plant Guilds (species/ha)
220
240
260
280
300
3.8
4.0
4.2
4.4
4.6
Topographic Wetness Index
$R^2 = 0.01$
$p = 0.43$
All Plant Guilds (species/ha)
220
240
260
280
300
20
25
30
Mean Canopy Height (m)
$R^2 = 0.21$
$p = 0.00093$
All Plant Guilds (species/ha)
220
240
260
280
300
1.8
2.0
2.2
2.4
Topographic Wetness Index (standard deviation)
$R^2 = 0.2$
$p = 0.0012$
All Plant Guilds (species/ha)
220
240
260
280
300
7
8
9
10
11
Mean Canopy Height (standard deviation)
$R^2 = 0.17$
$p = 0.0031$

Figure 2.3.

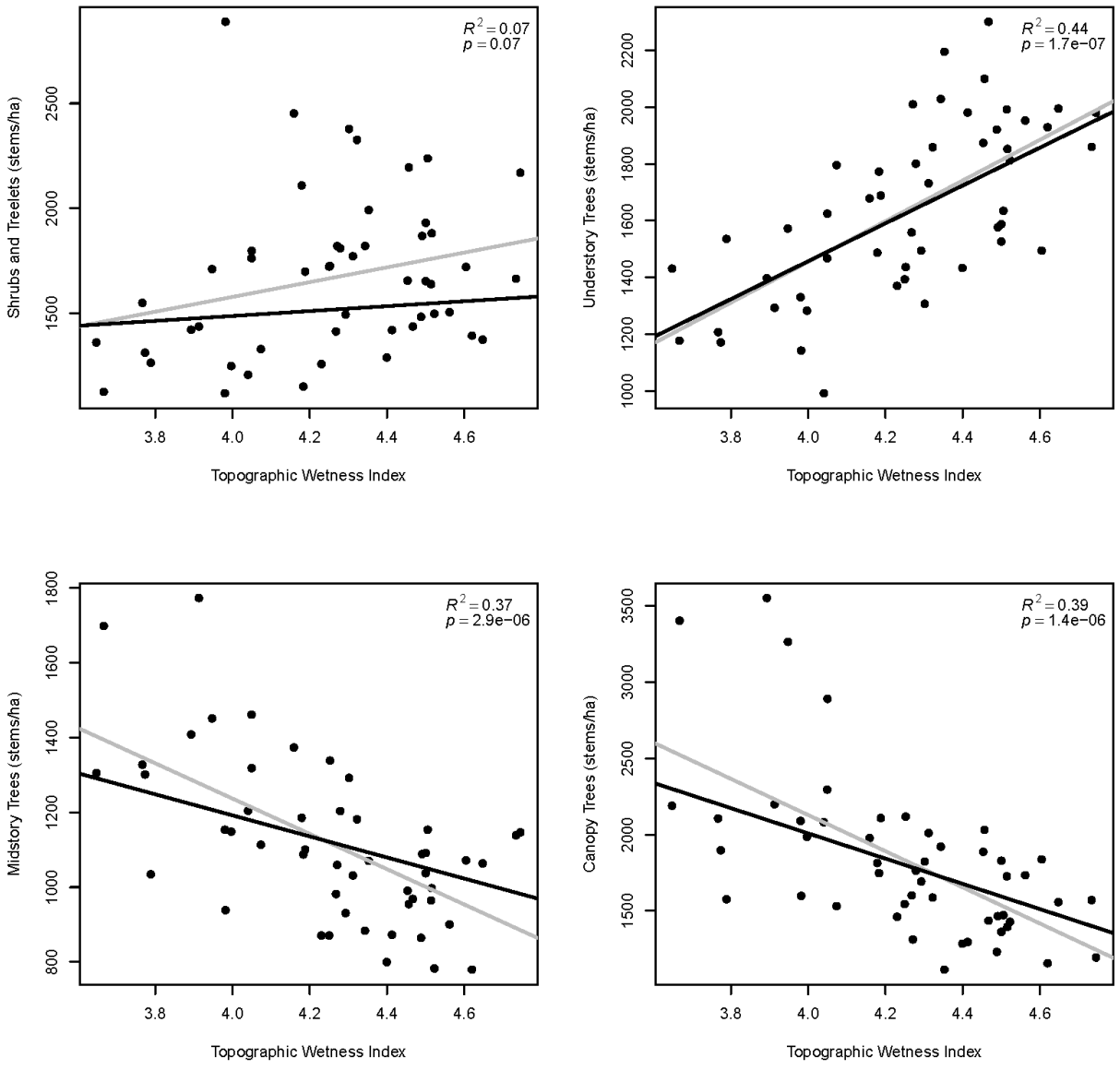
$R^2 = 0.07$
$p = 0.07$
Shrubs and Treelets (stems/ha)
1500
2000
2500
3.8
4.0
4.2
4.4
4.6
Topographic Wetness Index
$R^2 = 0.44$
$p = 1.7e{-}07$
Understory Trees (stems/ha)
1000
1200
1400
1600
1800
2000
2200
3.8
4.0
4.2
4.4
4.6
Topographic Wetness Index
$R^2 = 0.37$
$p = 2.9e{-}06$
Midstory Trees (stems/ha)
800
1000
1200
1400
1600
1800
3.8
4.0
4.2
4.4
4.6
Topographic Wetness Index
$R^2 = 0.39$
$p = 1.4e{-}06$
Canopy Trees (stems/ha)
1500
2000
2500
3000
3500
3.8
4.0
4.2
4.4
4.6
Topographic Wetness Index

Figure 2.4.

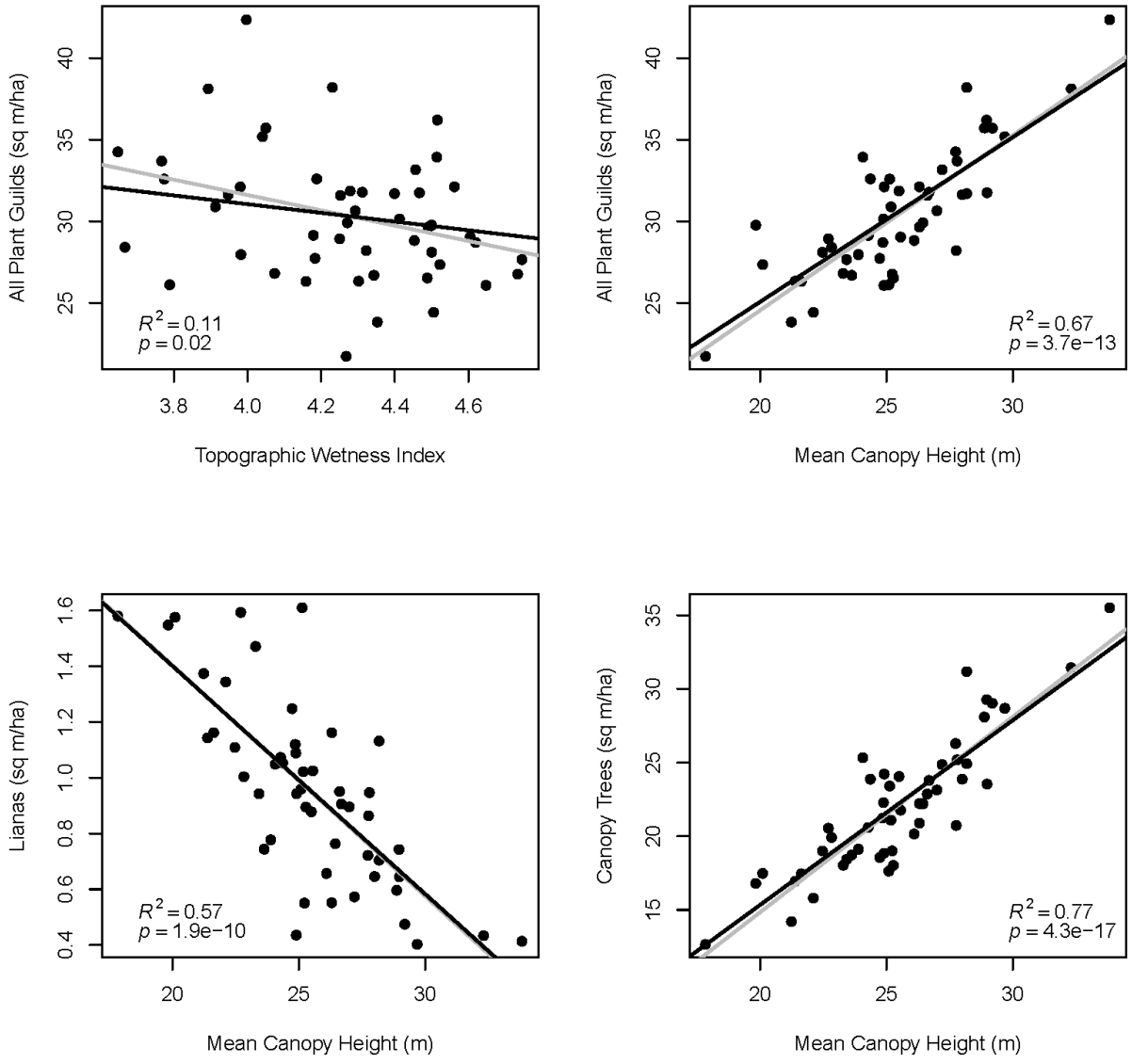
All Plant Guilds (sq m/ha)
25
30
35
40
$R^2 = 0.11$
$p = 0.02$
3.8
4.0
4.2
4.4
4.6
Topographic Wetness Index
All Plant Guilds (sq m/ha)
25
30
35
40
$R^2 = 0.67$
$p = 3.7e{-}13$
20
25
30
Mean Canopy Height (m)
Lianas (sq m/ha)
0.4
0.6
0.8
1.0
1.2
1.4
1.6
$R^2 = 0.57$
$p = 1.9e{-}10$
20
25
30
Mean Canopy Height (m)
Canopy Trees (sq m/ha)
15
20
25
30
35
$R^2 = 0.77$
$p = 4.3e{-}17$
20
25
30
Mean Canopy Height (m)

Figure 2.5.

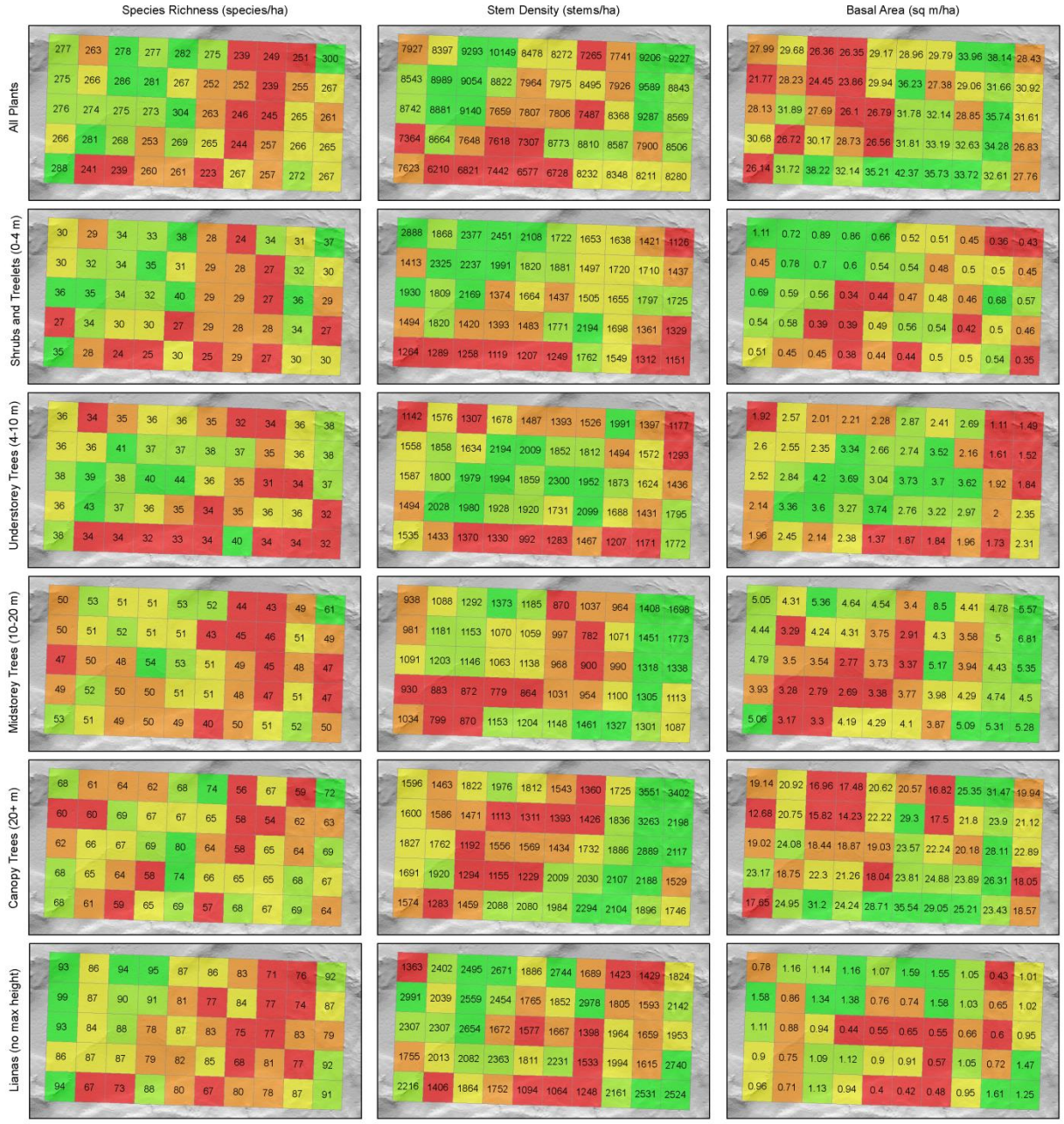
Species Richness (species/ha)
Stem Density (stems/ha)
Basal Area (sq m/ha)
All Plants
Shrubs and Treelets (0-4 m)
Understorey Trees (4-10 m)
Midstorey Trees (10-20 m)
Canopy Trees (20+ m)
Lianas (no max height)

Section 2.3: TABLES

Table 2.1. The growth form/guild classification systems based on maximum canopy architecture. Lianas are dependent on trees for structure and thus have no maximum height. Guild classification based on the system used by Comita et al. (2007).

Growth Form/Guild	Classification	Maximum Height
Shrubs and treelets	S	(≤ 4 m tall)
Understory trees	U	(4 - 10 m tall)
Midstory trees	M	(10 - 20 m tall)
Canopy trees	T	(≥ 20 m tall)
Lianas	L	(no maximum height)

Table 2.2. The diversity, density and basal area for the 50-ha plot, classified based on the maximum adult height of each plant species in Table 2.1.

Guild	Species Richness	Stem Density	Basal Area (m^2)
Shrubs and treelets	67	83,467	26.8
Understory trees	67	82,006	127.1
Midstory trees	73	55,740	214.8
Canopy trees	112	91,066	1,104.0
Lianas	182	99,256	47.6
Total	501	411,535	1,520.2

*not including 975 unidentified individuals and 19 hemi-epiphytes

Table 2.3. Pearson's r values for species richness (top), stem density (middle) and basal area (bottom) in relation to both the mean and standard deviation of Topographic Wetness Index (TWI) and Mean Canopy Height (MCH). All r values are reported at the community level (all) and at the individual guild level.

Species Richness (species/ha)

	All	shrubs	understory	midstory	canopy	lianas
TWI	-0.115	-0.015	0.204	-0.259	-0.126	-0.109
TWI sd	0.444	0.543	0.612	0.207	0.466	0.058
MCH	-0.454	-0.219	-0.129	-0.187	-0.077	-0.671
MCH sd	0.410	0.380	0.187	0.512	0.318	0.179

Stem Density (stems/ha)

	All	shrubs	understory	midstory	canopy	lianas
TWI	-0.128	0.258	0.661	-0.608	-0.622	0.128
TWI sd	0.111	0.135	0.172	0.174	-0.048	-0.054
MCH	-0.305	-0.247	-0.147	0.159	0.355	-0.686
MCH sd	0.322	-0.080	0.026	0.347	0.306	0.090

Basal Area (m^2/ha)

	All	shrubs	understory	midstory	canopy	lianas
TWI	-0.328	-0.011	0.751	-0.409	-0.313	0.044
TWI sd	-0.151	0.011	0.089	-0.106	-0.103	-0.259

MCH	0.819	-0.232	-0.293	-0.270	0.880	-0.758
MCH sd	0.006	-0.057	0.045	-0.095	0.030	-0.117

Section 2.4: APPENDICES

Appendix 2.1. LiDAR remote sensing variables: Topographic Wetness Index and Mean Canopy Height in the 50 ha Forest Dynamics Plot

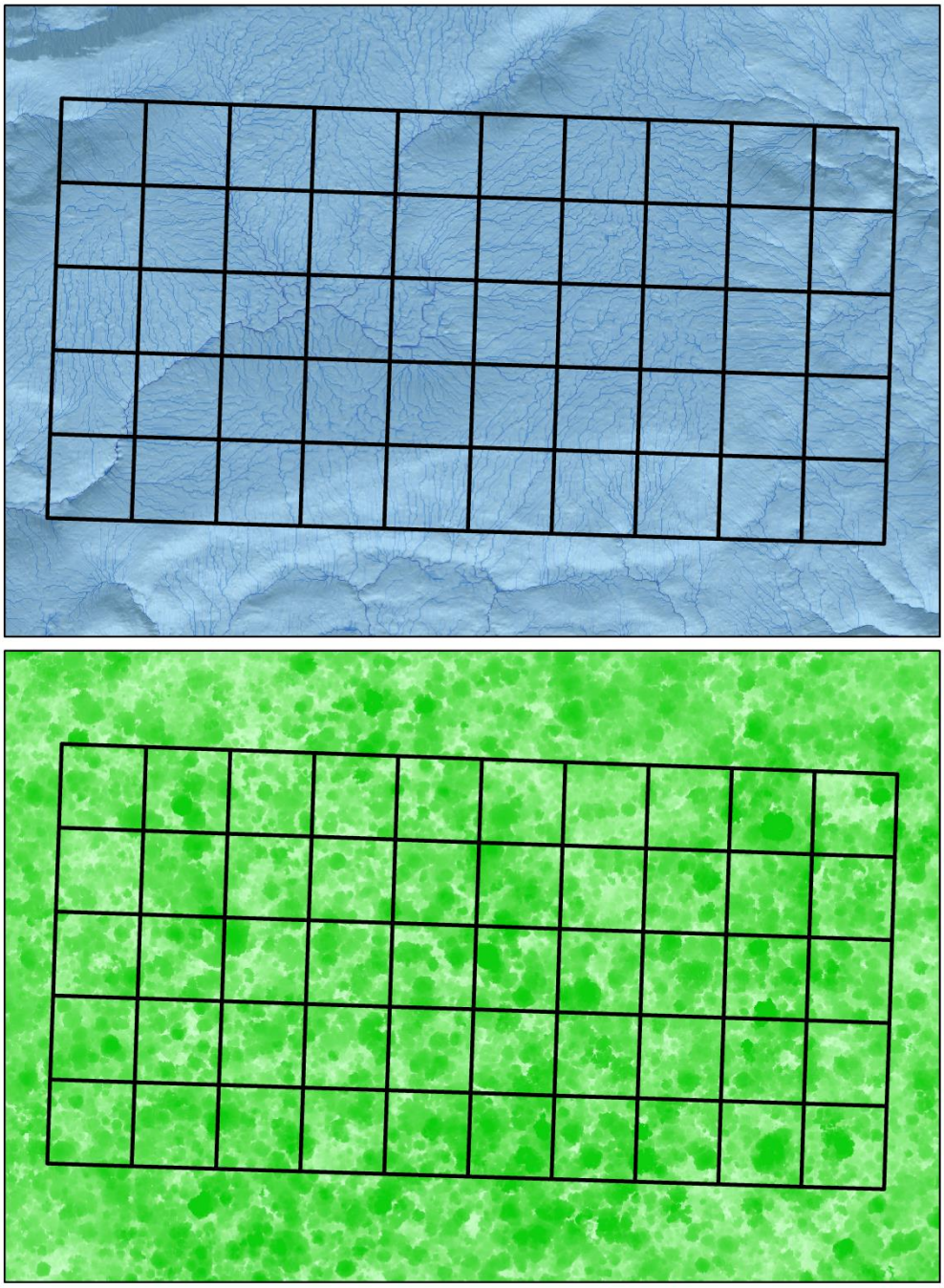

Appendix 2.2. Scatterplots of OLS and GLS regression models at the community and guild level for three response variables: species richness, stem density and basal area and four remote sensing predictor variables (MCH, MCH_{sd}, TWI, TWI_{sd}). R-squared and p-value statistics are reported for OLS regression only. The OLS regression fit line is in grey and the optimized GLS regression fit is shown as a black line. OLS vs. GLS scatterplots are presented for all plants and additionally by individual guild.

Appendix 2.2.1. Species Richness

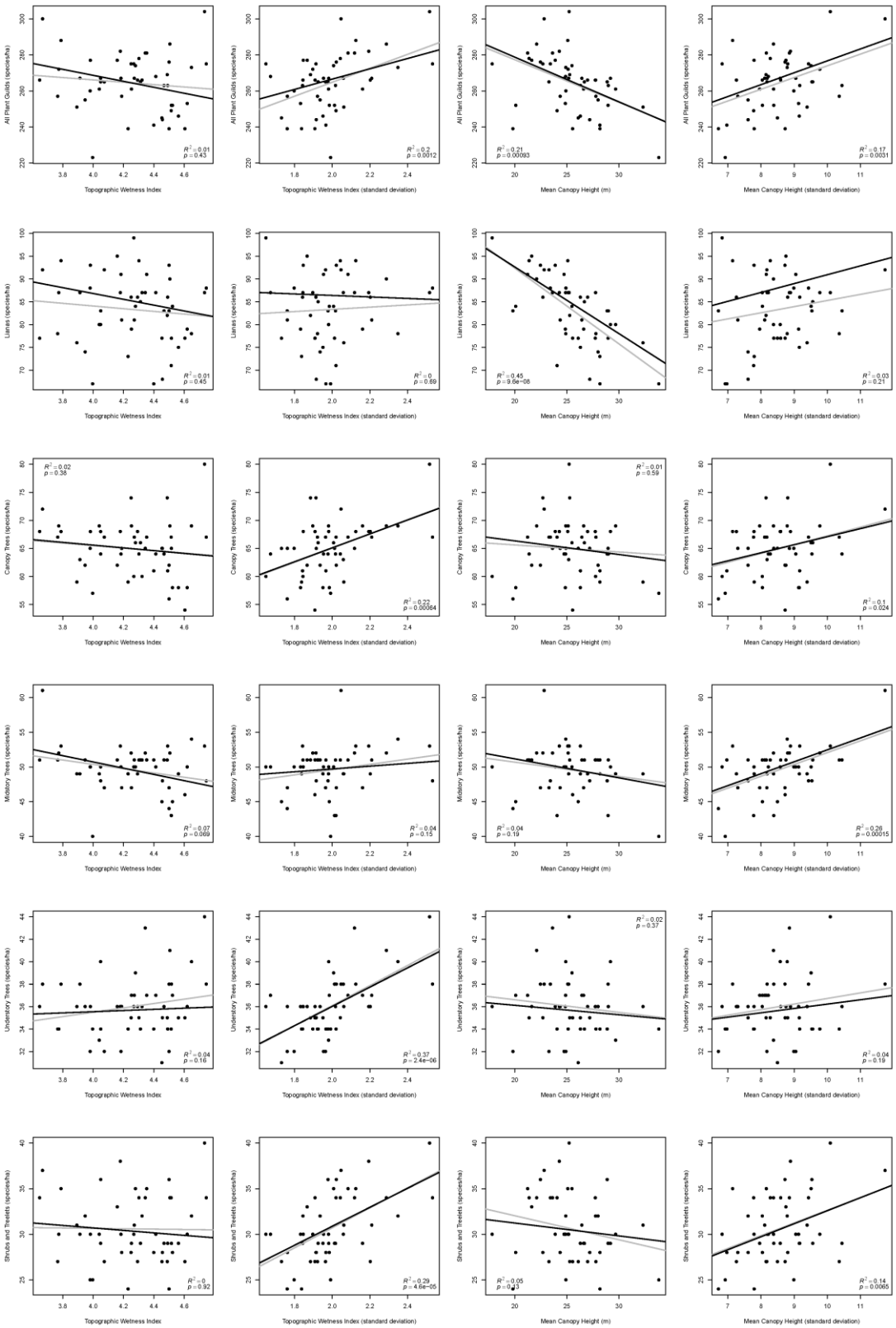

Appendix 2.2.2. Stem Density

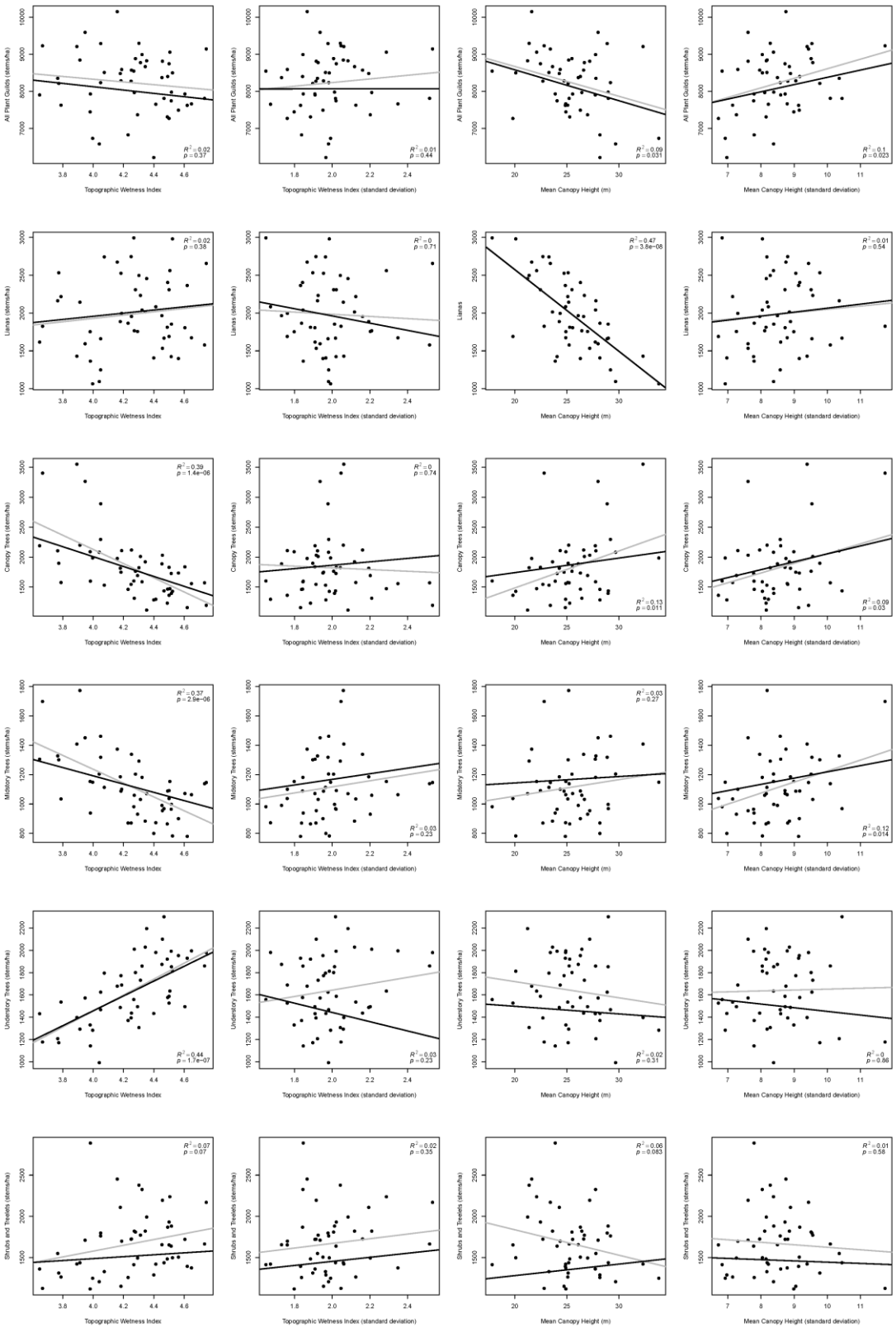

Appendix 2.2.3. Basal Area

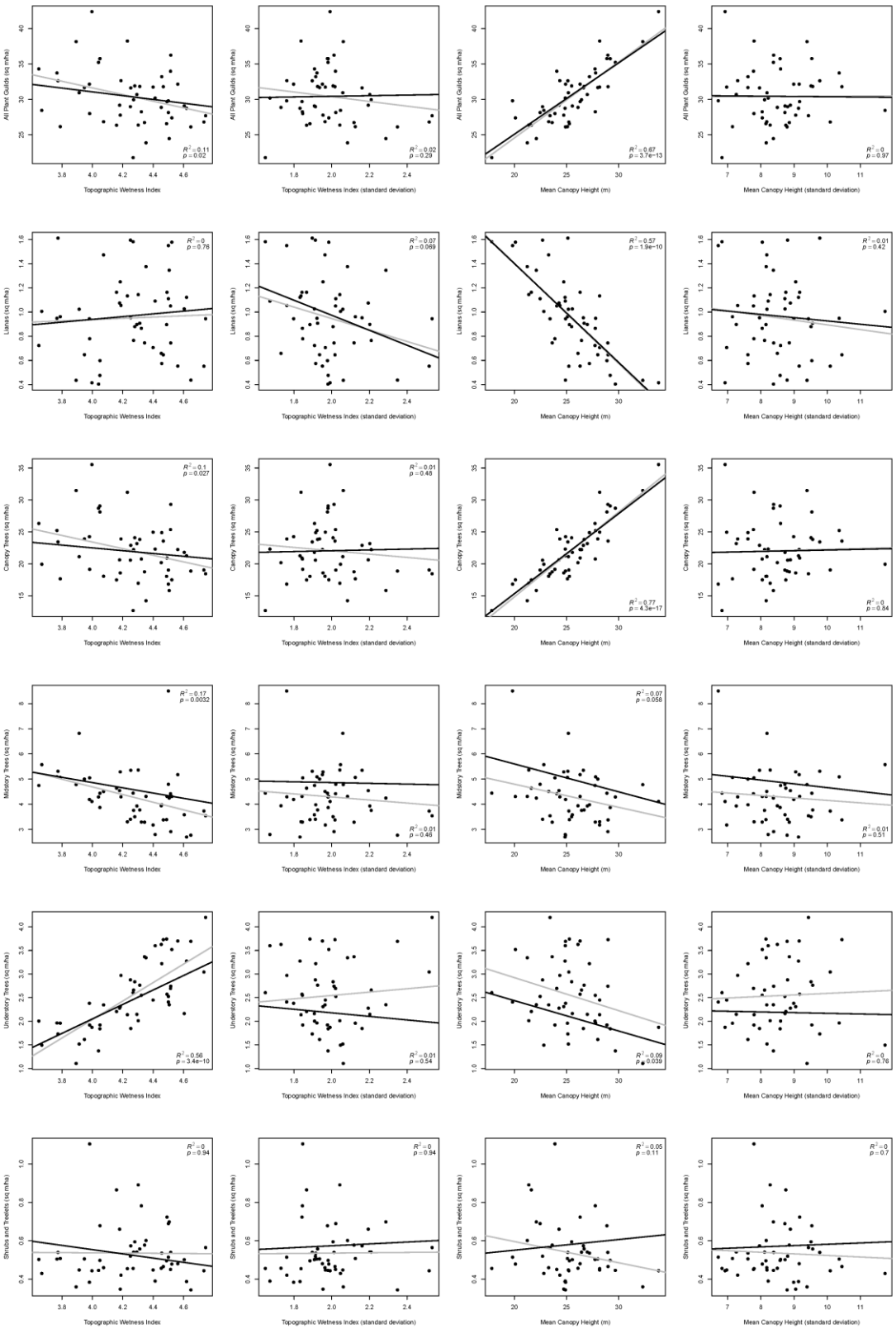

Appendix 2.3. List of Differential GPS points for the plot corners.

These coordinates are slightly different than the published STRI plot corners and have uncertainty values associated with them (se, sn, sup). GIS shapefiles were transformed to match these coordinates using the 'Affine' spatial adjustment method and GIS shapefiles are included in the supplementary materials. Affine spatial adjustment was written by Jeffrey Wolf and is freely available online at: https://github.com/jeffreywolf/afproj

dd_lat	dd_long	ell_ht	se	sn	sup
9.15124	-79.855	140.661	0.9159	0.4417	1.4076
9.15543	-79.846	152.347	0.0916	0.0267	0.1607
9.15578	-79.855	227.677	4.1791	2.5247	36.0178
9.15093	-79.846	132.957	0.6249	0.1511	0.349

CHAPTER 3

Section 3.1: Topographic and climatic influences on forest structure in Mesoamerica

ABSTRACT

Three-dimensional forest structure has been shown to vary in relation to topography at the local and forest census plot scale, however little research has been devoted to testing whether these patterns occur at regional to continental scales. In this study, I analyze vegetation height measured in 194,376 spaceborne laser footprints from the Geoscience Laser Altimeter System (GLAS) to study how forest structure varies in relation to topography, climate, biome, and spatial scale across Mesoamerica. Multivariate prediction models including topographic variables such as mean elevation, slope and the topographic wetness index explain the largest percentage of the variance (>20%) in average forest stand height across the region. Topography derived variables consistently were able to explain larger percentages of the variance (20-50%) in forest structure compared to climatic variables (<15%). Specifically, terrain slope dominates all of the models and is consistently the strongest predictor in multiple random forest regression (RFR) models which sample forest structure at varying spatial scales and control for outside factors like biome and forest type. The primary analysis treats each GLAS laser footprint as an independent sample, however to test the effects of aggregation and spatial scale, three additional sets of models were run which aggregate and average GLAS measurements into grid cells of varying resolution (1, 5, 10 km). By aggregating and averaging GLAS points within a grid cell, there is a reduction in random noise, the effects of outliers are lessened and model performance is assessed using multi-scale sampling strategies. Qualitatively, the relative importance of the strongest predictor variables remained insensitive to spatial scale with slope, elevation and topographic wetness index consistently the top three most important variables across all models,

generally followed by latitude and longitude. Climate variables generally had poor model performance, with annual precipitation and temperature of the warmest/wettest quarters the notable exceptions. Collectively, topography and climate variables could explain between 41-59% of the total variance in forest structure across spatial scales in random forest regression models. The findings suggest that compared to estimations of climate, local topography and terrain slope in particular may influence the spatial distribution of vegetation at the continental or global scale and these trends are directly measurable from spaceborne platforms.

Keywords: Forest structure, Topography, Central America, random forest regression, topographic wetness index, Geoscience Laser Altimeter System, ICESat, Shuttle Radar Topography Mission

INTRODUCTION

Three-dimensional vegetation spatial structure must be known to adequately monitor and model the terrestrial carbon cycle and forest ecosystem dynamics. Precise measurements of vertical forest structure have proven difficult from space. While radar remote sensing has improved in both vertical and horizontal resolution, issues with backscatter, topography, layover, band limitations and random noise prevent these sensors from reliably providing precise measurements of vegetation height at the tree to stand level. The Geoscience Laser Altimeter System (GLAS) has been shown to provide accurate approximations of vegetation height when compared to the medium altitude airborne Laser Vegetation Imaging Sensor and the Shuttle Radar Topography Mission (SRTM) digital surface model (DSM) (Sun et al. 2008). Others have used vegetation structure from GLAS waveforms in conjunction with passive optical imagery were used to create benchmark global biomass estimates and global forest canopy height maps (Lefsky 2010, Pan et al. 2011, Saatchi et al. 2011). Similarly, vertical forest structure from GLAS was incorporated into a multi-sensor satellite estimation of aboveground live woody vegetation carbon density for pan-tropical ecosystems with improved accuracy and spatial resolution (Baccini et al. 2012). A large-scale integrated airborne and satellite mapping effort using both imagery and LiDAR is necessary to support the United Nations Framework Convention on Climate Change (UNFCC) program to reduce deforestation and forest degradation (Asner 2009).

The majority of research which measure vegetation using GLAS waveforms is either focused on specific geographic regions where field validation data are available or at broader scales to sample forests which have little to no field validation measurements. At regional scales, GLAS LiDAR footprints have been used to measure peat topography and to collect large

numbers of forest biomass samples in the remote and highly inaccessible peatland forests of Kalimantan, Indonesia (Ballhorn et al. 2011). In Africa, estimates of aboveground biomass derived from satellite imagery were verified using GLAS estimates of biomass using the vertical height information contained in the vertical waveforms (Baccini et al. 2008), however it was later shown that such estimates must be carefully constrained using field inventory plots (Mitchard et al. 2009, Baccini et al. 2011). Field inventory plots, SRTM elevation data and GLAS footprints were used to estimate aboveground biomass in the mangrove systems in Ciénaga Grande de Santa Marta in Colombia (Simard et al. 2008). The results from a recent analysis of GLAS footprints over the Amazon basin demonstrate the potential of spaceborne LiDAR for sampling the vertical structure of tropical forests and measuring aboveground biomass at the regional scale (Lefsky et al. 2005b).

At local scales in a tropical moist forest in Panama, airborne LiDAR derived three-dimensional forest structure has been shown to vary in relation to hydrology networks and terrain curvature across the landscape (Detto et al. 2013). Vegetation structure derived from GLAS waveforms were found to generally confirm field measured canopy height in a diverse range of forest types from a coniferous forest in Oregon, to mixed hardwood/pine forest in Tennessee to old growth tropical rainforest in Tapajos, Brazil (Lefsky et al. 2005a). The GLAS laser pulses produce a waveform that represents the vertical extent of the forest profile which increases as a function of terrain slope and footprint size (x-y area on the ground illuminated by the laser). Over sloped terrain, the height of the waveform is insufficient to make estimates of tree height and algorithms are needed that are capable of retrieving information about terrain slope from the waveform itself. A recent study of this effect revealed that GLAS height estimates were accurate for areas with a slope up to 10° whereas waveforms of areas with terrain slope exceeding 15°

were problematic. Slopes between 10–15° have been found to be a critical crossover. Further, different waveform shape types and landscape structure classes were developed as a new possibility to explore the waveform in its whole structure. Based on the detailed analysis of some waveform examples, it could be demonstrated that the waveform shape can be regarded as a product of the complex interaction between surface and canopy structure (Hilbert and Schmullius 2012). Consequently, there is a great variety of waveform shapes which in turn considerably hampers GLAS tree height extraction in areas with steep slopes and complex forest conditions. The best method developed removes this slope effect using a second generation algorithm developed using datasets from diverse forests in which forest canopy height has been estimated in the field or via airborne LiDAR. This algorithm eliminates the need for an independent DEM by correcting for 'within footprint' topography and can explain 83% of the variance in forest canopy height with an RMSE of 5 m (Lefsky et al. 2007).

Numerous factors have been shown to influence forest structure across different forest types and spatial scales. Climate, topography and soil variables have proven important to forest structure across biomes. An East-West soil fertility and geology gradient coincide with forest structure and dynamics across the Amazon basin potentially impacting variations in forest biomass, growth and stem turnover rates (Quesada et al. 2009). A local/plot scale study of tropical rain forest structure in La Selva, Costa Rica analyzed soil type, slope angle and topographic position and found that although the plots on flat inceptisols had significantly larger and fewer trees than those on ultisols, above ground biomass did not vary over the relatively small edaphic gradient in upland areas. On residual soils, the largest trees were on the flattest topographic positions. Slope angle per se was not correlated with basal area or AGBM within the residual soils (Clark and Clark 2000). Compared to smaller shrubs and understory trees, canopy

tree species were found to be non-randomly spatially associated with dry forest subplots (1 ha) at the plot scale in Panama (Fricker in prep).

A latitudinal gradient in forest height has been documented with average heights increasing toward the equator and GLAS has been documented to have difficulty in mapping tall (>40 m) closed canopy forests (Simard et al. 2011). In addition to maximum plant height, wood density is another important functional trait in trees and a recent study found geographic and community variation in wood density, was significantly lower in temperate and high elevation communities, dominated by gymnosperms, than in tropical lowland communities, dominated by angiosperms, suggesting an increase in trait and, to some extent, clade filtering with latitude and elevation (Swenson and Enquist 2007).

Mesoamerica is distinct because of its "Biological Corridor" conservation strategy aligned along the long and narrow form of the landmass, divided by a central mountain range which has served as both a bridge and barrier for plants and animals between two continents and two oceans. Furthermore, humans have inhabited and impacted its biodiversity for at least 10,000 years and have heavily shaped the forests in Mesoamerica (DeClerck et al. 2010). Fragmentation alters forest-climate interactions in diverse ways, at a local scale elevated desiccation and wind disturbance near fragmented margins leads to sharply increased tree mortality. At landscape to regional scales (10-1000 km) habitat fragmentation may have complex effects on forest-climate interactions with important consequences for atmospheric circulation, water cycling and precipitation, which may be compounded by deforestation, regional climate change and fire. These interactions remain poorly understood (Laurance 2004).

Research questions

1. Using random forest regression modelling, how much of the total variance in vegetation height can be explained using predictor variables derived from topography and climate?
2. When explaining variation in vegetation height across Mesoamerica, do the topographic variables have stronger predictor associations relative to climate variables?
3. Are the relative trends between predictor variables constant across forest types or biomes and how are the results impacted by changing the spatial scale of analysis?

MATERIALS AND METHODS

Study Area

The biogeographical designation of Mesoamerica is distinct from the geopolitical designation of Central America. Mesoamerica stretches from the Darien in Panama north to the 5 southernmost states of Mexico, while Central America generally excludes Mexico entirely and sometimes Belize and Panama (DeClerck et al. 2010). For the purpose of this study, the formal definition of 'Mesoamerica' is extended to include all states including and between Mexico to Panama.

Forest Structure across Mesoamerica

Forest structure is measured by NASA's Geoscience Laser Altimeter System (GLAS), the sole instrument on the Ice, Cloud, and land Elevation Satellite (ICESat), launched in 2003 and collected data until 2009. The GLAS waveforms were processed following Lefsky et al. (2007) to correct vegetation height for 'within footprint' topographic slope. Clouds, non-terrestrial, and samples in urban areas were all removed from the GLAS sample. We tested GLAS footprints in the countries of Belize, Costa Rica, El Salvador, Guatemala, Honduras,

Mexico, Nicaragua and Panama. The two response variable metrics used to measure forest structure are maximum canopy height and basal area weighted height (e.g. Lorey's Height). Basal area weighting of trees heights increase the importance of the largest trees in a stand an in general represents the height of the stand's tallest trees (Lefsky 2010). All figures and maps in this study focus on Lorey's height as the primary response variable, however models were computed and are reported for maximum height as well. I present a comprehensive map of Lorey's height across Mesoamerica in Figure 3.1. This map shows Lorey's height plotted against latitude and longitude and overlaid on the land cover type. Although many different land cover types are represented in the GLAS sample, nearly half (46.86%) of the GLAS footprints are located in Evergreen Broadleaf Forests (dark green). The list describing the distribution of the GLAS points across land cover types can be found in Table 3.1.

Topographic Variables

Topographic variables are computed using the Version 3, void-filled 90 m resolution digital surface model (DSM) generated from the Shuttle Radar Topography Mission which collected a near-global elevation model in the year 2000 (SRTM) (Farr et al. 2000, Kobrick 2006, Farr et al. 2007). At each GLAS footprint location, the SRTM DSM is used to measure mean elevation, aspect, slope, curvature, flow accumulation and the Topographic Wetness Index (TWI) as predictor variables. Mean elevation is measured directly from the SRTM DSM, surface slope and curvature are the first and second derivatives of the DSM surface. Terrain slope is measured in degrees and curvature is unitless. A negative curvature value represents an upwardly concave surface (i.e. river valleys) while a positive curvature value represents an upwardly convex surface (i.e. ridges). Terrain aspect was measured as the cosine of aspect which is a

measure of ‘north-ness’ with 1 representing a due north-facing and -1 representing a due south-facing slope. Flow accumulation is an estimate of the number of upslope contributing cells which drain through each DSM cell based on the local flow direction. The TWI is a physically based model which considers upslope area contribution and weights the factor by the slope. TWI was first introduced by (Beven and Kirkby 1979) and is defined as $\ln(\alpha/\tan\beta)$ where α is the local upslope area draining through a certain point per unit contour length (i.e. flow accumulation) and $\tan\beta$ is the tangent of the local slope in radians. The TWI was an effective predictor of groundwater contamination in China (Rodríguez-Lado et al. 2013), approximates groundwater flow (Zinko et al. 2005) and is an effective metric to estimate species richness, soil pH, groundwater level, and soil moisture from digital elevation models (Sørensen 2006). The TWI equation is modified slightly to add a small constant to avoid slopes of zero and fill depressions (sinks) in the DEM. The arcpython script to calculate the TWI is available online at: (https://github.com/africker/Topographic-Wetness-Index).

Climate Variables

Climate is approximated using the current set of 19 WorldClim global data layers (http://www.worldclim.org). Bioclimatic variables are derived from the monthly temperature and rainfall values in order to generate more biologically meaningful variables which are commonly used in ecological niche modelling and are derived from national and international weather databases (Hijmans et al. 2005). Recently, patterns of maximum field measured vegetation height were examined globally using BioClim climatic variables and have shown significantly taller vegetation in the tropics (Moles et al. 2009). BioClim variables include annual

precipitation, temperature of the warmest quarter, temperature seasonality and precipitation of the wettest quarter. A full list of the BioClim variables can be found in Table 3.2.

Controlling for land cover/forest type, biome and spatial scale

Biome and land cover type are included as categorical variables in the RFR models in addition to the continuous topography and climatic variables. The overall trends in forest structure are first analyzed as only topographic and climatic variables, then again using the land cover and biome categories. The prediction accuracy of these categorical variables is tested relative to topography and climate to measure marked differences in prediction accuracy. The RFR models are also generated for each of the four different spatial scales to determine whether aggregating GLAS measurements over increasing larger window sizes changes model outputs. To test whether forest structure relates to predictors differently in different biomes or forest/land cover types, both the USGS Global Land Cover Characterization (GLCC) (Table 3.1) and biomes was obtained from the World Wildlife Federation (WWF) (Olson et al. 2001) are included as categorical variables.

The primary analysis focused on the GLAS shots themselves (~70 m diameter footprints), to reduce outlier noise and study the effects of spatial scale, GLAS shots were aggregated into 1 km, 5 km and 10 km grid cells. If a grid cell contained more than one GLAS shot, the vegetation heights were averaged to represent that grid cell. If only one GLAS shot was present in a single cell, the forest structure for that one shot represented the grid cell. Variables are ranked in each RFR models at each scale to determine whether size of the 'window of analysis' significantly changes the results and the relative importance of the predictor variables.

Statistical Analysis

1. Total variance explained in RFR models

Random Forest Regression (RFR) models were computed in R to determine the total proportion of variance which could be described using geographic position, topography and climatic predictor variables. The statistical analysis was performed in three separate steps for two response variables (Lorey's height and maximum height) and 27 predictor variables (latitude, longitude, 6 topographic and 19 climatic variables). The first step involved using RFR to determine how much of the total variance can be explained using all 27 predictors and the relative importance of each topography and climate variable.

2. Relative variable importance in RFR models

The second step was to assess relative variable importance between all variables. Random forest has a robust system of cross-validation (out-of-bag) utilizing training and testing datasets as well as the ability to account of variable co-linearity and complex interaction factors which cannot be easily accounted for in simple multiple-regression models (Breiman 2001). Variable importance is apparently a difficult concept to define in general because of the importance of a variable may be due to its (potentially complex) interactions with other variables. The random forest algorithm estimates the importance of a variable by looking at how much prediction error increases when "out-of-bag" cross-validation data for that variable are permuted while all others are left unchanged. The necessary calculations are carried out tree by tree as the random forest is constructed (Liaw and Wiener 2002). The RFR model for individual GLAS points is ranked by variable importance for all topographic, climatic and geographic position in Figure 3.2. Based on the results of the relative variable importance generated in the

RFR, the geographic distribution of all points is plotted (Figure 3.1) as well as the four most important topography/climate variables in a pairwise fashion using local regression (loess fit).

3. Effects of forest type/land cover, biome and spatial scale on model output

To control for the effects of land cover type and biome, we include land cover and biome as categorical variables in the RFR models to assess relative variable importance when compared to all available predictors. All topographic and climate variables are derived and computed using arcpython scripts in ArcGIS 10.2.2 (Environmental Systems Research Institute, Redlands, CA). Spatial sub-setting is performed in ArcGIS, and all regression analysis is performed in R statistical computing software (Team 2013).

RESULTS

Forest structure (Lorey's and Maximum height) is related to both latitude and longitude in Mesoamerica. Generally, forest height increases from northwestern Mexico to southeastern Panama. This trend is visible in Figure 3.1 showing Lorey's height mapped across Mesoamerica, overlaid on land cover type. Although there is a general trend, a visual inspection of Figure 3.1 suggests there is considerable variation in forest structure which cannot be explained by geographic position alone. The remainder of the results focuses primarily on the topographic and climatic variables in relation to forest structure.

1. Total variance explained in RFR models

The total variance in forest structure (Lorey's and maximum height) which could be explained in RFR models using topographic and climatic variables ranged from 56% (Lorey's

height) to 58% (maximum height) of the total variance when compared for all points and between 41-59% across all spatial scales (Table 3.4). When including all available predictor variables, terrain slope followed by mean elevation were the top two variables across all models, and the topographic wetness index was ranked 3rd in all but one model. Prediction accuracies were higher for all RFR models for maximum height compared to Lorey's height. Overall prediction accuracy was greater than 50% and only four out of 14 models could explain less than half the variance in any vegetation height metric at any scale due to poor model performance (Table 3.4).

2. Relative variable importance in RFR models

The results indicate that topographic variables are correlated with forest structure more than climatic variables at the continental scale. Topography predictor variables dominate climatic predictor variables in all the RFR models. Secondly, within the topographic predictor variables, slope is the dominant predictor even when controlling for confounding factors such as forest type and biome. Third, Mesoamerica's latitude and longitude are correlated due to the diagonal alignment of Mesoamerica relative to the geographic coordinate system, and longitude is generally ranked as a more important RFR variable relative to latitude. Geographic location on the x or y axis was not as important as terrain slope or elevation in any RFR model for either Lorey's height or maximum height.

The results of the variable importance in the random forest model using all topographic and climatic variables for the primary analysis (using the GLAS shots themselves not aggregative into cells) is illustrated in Figure 3.2. Of the top ten most important variables, six were either geographic position or a topographic variable and these were generally more

important than the top four climatic variables. The top ten variables in order of relative importance are: terrain slope, mean elevation, longitude, topographic wetness index, mean temperature of warmest quarter, latitude, terrain curvature, annual precipitation, mean temperature of the wettest quarter and temperature seasonality. The relationship between the top four topographic variables and the top four climatic variables are found in Figures 3.3 and 3.4 respectively.

3. *Effects of forest type/land cover, biome and spatial scale on model output*

Qualitatively, model results remain relatively insensitive to changes in the land cover/biome or spatial scale used in the analysis. Small changes in relative variable importance do occur when controlling for outside factors (particularly amongst climatic variables), the strongest predictors (topography) were consistent across all models. Biome or forest type accounted for <5% of the variance compared with the topographic and climatic variables. I tested the effects of spatial scale by computing the relative variable importance for the model analyzing individual GLAS shots, as well as the three models where GLAS shots were aggregated and averaged inside grid cells (1, 5 ,10 km cell size). The effects of spatial scale are present for the worst predictor variables (generally climate based), however the top predictors remained relatively constant and are ranked based on spatial scale. To simplify the results of the multi-scale analysis, I ranked four separate models (for each spatial scale and all points) and I summed across all models to report the relative variable importance while controlling for spatial scale. In order of importance, the top three ranked variables in the RFR models were consistently slope, average elevation and the topographic wetness index. Longitude, latitude and annual precipitation are the next strongest predictors followed by the remainder of the topographic and

climatic variables. A full list of ranked predictor variables across spatial scales is available in Table 3.3. Linear regression models for terrain slope for all GLAS points and the three most common land cover classes are available in Appendix 3.1.

DISCUSSION

The results provide evidence that steeper terrain slope may support taller stature forests at the continental scale. The effect of topography dominates climate variables across the region and these effects are generally insensitive to forest type, biome or spatial scale. I acknowledge that effects of waveform elongation in GLAS laser profiles can be heavily impacted by steep slopes and cannot provide definitive proof that this effect has been completely removed. However, the overall strength in the relationship between forest height and slope is robust and should not be discarded. Even at slopes of less than 15 degrees where terrain-vegetation contamination would be minimal, the overall trend is taller stature forest on steeper slopes (Figure 3.3A). The best available efforts were made to de-contaminate the effects of slope from the laser profiles following Lefsky et al. (2007). Elevation has a positive relationship with forest structure until about 500 m where most height measurements appear to plateau just below 20 m (Lorey's height) (Figure 3.3B). The TWI had a negative association with average forest height decreasing as the wetness index increased. The dominance of the terrain slope, elevation and wetness index predictor variables above all over predictors in all RFR models for vegetation height suggest strong topographic controls over forest structure at the continental scale.

The evidence that taller stature forest are occurring at steeper, higher elevation, and well drained regions, may have implications for land management and conservation efforts. It should be noted, that Mesoamerica is a highly fragmented ecosystem with a long history and high rates

of deforestation and human settlement. Human settlements generally occur on the drier (Pacific) side of the landmass and in flatter lowland areas with coastal access and as a result, most of the intact forest occurs at higher elevation and on steep slopes where deforestation is difficult. In addition to the contamination of slope in the GLAS waveform signal, this is an alternative explanation for why taller forests are observed on steeper slopes.

It is difficult to say with certainty whether hydrology is influencing forest structure or whether these are the effects of elevation and terrain slope. When viewed in a pairwise regression, there is an obvious trend towards taller forests occupying drier topographic positions (Figure 3.3C). The TWI is a proxy for water availability and is unbounded by field measurements, additionally it is a derivative product of both the elevation and terrain slope and therefore correlated with each. However, like terrain slope, the interpretation of the topographic wetness index results should be approached with these limitations in mind but not be discarded completely. This observation may be confirmed by the curvature results which indicate there is a slight, but significant preference towards taller trees in concave up areas (valleys) with slightly lower average height on ridges (Figure 3.3D). This would seem logical in the context of protection from high wind provided by valleys on the flanks of mountains and volcanoes as well as greater nutrient and water available in valleys, however the associations between forest structure and curvature are generally weak compared to elevation slope and TWI. There is local evidence to suggest that canopy and midstory tree species are non-randomly distributed in well drained soils (Fricker, in prep) and that terrain curvature was a significant predictor of tree species richness (Wolf et al. 2012) at the plot level in Panama. It was also found that the calculation of curvature is highly scale dependent, and these metrics could be expanded to follow

a multi-scale approach to curvature which has shown that valleys are more likely to have taller forests compared to plateaus and ridgetops (Detto et al. 2013).

This study is a proof-of-concept effort to study vertical forest structure in relation to topographic and climatic variables at the regional scale. Similar studies should be performed in other tropical forest regions, temperate and boreal forests and ultimately at the global scale. A better understanding of the environmental factors which impact forest structure can better parameterize estimates of biomass and terrestrial carbon storage. Lessons learned in this study should help inform studies of forest structure at a regional scale but can also be used to refine estimates of forest structure across Mesoamerica and thereby improving estimates of biomass at the landscape scale.

Individual GLAS footprints are sparsely spread across the landscape giving a sparse sampling of the vertical distribution of individual stands of trees. New spaceborne laser altimeters such as the ICESat-2 (Ice, Cloud, and land Elevation Satellite 2) planned for a 2017 launch will include a wider sampling design and will allow scientists to gain a more complete view of global vertical forest structure in the coming decade. ICESat-2's smaller footprints and wider sampling will help determine if the effects of slope have been fully removed from the GLAS laser footprints and how much of the observed terrain slope signal is actually present. In the near term, future research should be focused on whether associations between topographic variables such as slope and the topographic wetness index are consistent outside of Mesoamerica in tropical regions in South America, Africa, and Southeast Asia. A similar analysis should be extended to temperature and boreal forests as well to determine whether these associations are specific to the tropics or are perhaps universal.

CONCLUSION

The analysis of nearly 200,000 individual GLAS points across Mesoamerica provides evidence that terrain slope and topographically derived variables may have a controlling influence on the variation in forest canopy height at the continental scale. Topography dominates climatic predictor variables across land cover and biome which suggests that vertical forest structure may be driven by patterns in local topography more than climatic variables. Steeper terrain slope in particular was the strongest predictor of increased vegetation height across all forest types, land cover classes and biomes, and we suspect effects of slope contamination could not be completely eliminated in extreme terrain. Taller forest was generally located in upland areas on well-drained soils which suggest elevation and hydrology may influence forest structure at a regional scale. Climate variables such as the mean temperature of the warmest and wettest quarters, annual precipitation and temperature seasonality all had mixed effects on vegetation height, with taller forests generally occurring in wetter condition and in areas with higher temperature stability (less extreme high and low temperatures). This analysis across Mesoamerica provides a conceptual framework which can be extended to larger geographic areas to study forest structure globally.

Section 3.2: FIGURES

FIGURE LEGENDS

Figure 3.1. Map of Mesoamerica with land cover overlaid, USGS Land Use/Land Cover System Legend (Modified Level 2). Overlaid by all GLAS footprints used in analysis (red dots). Scatterplots indicate basal area weighted height (Lorey's Height) by latitude and longitude, with a Loess fitted curve (green).

Figure 3.2. Random Forest variable importance plot for all GLAS shots (without gridding). This graph shows the relative importance of each variable relative to all variables.

Figure 3.3. Four most important topography variables for all GLAS shots

Figure 3.4. Four most important climate variables for all GLAS shots

Figure 3.5. Scatterplots of Terrain slope and Lorey's Height for all GLAS points (top left), and the next three most numerous land cover classes, in order of GLAS shot abundance in each land cover class.

Figure 3.1.

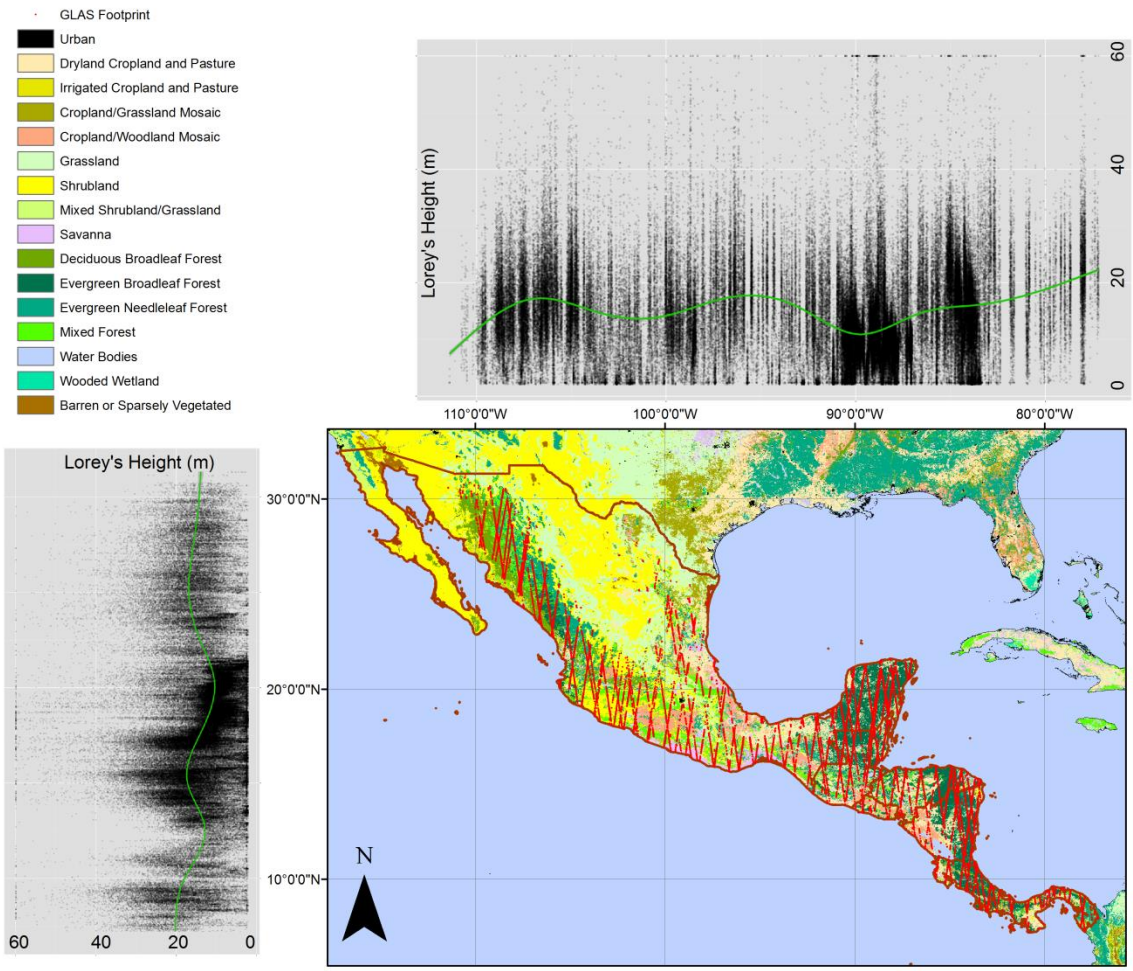
GLAS Footprint
Urban
Dryland Cropland and Pasture
Irrigated Cropland and Pasture
Cropland/Grassland Mosaic
Cropland/Woodland Mosaic
Grassland
Shrubland
Mixed Shrubland/Grassland
Savanna
Deciduous Broadleaf Forest
Evergreen Broadleaf Forest
Evergreen Needleleaf Forest
Mixed Forest
Water Bodies
Wooded Wetland
Barren or Sparsely Vegetated
Lorey's Height (m)
60
40
20
0
110°0'0"W
100°0'0"W
90°0'0"W
80°0'0"W
30°0'0"N
20°0'0"N
10°0'0"N
N

Figure 3.2.

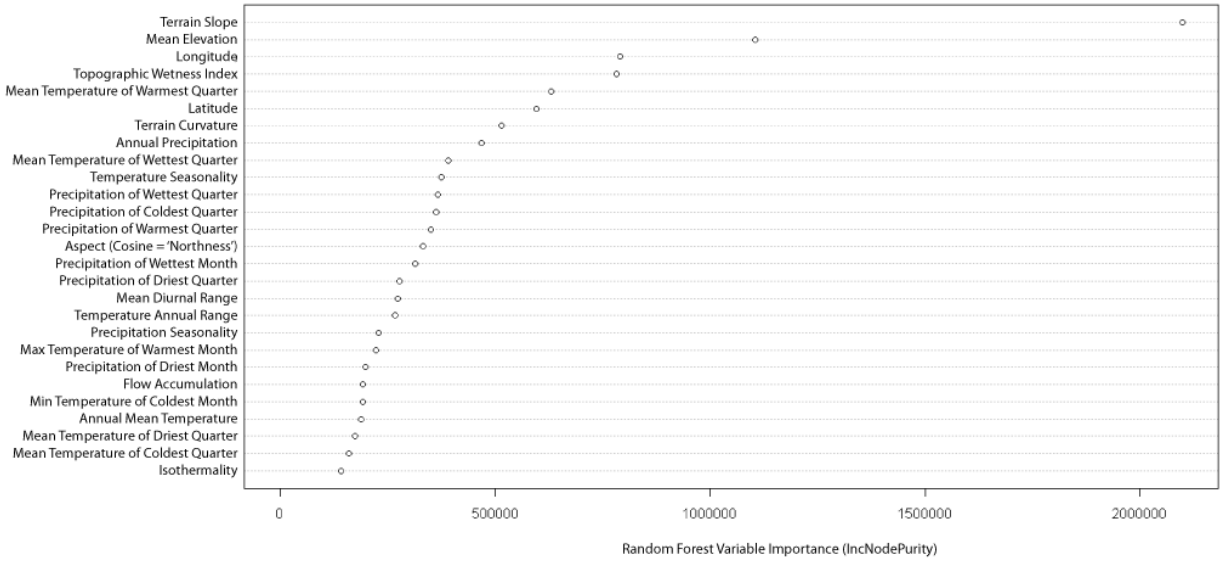
Terrain Slope
Mean Elevation
Longitude
Topographic Wetness Index
Mean Temperature of Warmest Quarter
Latitude
Terrain Curvature
Annual Precipitation
Mean Temperature of Wettest Quarter
Temperature Seasonality
Precipitation of Wettest Quarter
Precipitation of Coldest Quarter
Precipitation of Warmest Quarter
Aspect (Cosine = 'Northness')
Precipitation of Wettest Month
Precipitation of Driest Quarter
Mean Diurnal Range
Temperature Annual Range
Precipitation Seasonality
Max Temperature of Warmest Month
Precipitation of Driest Month
Flow Accumulation
Min Temperature of Coldest Month
Annual Mean Temperature
Mean Temperature of Driest Quarter
Mean Temperature of Coldest Quarter
Isothermality
0
500000
1000000
1500000
2000000
Random Forest Variable Importance (IncNodePurity)

Figure 3.3.

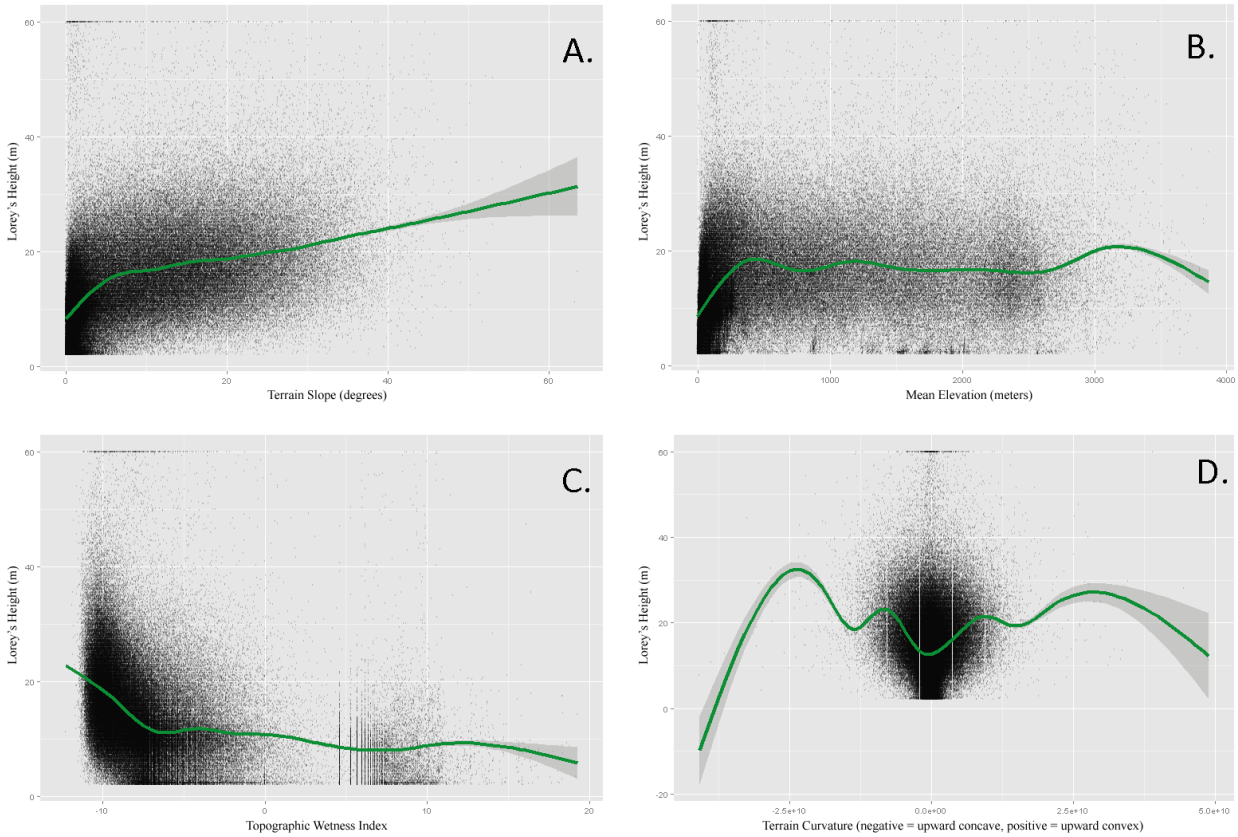
A.
Lorey's Height (m)
Terrain Slope (degrees)
B.
Lorey's Height (m)
Mean Elevation (meters)
C.
Lorey's Height (m)
Topographic Wetness Index
D.
Lorey's Height (m)
Terrain Curvature (negative = upward concave, positive = upward convex)

Figure 3.4.

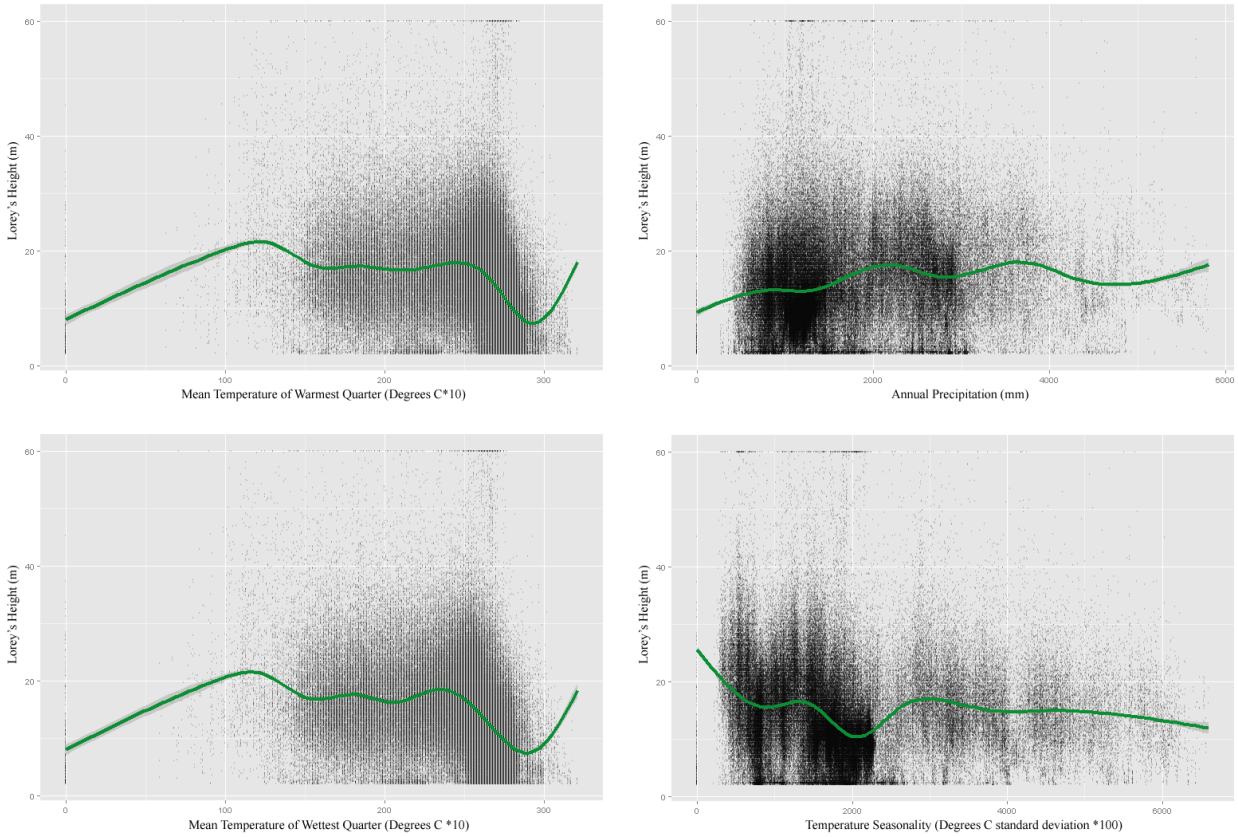
Lorey's Height (m)
Mean Temperature of Warmest Quarter (Degrees C*10)
Annual Precipitation (mm)
Mean Temperature of Wettest Quarter (Degrees C *10)
Temperature Seasonality (Degrees C standard deviation *100)

Section 3.3: TABLES

Table 3.1. Count of GLAS points and percentage of total by the USGS Land Use/Land Cover System (Modified Level 2).

LCD Value	Land Cover Description	GLAS Points in each class	% of total
1	Urban and Built-Up Land	20	0.01
2	Dryland Cropland and Pasture	23,745	12.22
3	Irrigated Cropland and Pasture	609	0.31
5	Cropland/Grassland Mosaic	906	0.47
6	Cropland/Woodland Mosaic	9,657	4.97
7	Grassland	5,912	3.04
8	Shrubland	7,933	4.08
10	Savanna	3,623	1.86
11	Deciduous Broadleaf Forest	7,586	3.90
13	Evergreen Broadleaf Forest	91,080	46.86
14	Evergreen Needleleaf Forest	16,273	8.37
15	Mixed Forest	24,911	12.82
16	Water Bodies	1,823	0.94
18	Wooded Wetland	296	0.15
21	Wooded Tundra	2	0.00
	Total	194,376	

Table 3.2. BioClim variables.

CODE	BioClim variable
BIO1	Annual Mean Temperature
BIO2	Mean Diurnal Range (Mean of monthly (max temp - min temp))
BIO3	Isothermality (BIO2/BIO7) (* 100)
BIO4	Temperature Seasonality (standard deviation *100)
BIO5	Max Temperature of Warmest Month
BIO6	Min Temperature of Coldest Month
BIO7	Temperature Annual Range (BIO5-BIO6)
BIO8	Mean Temperature of Wettest Quarter
BIO9	Mean Temperature of Driest Quarter
BIO10	Mean Temperature of Warmest Quarter
BIO11	Mean Temperature of Coldest Quarter
BIO12	Annual Precipitation
BIO13	Precipitation of Wettest Month
BIO14	Precipitation of Driest Month
BIO15	Precipitation Seasonality (Coefficient of Variation)
BIO16	Precipitation of Wettest Quarter
BIO17	Precipitation of Driest Quarter
BIO18	Precipitation of Warmest Quarter
BIO19	Precipitation of Coldest Quarter

Data available for download at: http://www.worldclim.org/current

Table 3.3. Random forest regression models ranking for each spatial scale. Each predictor variable is ranked for four spatial scales and the table is sorted based on the average ranking from highest relative variable importance (1) to lowest (27).

Variable	Code	10 km	5 km	1 km	points	average
Terrain Slope	slp	1	1	1	1	1
Mean Elevation	dem	2	2	2	2	2
Topographic Wetness Index	twi	3	3	3	4	3.3
Longitude	long	10	6	4	3	5.8
Annual Precipitation	BIO12	6	5	8	8	6.8
Latitude	lat	8	7	7	6	7
Precipitation of Coldest Quarter	BIO19	4	4	9	12	7.3
Curvature	curv	7	9	6	7	7.3
Mean Temperature of Warmest Quarter	BIO10	12	11	5	5	8.3
Mean Temperature of Wettest Quarter	BIO8	5	10	13	9	9.3
Precipitation of Warmest Quarter	BIO18	9	8	12	13	10.5
Temperature Seasonality (standard deviation *100)	BIO4	13	15	10	10	12
Precipitation of Wettest Quarter	BIO16	15	12	11	11	12.3
Precipitation of Driest Quarter	BIO17	11	13	15	16	13.8
Precipitation of Wettest Month	BIO13	14	14	14	15	14.3
Mean Diurnal Range (Mean of monthly (max temp - min temp))	BIO2	17	16	18	17	17
Precipitation Seasonality (Coefficient of Variation)	BIO15	16	17	19	19	17.8
Aspect (Cosine)	casp	21	22	16	14	18.3
Temperature Annual Range (BIO5-BIO6)	BIO7	19	20	17	18	18.5
Max Temperature of Warmest Month	BIO5	20	18	20	20	19.5
Precipitation of Driest Month	BIO14	18	19	21	21	19.8
Annual Mean Temperature	BIO1	23	21	22	24	22.5
Min Temperature of Coldest Month	BIO6	25	23	23	23	23.5
Isothermality (BIO2/BIO7) (* 100)	BIO3	22	24	25	27	24.5
Mean Temperature of Driest Quarter	BIO9	24	25	24	25	24.5
Flow Accumulation	fa	27	27	27	22	25.8
Mean Temperature of Coldest Quarter	BIO11	26	26	26	26	26

Table 3.4. Percentage of variance (%) explained by each Random Forest Regression model for both vegetation height metrics (Lorey's and Maximum), three sampling cell grid sizes (10,5,1 km^2) and the GLAS 'points' themselves (which cannot be averaged since they are singular measurements).

Vegetation Height Metric	10 km	5 km	1 km	points
Average Lorey's	54.52	56.61	55.20	-
Maximum Lorey's	41.33	44.89	49.22	56.09
Average Maximum	56.94	58.89	58.25	-
Maximum	48.54	52.11	54.36	58.41

Section 3.4: APPENDICES

Appendix 3.1. Linear regression models for Lorey's height and terrain slope between all points and the 3 most common land cover types (72% of total GLAS points).

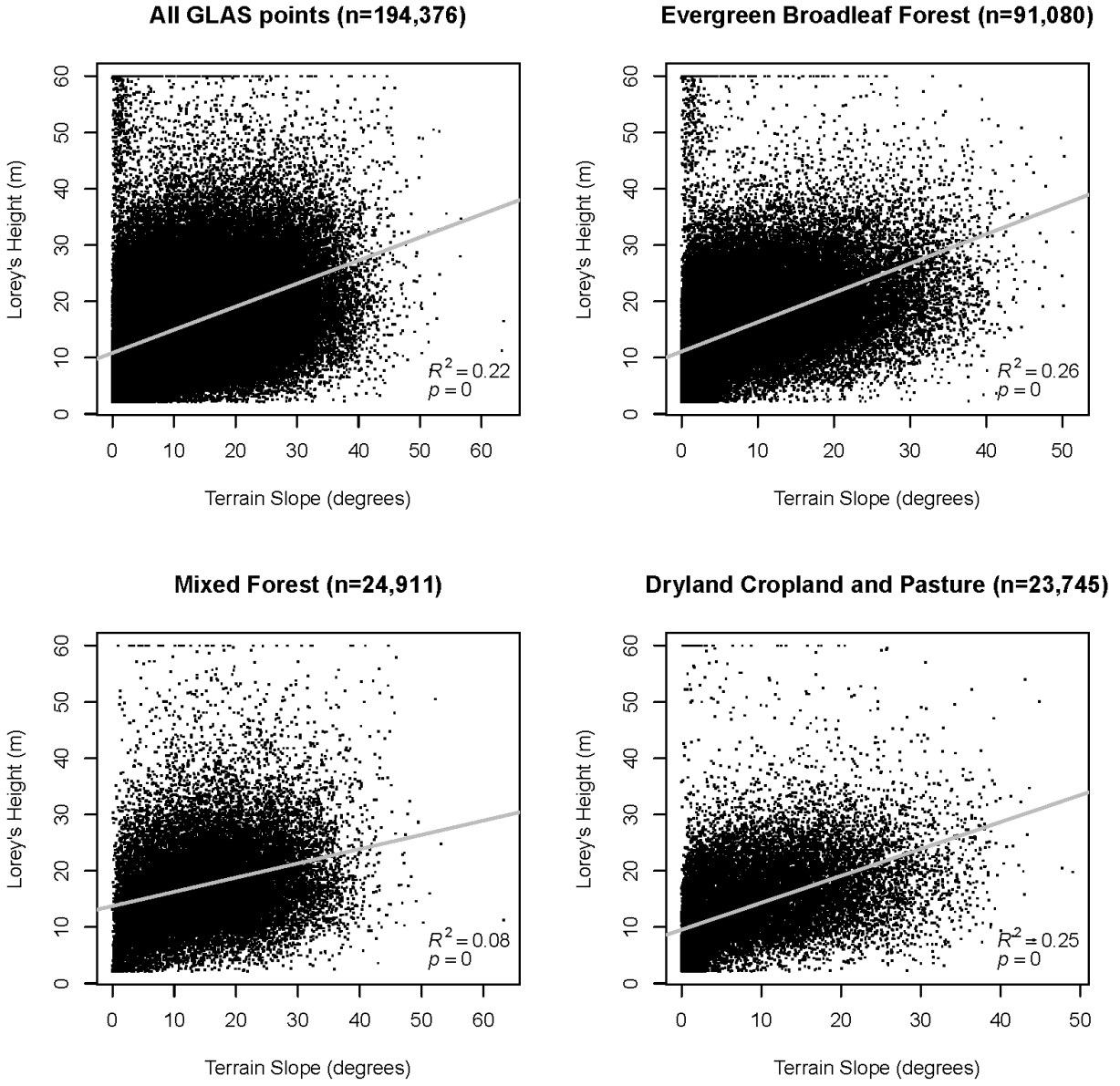

SYNTHESIS

The research presented is this dissertation examines metrics associated with biodiversity from the local plot (<50 ha) scale to the continental scale and narrows the spatial gap between broad scale remote sensing measurements and plot level measurements for forest richness and structure. As high resolution, three-dimensional remote sensing improves in resolution, geographic extent and cost, coupled with an even increasing forest plot network, the spatial gap will narrow further in the next decade. Research efforts should be focused on incorporating new and existing forest census data with LiDAR and optical remote sensing data to model diversity and dynamics at the landscape scale. Using ground-level plot data to make predictions outside of plot boundaries is critical for conservation prioritization, mapping and monitoring change in the world's tropical forests. Very few predictions of alpha-diversity exist in the tropical forests outside of forest census plots. This dissertation tests presents new predictions of species richness across Barro Colorado Island and a methodological framework for developing similar models wherever plot data and high resolution remote sensing data exists. Additionally, this research explores guild level patterns of diversity, density and size between lianas, shrubs, understory, midstory and canopy trees in relation to resource gradients of water and light. Finally, continental patterns of forest structure were found to be largely impacted by terrain slope and other topographic variables compared to climate variables such as temperature and precipitation.

The primary findings of the research indicate that increased alpha diversity is associated with environmental heterogeneity, particularly in the water and light environment and this environmental variation can be effectively detected from airborne remote sensing platforms. Diversity in heterogeneous environments is due to differences in resource acquisition strategies between plant guilds. The apparent filtering of freestanding trees along the hydrologic gradient is

manifested by smaller shrubs and understory trees occurring in higher densities in wet areas while midstory and canopy trees occur in higher densities in drier subplots. Similarly, woody climbing vines (lianas) and tall canopy trees occupy opposite ends of the light availability spectrum, with canopy trees occupying the upper reaches of the forest while lianas are strongly clustered in canopy gaps. At the continental scale, forest structure appears to be strongly influenced by terrain slope, elevation and water availability. These results indicate that environmental gradients influence tree richness, density and size from the fine plot scale to the coarse continental scale.

The accurate location of forest census plots in the field is an often overlooked aspect of forest ecology and remote sensing studies. The correct location (and associated positional errors) of forest census plots is critical to incorporating high-resolution remote sensing measurements since these coordinates are how local forest plot coordinates are translated into geographic space. Traditionally, field ecologists use handheld GPS receivers which only collect one GPS frequency (L1) and can report positional errors of over 10 m under tropical forest canopy cover. These residual errors are not reported from such consumer grade GPS equipment and are unfit for the task of accurately locating forest census plots under dense canopy. Residual GPS errors are almost never reported for geographic coordinates collected under dense forest canopy where errors are likely to be the highest. There should be a fundamental shift in how scientists report such coordinates, particularly when collected in difficult GPS environments (i.e. under dense tropical forest canopy). Each coordinate collected should also report the associated residual errors so locational accuracy can be assessed when converting plot level measurements to geographic space and this dissertation publishes the corner coordinates for the BCI FDP and associated measurement errors. This practice will facilitate the accurate alignment of forest

census plots by ensuring that high-resolution remote sensing is associated with the appropriate forest space and reduce measurement error.

As scientists adopt the practice of reporting accurate locational measurements and associated residual errors of forest plots, a more rigorous analysis using high-resolution remote sensing will be possible. Planned spaceborne LiDAR sensors and the plummeting cost of unmanned aerial platforms will eventually allow a high resolution estimate of the world's forests and a comprehensive view of the distribution of terrestrial biodiversity and forest structure. Finally, the ground based forest census plot network is constantly expanding in geographic extent and is starting to include non-tree life forms such as herbs, forbs and lianas. These ground level measurements are critical to training and testing remote sensing estimates and will provide the biological basis which informs estimates of biodiversity and biomass dynamics across the globe.

In the future, as climate changes and species distributions continue to shift their current geographic extents, these plots and remote sensing measurements will be critical to mapping and monitoring change. This dissertation provides a methodological framework for predicting alpha-diversity outside the extent of current plot boundaries, an approach for analyzing tree richness, density and size at the community and guild level, and uses machine learning Random Forest regression to study forest structure at the continental scale. Finally, I present recommendations for future research directed at testing the results in other forest census plots in a variety of forest types, analyzing forest census plot data at the guild level and using new statistical techniques to analyze large continental scale datasets. The research presented in this dissertation makes steps towards closing the spatial gap between the forest census plot and the landscape, in addition to presenting a clear path forward to better understanding forest richness, structure and dynamics.

REFERENCES

Anderson-Teixeira, K. J., S. J. Davies, A. C. Bennett, E. B. Gonzalez-Akre, H. C. Muller-Landau, S. Joseph Wright, K. Abu Salim, A. M. Almeyda Zambrano, A. Alonso, J. L. Baltzer, Y. Basset, N. A. Bourg, E. N. Broadbent, W. Y. Brockelman, S. Bunyavejchewin, D. F. R. P. Burslem, N. Butt, M. Cao, D. Cardenas, G. B. Chuyong, K. Clay, S. Cordell, H. S. Dattaraja, X. Deng, M. Detto, X. Du, A. Duque, D. L. Erikson, C. E. N. Ewango, G. A. Fischer, C. Fletcher, R. B. Foster, C. P. Giardina, G. S. Gilbert, N. Gunatilleke, S. Gunatilleke, Z. Hao, W. W. Hargrove, T. B. Hart, B. C. H. Hau, F. He, F. M. Hoffman, R. W. Howe, S. P. Hubbell, F. M. Inman-Narahari, P. A. Jansen, M. Jiang, D. J. Johnson, M. Kanzaki, A. R. Kassim, D. Kenfack, S. Kibet, M. F. Kinnaird, L. Korte, K. Kral, J. Kumar, A. J. Larson, Y. Li, X. Li, S. Liu, S. K. Y. Lum, J. A. Lutz, K. Ma, D. M. Maddalena, J.-R. Makana, Y. Malhi, T. Marthews, R. Mat Serudin, S. M. McMahon, W. J. McShea, H. R. Memiaghe, X. Mi, T. Mizuno, M. Morecroft, J. A. Myers, V. Novotny, A. A. de Oliveira, P. S. Ong, D. A. Orwig, R. Ostertag, J. den Ouden, G. G. Parker, R. P. Phillips, L. Sack, M. N. Sainge, W. Sang, K. Sri-ngernyuang, R. Sukumar, I. F. Sun, W. Sungpalee, H. S. Suresh, S. Tan, S. C. Thomas, D. W. Thomas, J. Thompson, B. L. Turner, M. Uriarte, R. Valencia, M. I. Vallejo, A. Vicentini, T. Vrška, X. Wang, X. Wang, G. Weiblen, A. Wolf, H. Xu, S. Yap, and J. Zimmerman. 2015. CTFS-ForestGEO: a worldwide network monitoring forests in an era of global change. Global Change Biology **21**:528-549.

Asner, G. P. 2009. Tropical forest carbon assessment: integrating satellite and airborne mapping approaches. Environmental Research Letters **4**:034009.

Asner, G. P., R. F. Hughes, P. M. Vitousek, D. E. Knapp, T. Kennedy-Bowdoin, J. Boardman, R. E. Martin, M. Eastwood, and R. O. Green. 2008. Invasive plants transform the three-dimensional structure of rain forests. Proceedings of the National Academy of Sciences of the United States of America **105**:4519-4523.

Asner, G. P., D. E. Knapp, T. Kennedy-Bowdoin, M. O. Jones, R. E. Martin, J. Boardman, and C. B. Field. 2007. Carnegie Airborne Observatory: in-flight fusion of hyperspectral imaging and waveform light detection and ranging for three-dimensional studies of ecosystems. Journal of Applied Remote Sensing **1**:013536-013536-013521.

Asner, G. P., and R. E. Martin. 2008a. Airborne spectranomics: mapping canopy chemical and taxonomic diversity in tropical forests. Frontiers in Ecology and the Environment **7**:269-276.

Asner, G. P., and R. E. Martin. 2008b. Spectral and chemical analysis of tropical forests: Scaling from leaf to canopy levels. Remote Sensing of Environment **112**:3958-3970.

Asner, G. P., R. E. Martin, D. E. Knapp, R. Tupayachi, C. Anderson, L. Carranza, P. Martinez, M. Houcheime, F. Sinca, and P. Weiss. 2011. Spectroscopy of canopy chemicals in humid tropical forests. Remote Sensing of Environment **115**:3587-3598.

Baccini, A., S. J. Goetz, N. Laporte, M. Sun, and H. Dong. 2011. Reply to Comment on 'A first map of tropical Africa's above-ground biomass derived from satellite imagery'. Environmental Research Letters **6**:049002.

Baccini, A., S. J. Goetz, W. S. Walker, N. T. Laporte, M. Sun, D. Sulla-Menashe, J. Hackler, P. S. A. Beck, R. Dubayah, M. A. Friedl, S. Samanta, and R. A. Houghton. 2012. Estimated carbon dioxide emissions from tropical deforestation improved by carbon-density maps. Nature Clim. Change **2**:182-185.

Baccini, A., N. Laporte, S. J. Goetz, M. Sun, and H. Dong. 2008. A first map of tropical Africa's above-ground biomass derived from satellite imagery. Environmental Research Letters **3**:045011.

Baldeck, C. A., K. E. Harms, J. B. Yavitt, R. John, B. L. Turner, R. Valencia, H. Navarrete, S. Bunyavejchewin, S. Kiratiprayoon, A. Yaacob, M. N. N. Supardi, S. J. Davies, S. P. Hubbell, G. B. Chuyong, D. Kenfack, D. W. Thomas, and J. W. Dalling. 2013a. Habitat filtering across tree life stages in tropical forest communities. Proceedings of the Royal Society of London B: Biological Sciences **280**.

Baldeck, C. A., K. E. Harms, J. B. Yavitt, R. John, B. L. Turner, R. Valencia, H. Navarrete, S. J. Davies, G. B. Chuyong, and D. Kenfack. 2013b. Soil resources and topography shape local tree community structure in tropical forests. Proceedings of the Royal Society B: Biological Sciences **280**:20122532.

Ballhorn, U., J. Jubanski, and F. Siegert. 2011. ICESat/GLAS data as a measurement tool for peatland topography and peat swamp forest biomass in Kalimantan, Indonesia. Remote Sensing **3**:1957-1982.

Barbier, N., P. Couteron, C. Proisy, Y. Malhi, and J.-P. Gastellu-Etchegorry. 2010. The variation of apparent crown size and canopy heterogeneity across lowland Amazonian forests. Global Ecology and Biogeography **19**:72-84.

Bawa, K. S., J. Rose, K. N. Ganeshaiah, B. N., K. M. C., and U. R. 2002. Assessing biodiversity from space: an example from the Western Ghats, India. Conservation Ecology **6 (2)**:7.

Bellard, C., C. Bertelsmeier, P. Leadley, W. Thuiller, and F. Courchamp. 2012. Impacts of climate change on the future of biodiversity. Ecology Letters **15**:365-377.

Bergen, K. M., S. J. Goetz, R. O. Dubayah, G. M. Henebry, C. T. Hunsaker, M. L. Imhoff, R. F. Nelson, G. G. Parker, and V. C. Radeloff. 2009. Remote sensing of vegetation 3-D structure for biodiversity and habitat: Review and implications for lidar and radar spaceborne missions. J. Geophys. Res. **114**:G00E06.

Beven, K. J., and M. J. Kirkby. 1979. A physically based, variable contributing area model of basin hydrology / Un modèle à base physique de zone d'appel variable de l'hydrologie du bassin versant. Hydrological Sciences Bulletin **24**:43-69.

Breiman, L. 2001. Random forests. Machine learning **45**:5-32.

Carlson, K. M., G. P. Asner, R. F. Hughes, R. Ostertag, and R. E. Martin. 2007. Hyperspectral remote sensing of canopy biodiversity in Hawaiian lowland rainforests. Ecosystems **10**:536-549.

Cayuela, L., J. M. R. Benayas, A. Justel, and J. Salas-Rey. 2006. Modelling tree diversity in a highly fragmented tropical montane landscape. Global Ecology and Biogeography **15**:602-613.

Chambers, J. Q., G. P. Asner, D. C. Morton, L. O. Anderson, S. S. Saatch, F. D. B. Espirito-Santo, M. Palace, and C. Souza. 2007. Regional ecosystem structure and function: ecological insights from remote sensing of tropical forests. Trends in Ecology & Evolution **22**:414-423.

Chave, J., R. Condit, S. Aguilar, A. Hernandez, S. Lao, and R. Perez. 2004. Error propagation and scaling for tropical forest biomass estimates. Philosophical Transactions of the Royal Society of London. Series B: Biological Sciences **359**:409-420.

Chen, J. M., G. Pavlic, L. Brown, J. Cihlar, S. G. Leblanc, H. P. White, R. J. Hall, D. R. Peddle, D. J. King, J. A. Trofymow, E. Swift, J. Van der Sanden, and P. K. E. Pellikka. 2002. Derivation and validation of Canada-wide coarse-resolution leaf area index maps using high-resolution satellite imagery and ground measurements. Remote Sensing of Environment **80**:165-184.

Chisholm, R. A., H. C. Muller-Landau, K. Abdul Rahman, D. P. Bebber, Y. Bin, S. A. Bohlman, N. A. Bourg, J. Brinks, S. Bunyavejchewin, N. Butt, H. Cao, M. Cao, D. Cárdenas, L.-W. Chang, J.-M. Chiang, G. Chuyong, R. Condit, H. S. Dattaraja, S. Davies, A. Duque, C. Fletcher, N. Gunatilleke, S. Gunatilleke, Z. Hao, R. D. Harrison, R. Howe, C.-F. Hsieh, S. P. Hubbell, A. Itoh, D. Kenfack, S. Kiratiprayoon, A. J. Larson, J. Lian, D. Lin, H. Liu, J. A. Lutz, K. Ma, Y. Malhi, S. McMahon, W. McShea, M. Meegaskumbura, S. Mohd. Razman, M. D. Morecroft, C. J. Nytch, A. Oliveira, G. G. Parker, S. Pulla, R. Punchi-Manage, H. Romero-Saltos, W. Sang, J. Schurman, S.-H. Su, R. Sukumar, I. F. Sun, H. S. Suresh, S. Tan, D. Thomas, S. Thomas, J. Thompson, R. Valencia, A. Wolf, S. Yap, W. Ye, Z. Yuan, and J. K. Zimmerman. 2013. Scale-dependent relationships between tree species richness and ecosystem function in forests. Journal of Ecology **101**:1214-1224.

Clark, D. B., and D. A. Clark. 2000. Landscape-scale variation in forest structure and biomass in a tropical rain forest. Forest Ecology and Management **137**:185-198.

Clark, D. B., D. A. Clark, and J. M. Read. 1998. Edaphic variation and the mesoscale distribution of tree species in a neotropical rain forest. Journal of Ecology **86**:101-112.

Clark, D. B., J. M. Read, M. L. Clark, A. M. Cruz, M. F. Dotti, and D. A. Clark. 2004. Application of 1-m and 4-m resolution satellite data to studies of tree demography, stand structure and land-use classification in tropical rain forest landscapes. Ecological Applications **14**:61-74.

Clark, J. S., D. M. Bell, M. H. Hersh, and L. Nichols. 2011. Climate change vulnerability of forest biodiversity: climate and competition tracking of demographic rates. Global Change Biology **17**:1834-1849.

Comita, L. S., S. Aguilar, R. Pérez, S. Lao, and S. P. Hubbell. 2007. Patterns of woody plant species abundance and diversity in the seedling layer of a tropical forest. Journal of Vegetation Science **18**:163-174.

Comita, L. S., and B. M. J. Engelbrecht. 2009. Seasonal and spatial variation in water availability drive habitat associations in a tropical forest. Ecology **90**:2755-2765.

Condit, R. 1998. Tropical Forest Census Plots: Methods and results from Barro Colorado Island, Panama and a comparison with other plots, Berlin.

Condit, R., B. M. J. Engelbrecht, D. Pino, R. Pérez, and B. L. Turner. 2013. Species distributions in response to individual soil nutrients and seasonal drought across a community of tropical trees. Proceedings of the National Academy of Sciences **110**:5064-5068.

Condit, R., S. P. Hubbell, J. V. Lafrankie, R. Sukumar, N. Manokaran, R. B. Foster, and P. S. Ashton. 1996. Species-area and species-individual relationships for tropical trees: A comparison of three 50-ha plots. Journal of Ecology **84**:549-562.

Couteron, P., R. Pelissier, E. A. Nicolini, and D. Paget. 2005. Predicting tropical forest stand structure parameters from Fourier transform of very high-resolution remotely sensed canopy images. Journal of Applied Ecology **42**:1121-1128.

Croat, T., editor. 1978. Flora of Barro Colorado Island. Stanford University, Stanford, California.

Dalling, J. W., S. A. Schnitzer, C. Baldeck, K. E. Harms, R. John, S. A. Mangan, E. Lobo, J. B. Yavitt, and S. P. Hubbell. 2012. Resource-based habitat associations in a neotropical liana community. Journal of Ecology **100**:1174-1182.

Daws, M., C. Mullins, D. R. P. Burslem, S. Paton, and J. Dalling. 2002. Topographic position affects the water regime in a semideciduous tropical forest in Panamá. Plant and Soil **238**:79-89.

DeClerck, F. A. J., R. Chazdon, K. D. Holl, J. C. Milder, B. Finegan, A. Martinez-Salinas, P. Imbach, L. Canet, and Z. Ramos. 2010. Biodiversity conservation in human-modified landscapes of Mesoamerica: Past, present and future. Biological Conservation **143**:2301-2313.

Denslow, J. S. 1995. Disturbance and diversity in tropical rain forests: The density effect. Ecological Applications **5**:962-968.

Detto, M., H. C. Muller-Landau, J. Mascaro, and G. P. Asner. 2013. Hydrological networks and associated topographic variation as templates for the spatial organization of tropical forest vegetation. PLoS ONE **8**:e76296.

Dornelas, M., N. J. Gotelli, B. McGill, H. Shimadzu, F. Moyes, C. Sievers, and A. E. Magurran. 2014. Assemblage time series reveal biodiversity change but not systematic loss. Science **344**:296-299.

Engelbrecht, B. M. J., L. S. Comita, R. Condit, T. A. Kursar, M. T. Tyree, B. L. Turner, and S. P. Hubbell. 2007. Drought sensitivity shapes species distribution patterns in tropical forests. Nature **447**:80-82.

Evans, K. L., P. H. Warren, and K. J. Gaston. 2005. Species–energy relationships at the macroecological scale: a review of the mechanisms. Biological Reviews **80**:1-25.

Fairbanks, D. H. K., and K. C. McGwire. 2004. Patterns of floristic richness in vegetation communities of California: regional scale analysis with multi-temporal NDVI. Global Ecology and Biogeography **13**:221-235.

Farr, T. G., S. Hensley, E. Rodriguez, J. Martin, and M. Kobrick. 2000. The shuttle radar topography mission. European Space Agency-Publications-ESA SP **450**:361-364.

Farr, T. G., P. A. Rosen, E. Caro, R. Crippen, R. Duren, S. Hensley, M. Kobrick, M. Paller, E. Rodriguez, and L. Roth. 2007. The shuttle radar topography mission. Reviews of geophysics **45**.

Feeley, K. J., T. W. Gillespie, and J. W. Terborgh. 2005. The utility of spectral indices from Landsat ETM+ for measuring the structure and composition of tropical dry forests. Biotropica **37**:508-519.

Fricker, G.A., Wolf, J.A., Saatchi, S.S., Gillespie, T.G., Predicting spatial variations of tree species richness in tropical forests from high spatial resolution remote sensing. *Ecological Applications*. In Press, preprint available at: http://www.esajournals.org/toc/ecap/0/0.

Gentry, A. H. 1982. Neotropical floristic diversity: phytogeographical connections between Central and South America, pleistocene climatic fluctuations, or an accident of the Andean orogeny? Annals of the Missouri Botanical Garden **69**:557-593.

Gillespie, T. W. 2005. Predicting woody-plant species richness in tropical dry forests: a case study from South Florida, USA. Ecological applications **15**:27-37.

Gillespie, T. W., J. Brock, and C. W. Wright. 2004. Prospects for quantifying structure, floristic composition and species richness of tropical forests. International Journal of Remote Sensing **25**:707-715.

Gillespie, T. W., S. Saatchi, S. Pau, S. Bohlman, A. P. Giorgi, and S. Lewis. 2009. Towards quantifying tropical tree species richness in tropical forests. International Journal of Remote Sensing **30**:1629-1634.

Goetz, S., D. Steinberg, R. Dubayah, and B. Blair. 2007. Laser remote sensing of canopy habitat heterogeneity as a predictor of bird species richness in an eastern temperate forest, USA. Remote Sensing of Environment **108**:254-263.

Goetz, S. J., D. Steinberg, M. G. Betts, R. T. Holmes, P. J. Doran, R. Dubayah, and M. Hofton. 2010. Lidar remote sensing variables predict breeding habitat of a Neotropical migrant bird. Ecology **91**:1569-1576.

Gould, W. 2000. Remote sensing of vegetation, plant species richness, and regional biodiversity hotspots. Ecological Applications **10**:1861-1870.

Hansen, M. C., P. V. Potapov, R. Moore, M. Hancher, S. A. Turubanova, A. Tyukavina, D. Thau, S. V. Stehman, S. J. Goetz, T. R. Loveland, A. Kommareddy, A. Egorov, L. Chini, C. O. Justice, and J. R. G. Townshend. 2013. High-resolution global maps of 21st-century forest cover change. Science **342**:850-853.

Harms, K. E., R. Condit, S. P. Hubbell, and R. B. Foster. 2001. Habitat associations of trees and shrubs in a 50-ha neotropical forest plot. Journal of Ecology **89**:947-959.

Harris, N. L., S. Brown, S. C. Hagen, S. S. Saatchi, S. Petrova, W. Salas, M. C. Hansen, P. V. Potapov, and A. Lotsch. 2012. Baseline map of carbon emissions from deforestation in tropical regions. Science **336**:1573-1576.

Hijmans, R. J., S. E. Cameron, J. L. Parra, P. G. Jones, and A. Jarvis. 2005. Very high resolution interpolated climate surfaces for global land areas. International Journal of Climatology **25**:1965-1978.

Hilbert, C., and C. Schmullius. 2012. Influence of surface topography on ICESat/GLAS forest height estimation and waveform shape. Remote Sensing **4**:2210-2235.

Hopkinson, C., and L. Chasmer. 2009. Testing LiDAR models of fractional cover across multiple forest ecozones. Remote Sensing of Environment **113**:275-288.

Hubbell, S. P., and R. B. Foster. 1983. Diversity of canopy trees in a neotropical forest and implications for conservation. Special publications series of the British Ecological Society.

Hubbell, S. P., and R. B. Foster. 1986. Biology, chance, and history and the structure of tropical rain forest tree communities. Community ecology **314**:330.

Hubbell, S. P., R. B. Foster, S. T. O'Brien, K. E. Harms, R. Condit, B. Wechsler, S. J. Wright, and S. L. de Lao. 1999. Light-gap disturbances, recruitment limitation, and tree diversity in a neotropical forest. Science **283**:554-557.

Ishii, H. T., S.-i. Tanabe, and T. Hiura. 2004. Exploring the relationships among canopy structure, stand productivity, and biodiversity of temperate forest ecosystems. Forest Science **50**:342-355.

John, R., J. W. Dalling, K. E. Harms, J. B. Yavitt, R. F. Stallard, M. Mirabello, S. P. Hubbell, R. Valencia, H. Navarrete, M. Vallejo, and R. B. Foster. 2007. Soil nutrients influence spatial distributions of tropical tree species. Proceedings of the National Academy of Sciences **104**:864-869.

Keith, H., B. G. Mackey, and D. B. Lindenmayer. 2009. Re-evaluation of forest biomass carbon stocks and lessons from the world's most carbon-dense forests. Proceedings of the National Academy of Sciences **106**:11635-11640.

Kembel, S. W., and S. P. Hubbell. 2006. The phylogenetic structure of a neotropical forest tree community. Ecology **87**:S86-S99.

Kerr, J. T., and M. Ostrovsky. 2003. From space to species: ecological applications for remote sensing. Trends in Ecology & Evolution **18**:299-305.

Kobe, R. K. 1999. Light gradient partitioning among tropical tree species through differential seedling mortaility and growth. Ecology **80**:187-201.

Kobrick, M. 2006. On the toes of giants-How SRTM was born. Photogrammetric Engineering and Remote Sensing **72**:206-210.

Laurance, W. F. 2004. Forest-climate interactions in fragmented tropical landscapes. Philosophical Transactions of the Royal Society of London B: Biological Sciences **359**:345-352.

Lefsky, M. A. 2010. A global forest canopy height map from the Moderate Resolution Imaging Spectroradiometer and the Geoscience Laser Altimeter System. Geophys. Res. Lett. **37**:L15401.

Lefsky, M. A., W. B. Cohen, G. G. Parker, and D. J. Harding. 2002. Lidar remote sensing for ecosystem studies. Bioscience **52**:19-30.

Lefsky, M. A., D. J. Harding, M. Keller, W. B. Cohen, C. C. Carabajal, F. Del Bom Espirito-Santo, M. O. Hunter, and R. de Oliveira, Jr. 2005a. Estimates of forest canopy height and aboveground biomass using ICESat. Geophys. Res. Lett. **32**:L22S02.

Lefsky, M. A., M. Keller, Y. Pang, P. B. De Camargo, and M. O. Hunter. 2007. Revised method for forest canopy height estimation from Geoscience Laser Altimeter System waveforms. Journal of Applied Remote Sensing **1**:013537-013518.

Lefsky, M. A., D. P. Turner, M. Guzy, and W. B. Cohen. 2005b. Combining lidar estimates of aboveground biomass and Landsat estimates of stand age for spatially extensive validation of modeled forest productivity. Remote Sensing of Environment **95**:549-558.

Levin, N., A. Shmida, O. Levanoni, H. Tamari, and S. Kark. 2007. Predicting mountain plant richness and rarity from space using satellite-derived vegetation indices. Diversity and Distributions **13**:692-703.

Leyequien, E., J. Verrelst, M. Slot, G. Schaepman-Strub, I. M. A. Heitkönig, and A. Skidmore. 2007. Capturing the fugitive: Applying remote sensing to terrestrial animal distribution and diversity. International Journal of Applied Earth Observation and Geoinformation **9**:1-20.

Liaw, A., and M. Wiener. 2002. Classification and Regression by randomForest. R news **2**:18-22.

Lo Seen Chong, D., E. Mougin, and J. P. Gastellu-Etchegorry. 1993. Relating the global vegetation index to net primary productivity and actual evapotranspiration over Africa. International Journal of Remote Sensing **14**:1517-1546.

MacArthur, R. H., and J. W. MacArthur. 1961. On bird species diversity. Ecology **42**:594-598.

Meinzer, F. C., J. L. Andrade, G. Goldstein, N. M. Holbrook, J. Cavelier, and S. J. Wright. 1999. Partitioning of soil water among canopy trees in a seasonally dry tropical forest. Oecologia **121**:293-301.

Mitchard, E. T. A., S. S. Saatchi, I. H. Woodhouse, G. Nangendo, N. S. Ribeiro, M. Williams, C. M. Ryan, S. L. Lewis, T. R. Feldpausch, and P. Meir. 2009. Using satellite radar backscatter to predict above-ground woody biomass: A consistent relationship across four different African landscapes. Geophysical Research Letters **36**.

Moles, A. T., D. I. Warton, L. Warman, N. G. Swenson, S. W. Laffan, A. E. Zanne, A. Pitman, F. A. Hemmings, and M. R. Leishman. 2009. Global patterns in plant height. Journal of Ecology **97**:923-932.

Moore, I. D., R. B. Grayson, and A. R. Ladson. 1991. Digital terrain modelling: A review of hydrological, geomorphological, and biological applications. Hydrological Processes **5**:3-30.

Morton, D. C., J. Nagol, C. C. Carabajal, J. Rosette, M. Palace, B. D. Cook, E. F. Vermote, D. J. Harding, and P. R. J. North. 2014. Amazon forests maintain consistent canopy structure and greenness during the dry season. Nature **506**:221-224.

Müller, J., and R. Brandl. 2009. Assessing biodiversity by remote sensing in mountainous terrain: the potential of LiDAR to predict forest beetle assemblages. Journal of Applied Ecology **46**:897-905.

Nagendra, H. 2001. Using remote sensing to assess biodiversity. International Journal of Remote Sensing **22**:2377-2400.

Nagendra, H., and D. Rocchini. 2008. High resolution satellite imagery for tropical biodiversity studies: the devil is in the detail. Biodiversity and Conservation **17**:3431-3442.

Olson, D. M., E. Dinerstein, E. D. Wikramanayake, N. D. Burgess, G. V. N. Powell, E. C. Underwood, J. A. D'Amico, I. Itoua, H. E. Strand, and J. C. Morrison. 2001. Terrestrial ecoregions of the world: A new map of life on earth A new global map of terrestrial ecoregions provides an innovative tool for conserving biodiversity. BioScience **51**:933-938.

Palmer, M. W., P. G. Earls, B. W. Hoagland, P. S. White, and T. Wohlgemuth. 2002. Quantitative tools for perfecting species lists. Environmetrics **13**:121-137.

Pan, Y., R. A. Birdsey, J. Fang, R. Houghton, P. E. Kauppi, W. A. Kurz, O. L. Phillips, A. Shvidenko, S. L. Lewis, J. G. Canadell, P. Ciais, R. B. Jackson, S. W. Pacala, A. D. McGuire, S. Piao, A. Rautiainen, S. Sitch, and D. Hayes. 2011. A large and persistent carbon sink in the world's forests. Science **333**:988-993.

Phillips, O. L., R. Vasquez Martinez, L. Arroyo, T. R. Baker, T. Killeen, S. L. Lewis, Y. Malhi, A. Monteagudo Mendoza, D. Neill, P. Nunez Vargas, M. Alexiades, C. Ceron, A. Di Fiore, T. Erwin, A. Jardim, W. Palacios, M. Saldias, and B. Vinceti. 2002. Increasing dominance of large lianas in Amazonian forests. Nature **418**:770-774.

Putz, F. E. 1984. The natural history of lianas on Barro Colorado Island, Panama. Ecology **65**:1713-1724.

Quesada, C. A., J. Lloyd, M. Schwarz, T. R. Baker, O. L. Phillips, S. Patino, C. Czimczik, M. G. Hodnett, R. Herrera, and A. Arneth. 2009. Regional and large-scale patterns in Amazon forest structure and function are mediated by variations in soil physical and chemical properties. Biogeosciences Discussion **6**:3993-4057.

Questad, E. J., J. R. Kellner, K. Kinney, S. Cordell, G. P. Asner, J. Thaxton, J. Diep, A. Uowolo, S. Brooks, N. Inman-Narahari, S. A. Evans, and B. Tucker. 2014. Mapping habitat suitability for at-risk plant species and its implications for restoration and reintroduction. Ecological Applications **24**:385-395.

Rocchini, D., A. Chiarucci, and S. A. Loiselle. 2004a. Testing the spectral variation hypothesis by using satellite multispectral images. Acta Oecologica-International Journal of Ecology **26**:117-120.

Rocchini, D., A. Chiarucci, and S. A. Loiselle. 2004b. Testing the spectral variation hypothesis by using satellite multispectral images. Acta Oecologica **26**:117-120.

Rocchini, D., C. Ricotta, and A. Chiarucci. 2007. Using satellite imagery to assess plant species richness: The role of multispectral systems. Applied Vegetation Science **10**:325-331.

Rocha, A. V., and G. R. Shaver. 2009. Advantages of a two band EVI calculated from solar and photosynthetically active radiation fluxes. Agricultural and Forest Meteorology **149**:1560-1563.

Rodríguez-Lado, L., G. Sun, M. Berg, Q. Zhang, H. Xue, Q. Zheng, and C. A. Johnson. 2013. Groundwater Arsenic Contamination Throughout China. Science **341**:866-868.

Saatchi, S., W. Buermann, H. ter Steege, S. Mori, and T. B. Smith. 2008. Modeling distribution of Amazonian tree species and diversity using remote sensing measurements. Remote Sensing of Environment **112**:2000-2017.

Saatchi, S. S., N. L. Harris, S. Brown, M. Lefsky, E. T. A. Mitchard, W. Salas, B. R. Zutta, W. Buermann, S. L. Lewis, S. Hagen, S. Petrova, L. White, M. Silman, and A. Morel. 2011. Benchmark map of forest carbon stocks in tropical regions across three continents. Proceedings of the National Academy of Sciences **108**:9899-9904.

Schimel, D., R. Pavlick, J. B. Fisher, G. P. Asner, S. Saatchi, P. Townsend, C. Miller, C. Frankenberg, K. Hibbard, and P. Cox. 2014. Observing terrestrial ecosystems and the carbon cycle from space. Global Change Biology:n/a-n/a.

Schnitzer, S. A., and F. Bongers. 2002. The ecology of lianas and their role in forests. Trends in Ecology & Evolution **17**:223-230.

Schnitzer, S. A., and F. Bongers. 2011. Increasing liana abundance and biomass in tropical forests: emerging patterns and putative mechanisms. Ecology Letters **14**:397-406.

Schnitzer, S. A., and W. P. Carson. 2001. Treefall gaps and the maintenance of species diversity in a tropical forest. Ecology **82**:913-919.

Schnitzer, S. A., S. A. Mangan, J. W. Dalling, C. A. Baldeck, S. P. Hubbell, A. Ledo, H. Muller-Landau, M. F. Tobin, S. Aguilar, D. Brassfield, A. Hernandez, S. Lao, R. Perez, O. Valdes, and S. R. Yorke. 2012. Liana abundance, diversity, and distribution on Barro Colorado Island, Panama. PLoS ONE **7**:e52114.

Schwartz, M. W., C. A. Brigham, J. D. Hoeksema, K. G. Lyons, M. H. Mills, and P. J. van Mantgem. 2000. Linking biodiversity to ecosystem function: implications for conservation ecology. Oecologia **122**:297-305.

Sedio, B. E., S. J. Wright, and C. W. Dick. 2012. Trait evolution and the coexistence of a species swarm in the tropical forest understorey. Journal of Ecology **100**:1183-1193.

Simard, M., N. Pinto, J. B. Fisher, and A. Baccini. 2011. Mapping forest canopy height globally with spaceborne lidar. Journal of Geophysical Research: Biogeosciences **116**:G04021.

Simard, M., V. H. Rivera-Monroy, J. E. Mancera-Pineda, E. Castañeda-Moya, and R. R. Twilley. 2008. A systematic method for 3D mapping of mangrove forests based on Shuttle Radar Topography Mission elevation data, ICEsat/GLAS waveforms and field data: Application to Ciénaga Grande de Santa Marta, Colombia. Remote Sensing of Environment **112**:2131-2144.

Srivastava, D. S., and M. Vellend. 2005. Biodiversity-ecosystem function research: Is it relevant to conservation? Annual Review of Ecology, Evolution, and Systematics **36**:267-294.

Sun, G., K. J. Ranson, D. S. Kimes, J. B. Blair, and K. Kovacs. 2008. Forest vertical structure from GLAS: An evaluation using LVIS and SRTM data. Remote Sensing of Environment **112**:107-117.

Swenson, N. G., and B. J. Enquist. 2007. Ecological and evolutionary determinants of a key plant functional trait: wood density and its community-wide variation across latitude and elevation. American Journal of Botany **94**:451-459.

Sørensen, R., and J. Seibert. 2007. Effects of DEM resolution on the calculation of topographical indices: TWI and its components. Journal of Hydrology **347**:79-89.

Sørensen, R. Z., U. Seibert, J. 2006. On the calculation of the topographic wetness index: evaluation of different methods based on field observations. Hydrol. Earth Syst. Sci. **10**:101-112.

Tang, H., R. Dubayah, A. Swatantran, M. Hofton, S. Sheldon, D. B. Clark, and B. Blair. 2012. Retrieval of vertical LAI profiles over tropical rain forests using waveform lidar at La Selva, Costa Rica. Remote Sensing of Environment **124**:242-250.

R Core Development Team. C. 2013. R: A language and environment for statistical computing.*in* R. F. f. S. Computing, editor., Vienna, Austria.

Terborgh, J. 1985. The vertical component of plant species diversity in temperate and tropical forests. The American Naturalist **126**:760-776.

Tittensor, D. P., M. Walpole, S. L. L. Hill, D. G. Boyce, G. L. Britten, N. D. Burgess, S. H. M. Butchart, P. W. Leadley, E. C. Regan, R. Alkemade, R. Baumung, C. Bellard, L.

Bouwman, N. J. Bowles-Newark, A. M. Chenery, W. W. L. Cheung, V. Christensen, H. D. Cooper, A. R. Crowther, M. J. R. Dixon, A. Galli, V. Gaveau, R. D. Gregory, N. L. Gutierrez, T. L. Hirsch, R. Höft, S. R. Januchowski-Hartley, M. Karmann, C. B. Krug, F. J. Leverington, J. Loh, R. K. Lojenga, K. Malsch, A. Marques, D. H. W. Morgan, P. J. Mumby, T. Newbold, K. Noonan-Mooney, S. N. Pagad, B. C. Parks, H. M. Pereira, T. Robertson, C. Rondinini, L. Santini, J. P. W. Scharlemann, S. Schindler, U. R. Sumaila, L. S. L. Teh, J. van Kolck, P. Visconti, and Y. Ye. 2014. A mid-term analysis of progress toward international biodiversity targets. Science **346**:241-244.

Townsend, A. R., G. P. Asner, and C. C. Cleveland. 2008. The biogeochemical heterogeneity of tropical forests. Trends in Ecology & Evolution **23**:424-431.

Wilson, E. O. 1988. The current state of biological diversity. Biodiversity **3**:18.

Windsor, D. M. 1990. Climate and moisture variability in a tropical forest: long term records from Barro Colorado Island, Panama. Smithsonian Contributions to the Earth Sciences **29**:1-145.

Wolf, J., G. Fricker, V. Meyer, S. Hubbell, T. Gillespie, and S. Saatchi. 2012. Plant species richness is associated with canopy height and topography in a neotropical forest. Remote Sensing **4**:4010-4021.

Wolf, J.A., Hubbell, S.P., Fricker, G.A., Turner, B.L., Geospatial Observations on tropical forest subsurface soil chemistry (Data Paper). Ecology (Accepted 5/19/2015).

Wright, S. J., O. Calderón, A. Hernandéz, and S. Paton. 2004. Are lianas increasing in importance in tropical forests? A 17-year record from Panama. Ecology **85**:484-489.

Wright, S. J., and C. P. v. Schaik. 1994. Light and the phenology of tropical trees. The American Naturalist **143**:192-199.

Zinko, U., J. Seibert, M. Dynesius, and C. Nilsson. 2005. Plant species numbers predicted by a topography-based groundwater flow index. Ecosystems **8**:430-441.